

Athanasios Kallioras

Urban flood hazard management – Case study: Shanghai



Urban flood hazard management – Case study: Shanghai

By

Athanasios Kallioras

in partial fulfilment of the requirements for the degree of

Master of Science
in Civil Engineering

at the Delft University of Technology,
to be defended publicly on Friday February 21, 2020 at 1:00 PM.

Student number: 4724550

Thesis committee:	Dr. ir. J.D. Bricker,	TU Delft
	Dr. Q. Ke,	TU Delft
	Dr. ir. F.H.M. van de Ven,	TU Delft

An electronic version of this thesis is available at <http://repository.tudelft.nl/>.

Cover image: How Shanghai would look with a rise of just 2C: the UN warned this week of a potential 3C scenario. Photograph: Nickolay Lamm/Courtesy Climate Central.

Source: The Guardian. From Miami to Shanghai: 3C of warming will leave world cities below sea level.

<https://www.theguardian.com/cities/2017/nov/03/miami-shanghai-3c-warming-cities-underwater>

CONTENTS

CONTENTS	ii
LIST OF FIGURES	v
LIST OF TABLES	ix
ABSTRACT	x
ACKNOWLEDGEMENTS	xi
1 INTRODUCTION	1
1.1 Background	1
1.1.1 Floods in urban areas and China	1
1.1.2 Floods in Shanghai	2
1.2 Research description.....	2
1.2.1 Research problem	3
1.2.2 Research objective.....	3
1.2.3 Scope	3
1.2.4 Research strategy.....	3
2 LITERATURE REVIEW	5
2.1 Hydrologic processes during urban flooding	5
2.2 Types of flooding	5
2.3 Urban drainage system	7
2.4 Flooding in urban drainage systems	7
2.5 Surcharge in urban drainage systems	7
2.6 Simulation of urban flooding	8
2.6.1 Hydrological models	9
2.6.2 Hydraulic model (dual drainage model).....	9
2.7 Digital Elevation Model (DEM).....	13
2.8 Design storms	14
2.9 Flood Management – Proposed flood reduction measures.....	15
2.9.1 Sustainable urban Drainage Systems (SuDS).....	15
2.9.2 Sponge Cities in China	15
2.9.3 Upgrade of drainage system – Creation of water storage areas	16
3 STUDY AREA AND METHODOLOGY	17
3.1 Study area.....	17
3.2 Availability and quality of data	17
3.3 Flood hazard in Delft3D Flexible Mesh (Delft3D FM)	18
3.3.1 Delft3D Flexible Mesh (Delft3D FM)	18
3.3.2 Simulation models and sensitivity analysis	18
3.4 Additional software	20
3.4.1 SOBEK.....	20
3.4.2 Other software	21
4 DATA PREPROCESSING AND SIMULATION	22
4.1 Generation of unstructured grid in DFM.....	22
4.2 Digital Surface Model (DSM – 5 meters)	23
4.3 Sources and sinks	25
4.4 Rainfall events.....	27

4.4.1	Rainfall events from Chicago design storm	27
4.4.2	Historical rainfall events.....	28
4.5	Simulation	29
4.5.1	Set-up of flood hazard model	29
4.5.2	Limitations.....	31
5	RESULTS AND ANALYSIS	32
5.1	Validation - Model 1: Rainfall event of August 2005, including the drainage system	32
5.2	Historical rainfall events	34
5.2.1	Model 2: Rainfall event of August 1997, including the drainage system	34
5.2.2	Model 3: Rainfall event of September 2013, including the drainage system	34
5.3	Rainfall events from Chicago hydrograph	35
5.3.1	Model 4b: Rainfall event of 1-year return period, including the drainage system	36
5.3.2	Model 5b: Rainfall event of 3-years return period, including the drainage system.....	37
5.3.3	Model 6b: Rainfall event of 5-years return period, including the drainage system.....	38
5.3.4	Model 7b: Rainfall event of 10-years return period, including the drainage system.....	39
5.3.5	Model 8b: Rainfall event of 50-years return period, including the drainage system.....	40
5.4	Effectiveness of the drainage system	41
5.5	Comparison of inundation maps after simulation in SOBEK and DFM	42
5.6	Effectiveness of the proposed flood reduction measures	44
5.6.1	Model 9: Rainfall event of 5-years return period including the drainage system and the development of water storage areas.....	44
5.6.2	Model 10: Rainfall event of 5-years return period including the drainage system and the increased drainage capacity in a single location.....	47
5.6.3	Model 11: Rainfall event of 5-years return period including the drainage system, the development of water storage areas and the increased drainage capacity in a single location.....	49
5.6.4	Model 12: Rainfall event of 5-years return period including the drainage system and the increased drainage capacity in multiple locations	50
6	DISCUSSION.....	52
6.1	Input data.....	52
6.2	Flood hazard maps.....	53
7	CONCLUSIONS AND RECOMMENDATIONS	54
7.1	Conclusions	54
7.1.1	Validation of model.....	54
7.1.2	Flood hazard maps and DSM	54
7.1.3	Flood hazard maps for the historical rainfall events.....	54
7.1.4	Comparison of 1D and 2D inundation model simulation.....	54
7.1.5	Effectiveness of drainage system	55
7.1.6	Effectiveness of flood reduction measures	55
7.2	Recommendations	55
	BIBLIOGRAPHY	57
	APPENDIX A: RAINFALL EVENTS	60
A.1	Rainfall events from Chicago design storm	60
A.2	Historical rainfall events.....	61
	APPENDIX B: SEWER SYSTEM IN SOBEK	65
B.1	Settings	65

B.2	Meteorological data.....	65
B.3	Schematization	66
B.4	Integration of rainfall in SOBEK	67
B.4.1	Assumptions	67
B.4.2	Calculation of runoff area.....	68
B.5	Output of SOBEK and connection with 2D model	69
APPENDIX C: RESULTS (EFFECTIVENESS OF THE DRAINAGE SYSTEM)		70
C.1	Model 4: Rainfall event with 1-year return period	70
C.2	Model 5: Rainfall event with 3-years return period	70
C.3	Model 6: Rainfall event with 5-years return period	70
C.4	Model 7: Rainfall event with 10-years return period	71
C.5	Model 8: Rainfall event with 50-years return period	71
APPENDIX D: MATLAB CODES.....		73
D.1	Preprocessing of surface elevation map	73
D.2	Generation of PLI and TIM files	75
APPENDIX E: FIELDWORK IN SHANGHAI.....		77
E.1	Correction of surface elevation map.....	77
E.1.1	Introduction – Definition of problems.....	77
E.1.2	Measurements – Correction of unrealistic values in DEM.....	79
E.2	Green areas in Jingan district	81
E.2.1	Environmental Theme Park of Suzhouhe Mengqing Garden.....	82
E.2.2	Jingan Park	85
E.2.3	Shanghai Rose Garden	86
E.2.4	Jingan Sculpture Park.....	86
E.2.5	Green areas across the road system	88
E.3	New buildings vs Old buildings	90
E.4	Flood event / Bad maintenance / Possible outlet locations	91
E.4.1	Flood event (6th September 2019)	91
E.4.2	Bad maintenance	92
E.4.3	Possible outlet locations	93
E.5	Expert Judgement.....	93
E.6	Questionnaire.....	94

LIST OF FIGURES

Figure 1: Economic losses in China during 2013 urban flood (Jiang et al. 2018)	1
Figure 2: Water system of Shanghai (Ke et al. 2018)	2
Figure 3: Hydrologic processes during an urban flood event (Awakimjan, 2015)	5
Figure 4: Pluvial flooding due to torrential rain in the United Kingdom (summer of 2007) (INTERMAP)	6
Figure 5: Sewer surcharge (Schmitt et al. 2004)	8
Figure 6: Approach for modelling a flooded urban drainage system (Mark et al. 2004)	8
Figure 7: Flow interactions between the overland flow (surface flow) and the sewer system (subsurface flow) (Chang et al. 2015)	9
Figure 8: Connection between a street and a pipe system (Mark et al. 2004)	10
Figure 9: 1D-1D modelling approach (left panel), Virtual storage on top of a manhole using MOUSE Pipe Flow software (right panel), (Henonin et al. 2013)	12
Figure 10: 1D-2D modelling approach (Henonin et al. 2013)	13
Figure 11: Digital Surface Model and Digital Terrain Model (PagerPower)	14
Figure 12: Rainstorm profile proposed by Sifalda (Van de Ven 2016)	15
Figure 13: Patterns of Sponge City and conventional management of urban pluvial flooding (Lashford et al. 2019)	16
Figure 14: Location of Shanghai and Jingan District (upper panels) (Google Maps), area of interest (lower panel) (Open Street Map in QGIS)	17
Figure 15: Location of Pudong and Longhua stations	19
Figure 16: Unstructured grid for Jingan District (left), zoom in area to illustrate the connection between streets and blocks (right) – grid resolution: 15 meters	23
Figure 17: Initial DSM (5 meters) interpolated for the area of interest (without negative values)	23
Figure 18: Final DSM (5 meters) interpolated for the area of interest	24
Figure 19: Average runoff discharges for rainfall events with return period of 1-year (top left), 3-years (top right), 5-years (middle left), 10-years (middle right) and 50-years (bottom)	26
Figure 20: DDF curves for rainfall duration between 5 and 180 minutes	27
Figure 21: Hydrograph for rainfall duration of 3 hours and 1, 3, 5, 10 and 50 years return periods	27
Figure 22: Rainfall hydrograph for August 2005, duration: 59 hours	28
Figure 23: Rainfall hydrograph for August 1997, duration: 41 hours	29
Figure 24: Rainfall hydrograph for September 2013, duration: 3 hours	29
Figure 25: Unstructured grid with 15 meters resolution for Jingan District, used for the simulation	31
Figure 26: DSM with 5 meters resolution, used for the simulation	31
Figure 27: Maximum inundation depths for the rainfall event of August 2005 (07/08 at 10:00:00)	32
Figure 28: Maximum inundation depths for the rainfall event of August 2005 (Meng et al. 2019)	33
Figure 29: Maximum inundation depths and most inundated areas for the rainfall event of August 1997 (19/08 at 9:00:00)	34

Figure 30: Maximum inundation depths and most inundated areas for the rainfall event of September 2013 (13/09 at 18:00:00)	35
Figure 31: Maximum inundation depth for the rainfall event of 1-year return period at 3:00:00 (including drainage system).....	36
Figure 32: Maximum inundation depth at 3:00:00 (left panel) and most inundated areas 2:00:00 (right panel) for the rainfall event of 1-year return period (including drainage system)	36
Figure 33: Maximum inundation depth for the rainfall event of 3-years return period at 2:55:00 (including drainage system).....	37
Figure 34: Maximum inundation depth at 2:55:00 (left panel) and most inundated areas 1:45:00 (right panel) for the rainfall event of 3-years return period (including drainage system)	37
Figure 35: Maximum inundation depth for the rainfall event of 5-years return period at 2:40:00 (including drainage system).....	38
Figure 36: Maximum inundation depth at 2:40:00 (left panel) and most inundated areas 1:40:00 (right panel) for the rainfall event of 5-years return period (including drainage system)	38
Figure 37: Maximum inundation depth for the rainfall event of 10-years return period at 2:25:00 (including drainage system).....	39
Figure 38: Maximum inundation depth at 2:25:00 (left panel) and most inundated areas 1:30:00 (right panel) for the rainfall event of 10-years return period (including drainage system)	39
Figure 39: Maximum inundation depth for the rainfall event of 50-years return period at 2:00:00 (including drainage system).....	40
Figure 40: Maximum inundation depth at 2:00:00 (left panel) and most inundated areas 1:25:00 (right panel) for the rainfall event of 50-years return period (including drainage system)	40
Figure 41: Water on street for the rainfall event of 5-years return period after the simulation in SOBEK	43
Figure 42: Maximum inundation depths for the rainfall event of 5-years return period, including the drainage system after the simulation in DFM	43
Figure 43: Modified DSM for model 9 including the water storage areas in the blocks	45
Figure 44: Maximum inundation depth for the rainfall event of 5-years return period including the drainage system, without the water storage areas at 2:40:00 (upper panel) and with the water storage areas at 3:00:00 (lower panel)	46
Figure 45: Maximum inundation depth for the rainfall event of 5-years return period including the drainage system, without the increased drainage capacity at 2:40:00 (upper panel) and with the increased drainage capacity at 2:30:00 (lower panel)	48
Figure 46: Maximum inundation depth for the rainfall event of 5-years return period including the drainage system, without the water storage areas and the increased drainage capacity at 2:40:00 (upper panel) and with the water storage areas and the increased drainage capacity at 3:00:00 (lower panel)	49
Figure 47: Maximum inundation depth for the rainfall event of 5-years return period including the drainage system, without the increased drainage capacity at 2:40:00 (upper panel) and with the increased drainage capacity at 1:55:00 (lower panel)	50

Figure 48: Rainfall hydrograph for August 1997 at Pudong station	61
Figure 49: Rainfall hydrograph for August 1997 at Longhua station	61
Figure 50: Rainfall hydrograph for September 2013 at Pudong station.....	62
Figure 51: Rainfall hydrograph for September 2013 at Longhua station.....	62
Figure 52: Selected simulation mode	65
Figure 53: Initial plan of pipeline network – manholes do not allow runoff.....	66
Figure 54: Final plan of pipeline network – manholes allow runoff.....	67
Figure 55: Calculation of the block surface area using QGIS	68
Figure 56: Schematic representation of blocks in the pipeline network.....	69
Figure 57: Maximum inundation depths for the rainfall event of 1-year return period, not including the drainage system (left panel), including the drainage system (right panel).....	70
Figure 58: Maximum inundation depths for the rainfall event of 3-years return period, not including the drainage system (left panel), including the drainage system (right panel).....	70
Figure 59: Maximum inundation depths for the rainfall event of 5-years return period, not including the drainage system (left panel), including the drainage system (right panel).....	70
Figure 60: Maximum inundation depths for the rainfall event of 10-years return period, not including the drainage system (left panel), including the drainage system (right panel).....	71
Figure 61: Maximum inundation depths for the rainfall event of 50-years return period, not including the drainage system (left panel), including the drainage system (right panel).....	71
Figure 62: Estimation of the width of the road in Jingan District using QGIS	77
Figure 63: Road in Jingan District	78
Figure 64: Elevated Roads in Jingan District (Mapcarta)	78
Figure 65: Elevated roads in Jingan District, Huashan Rd – Yan’an Middle Rd (top left panel), Weihai Rd – Yan’an Middle Rd (top right panel), Maoming N Rd – Yan’an Middle Rd (bottom left panel), Chengdu N Rd – Nanjing W Rd (bottom right panel).....	79
Figure 66: Locations of measurements across the elevated roads (Mapcarta).....	80
Figure 67: Locations of visited green areas (Mapcarta).....	82
Figure 68: Location of underground rainwater storage tank	83
Figure 69: Model for sewer treatment plant and rainwater storage tank.....	83
Figure 70: Pool and elevated water channel (left panel) and pumping system (right panel)	84
Figure 71: Elevated water channel and flow direction	84
Figure 72: Reservoir that collects the water from the elevated channel.....	84
Figure 73: Location of outfall to the Suzhou River for the water after purification	85
Figure 74: Sloped green area in Jingan Park.....	85
Figure 75: Flat green area in Jingan Park.....	86
Figure 76: Green space in Shanghai Rose Garden	86
Figure 77: Roof garden on the main building in Jingan Sculpture Park	87
Figure 78: Side view of the main building in Jingan Sculpture Park.....	87

Figure 79: Green areas in Jingan Sculpture Park	88
Figure 80: Green areas across the Nanjing W Road.....	89
Figure 81: Green area in Qinghai Road.....	89
Figure 82: Green areas across the Chengdu N Road.....	90
Figure 83: Elevated entrances in new buildings (upper panels) vs street level entrances in the old buildings (lower panels).....	91
Figure 84: Inundation in the campus of Shanghai Normal University.....	91
Figure 85: Stagnant water on top of inlets (Shanghai Normal University campus).....	92
Figure 86: Examples of inlets for the rainwater in Jingan District.....	92
Figure 87: Inlets and manholes across the river	93

LIST OF TABLES

Table 1: Summary of research strategy	4
Table 2: Overview of models for historical rainfall events	19
Table 3: Overview of models for rainfall events generated by Chicago hydrograph.....	20
Table 4: Overview of the models for flood reduction measures	20
Table 5: Overview of the input data	22
Table 6: Start, end and duration (hours) of historical rainfall events	28
Table 7: Set-up of time parameters	30
Table 8: Set-up of boundary conditions parameters.....	30
Table 9: Summarized results for models 4-8, including the drainage system	41
Table 10: Summarized results for models 4-8, without including the drainage system.....	42
Table 11: Reduction of maximum water depth in specific points	47
Table 12: Rainfall distribution over time	60
Table 13: Time series of rainfall event of August 1997 for Pudong and Longhua station.....	63
Table 14: Time series of rainfall event of September 2013 for Pudong and Longhua station	64
Table 15: Surface area of water storage areas as estimated in DFM.....	71
Table 16: Measured elevation, DEM and estimated elevation under the elevated roads	80

ABSTRACT

Shanghai is one of the numerous megacities worldwide that experience severe flood events triggered by torrential rainfall. To deal with the undesirable consequences of these events and mitigate the flood hazard, the research of flood reduction measures is necessary. In this effort, the hydrodynamic modelling is a useful tool.

In this master thesis a 2D model was developed for the simulation of urban flood events in Jingan District in the downtown of Shanghai. The main objectives of the thesis were the production of the flood hazard maps for numerous rainfall events and the assessment of the proposed flood mitigation measures. Delft3D Flexible Mesh was used as a tool to produce the inundation maps. Also, several data were considered regarding the grid for the numerical calculation, the surface elevation, the local drainage system and the rainfall events. SOBEK was used for the set up and the preprocessing of the sewer system. For the simulations, data from three historical rainfall events were used: August 2005, August 1997 and September 2013 and five rainfall events with return periods of 1, 3, 5, 10 and 50 years were generated by using the Chicago hydrograph.

For the validation of the model, the rainfall event of August 2005 was used. Although the validation of the model was not proven due to the simplifications that were made in the input data and the lack of data, the model showed that some processes can be simulated, and inundation maps can be produced. By comparing the results that occur with and without the inclusion of the drainage system, it was concluded that the local drainage system should be included in the analysis for the assessment of the flood hazard in an urban area, since its presence plays an important role in the flood reduction. The results showed that the maximum inundation depth can decrease by around 45%. As flood reduction measures, the creation of water storage areas and the increase of the drainage capacity were considered. The water storage areas covered around 10%, or less, of the block areas with available space, leading to a water depth reduction that depends on the location in the map. For the increase of the drainage capacity, the value of $1 \text{ m}^3/\text{s}$ was assigned in a single and in multiple locations in a specific area of investigation. The results showed a percentage of water depth reduction around 15.9% and 45.5%, respectively. For the same location the percentage of water depth reduction due to the water storage areas was 22.5%.

Finally, uncertainties were introduced in the model due to the assumptions and the simplifications that were made in the input data. However, this model can work as a base for future researches to accomplish more realistic results, by improving the current model and adding more updated and precise data.

ACKNOWLEDGEMENTS

This research was performed under the guidance and supervision of professor Jeremy Bricker, professor Frans van de Ven and researcher Qian Ke. I would like to express my gratitude to all of them for their advices, insightful comments and encouragement during these months. It has been a pleasure for me to work under their guidance and gain from their experience.

I would like to thank professor Jiahong Wen and his team in Shanghai Normal University for supporting our fieldwork investigation in Shanghai during September of 2019, by providing an ideal studying place and useful guidance. The knowledge I gained during the fieldwork helped me in conducting my research.

I am also grateful to the Bakala Brothers Foundation for the funding I received to undertake my postgraduate studies during years 2017-2019.

Additionally, I would like to thank all my fellow students at TU Delft, who I met during my postgraduate studies. They played an essential role in enjoying my research experience and improving my social life.

I am also extremely grateful to my girlfriend Fotini for being always by my side. Her understanding, encouragement and love helped me to overcome all the difficult moments and accomplish my goal.

Finally, I would like to thank my father, my mother and my brother, who always support and encourage me and never stop believing in me.

*Athanasios Kallioras
Delft, February 2020*

1 INTRODUCTION

1.1 Background

In this chapter, the background of the problem that was investigated in this master thesis is presented.

1.1.1 Floods in urban areas and China

In recent years, many coastal mega-cities globally have suffered exposure to flood events caused by torrential rainfalls. According to environmental surveys, these events are triggered by the effects of global warming and climate change, the origin of which is imputed to urbanization (Yuan et al. 2017). In particular, the direct consequences of global warming such as the heating up of the earth and the sea level rise, lead to the rise of the likelihood of occurrence of heavy rainfall events, especially in areas located near the sea (Yuan et al. 2017). This growing number of torrential rainfall events leads to increasing risks regarding urban pluvial flooding, thus putting the urban safety into peril (Yuan et al. 2017).

China is one of the countries that encounter severe flooding events that have become more intense in metropolitan regions, endangering their development concerning societal and economic issues (Jiang et al. 2018). The origins of these pluvial flooding disasters are pinpointed to factors such as climate change, extensive urbanization and the combined effect of management failure and unsustainable development of the urban areas. According to a study of the Ministry of Housing and Urban Rural Development (MHURD), during the period 2008-2010, 351 cities were investigated and it was found that 62% of them were exposed to urban pluvial flooding whereas 39% of them faced with flooding more than three times (Jiang et al. 2018). Also, over the last years the cities of China that have been affected by floods are almost twice the number of those before 2008. Urban pluvial flooding events led to property damages, hampering the economic activities and therefore causing serious societal problems in the country. The flash flood in Beijing in 2012, that affected 1.6 million citizens and caused around US\$1.6 billion direct economic losses and the big floods across the South and North boundaries of China in 2016, that impacted 60 million citizens and costed approximately US\$44.7 billion, are two examples of urban pluvial flood disaster in China (Jiang et al. 2018). Another urban pluvial flood event in China happened in 2013 that resulted in economic losses as shown in Figure 1 (Jiang et al. 2018).

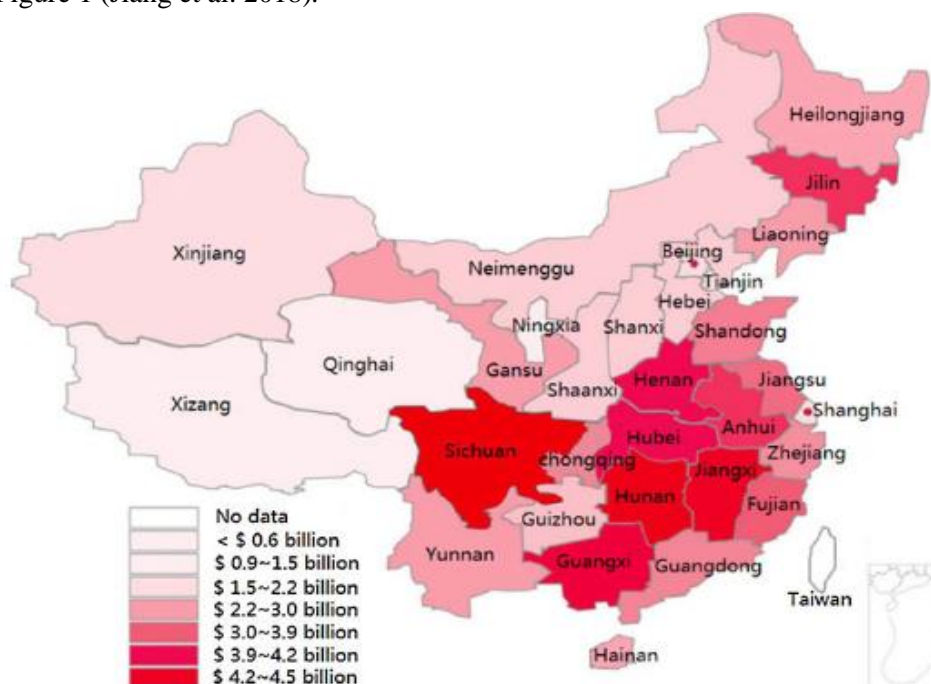


Figure 1: Economic losses in China during 2013 urban flood (Jiang et al. 2018)

1.1.2 Floods in Shanghai

Shanghai lies on the Asian Continent's eastern coastal line, at 31° 14' north latitude and 121° 29' east longitude (Shanghai Municipal People's Government), facing the Pacific Ocean. It is placed in the middle of China's east coast and it is one of the largest cities worldwide bordering the sea. In particular, the city is situated in the eastern edge of the Yangtze River Delta and its total coverage area is 6340 km² (Yuan et al. 2017). Shanghai is enclosed by water, since in the north it is bordered by the estuary of Yangtze River, in the east by the East China Sea, in the south by the Hangzhou Bay and in the west by the Tai Lake. Also, the city is crossed by the last tributary of Yangtze River named Huangpu River. This tidal river has its origins in the Tai and Dianshan Lakes and runs from the west to the east while in the midway it changes direction from south to east (Ke et al. 2018). Due to its advantageous geographical features, Shanghai is considered the world's largest port and a global financial and commercial center. Its geographic location and its water system are depicted in Figure 2 (Ke et al. 2018).



Figure 2: Water system of Shanghai (Ke et al. 2018)

However, Shanghai is a city that experiences the hostile consequences of global warming (Yuan et al. 2017). Due to the combination of its geographic location and its flat and lowland area, and the effects of land subsidence and climate change, Shanghai is prone to flood events (Ke et al. 2018). In particular, the downtown area of Shanghai is vulnerable to three different types of flooding events which may take place during the typhoon season: coastal flooding caused by storm surge, fluvial flooding due to the insufficient flood protection system across the Huangpu river and urban pluvial flooding caused by extreme rainfall events and deficient drainage system (Sutter V. 2019). These flood events endanger the city's social advancement and economic sustainability, whereas in extreme situations they cause loss of life and severe economic damages. A conservative study states that the annual risk is expected to cause 2000 fatalities per year and cost US\$73 million damages per year, while a more optimistic view claims that the flood risk is estimated at US\$63 million per year with a protection level of 1/1000 per year (Ke 2014). Thus, to mitigate the undesirable situations of loss of life and economic damage, it is urgent to develop the proper measures against floods in urban areas. To achieve this, the hydrodynamic modelling plays a crucial role.

1.2 Research description

In this chapter the grounds for the research are described by introducing the research problem. Also, the main research objective, the scope and the strategy of the thesis are formulated.

1.2.1 Research problem

As stated in the introduction, there is an increasing need for implementation of management strategies against storm water events to diminish the flood hazard in urban areas. To achieve this, flood hazard maps are useful and essential tools that provide the local authorities with adequate information with respect to the vulnerability and the exposure of the area of interest to flood events (WMO 2008). For this reason, the simulation of flood events originating from past torrential events and from forecasted rainfall events with diverse return periods is of great importance. In this case, the hydrodynamic models are called up, since they are considered solid tools regarding this topic. More specific, the numerical simulation of urban floods plays a major role when dealing with the design and planning of urban drainage systems and enables the research of effective management and control strategies against urban flood disasters. However, in contrast to the development of models for coastal and river flooding simulations, urban flooding models are not yet fully developed because of the complexity of the flow in urban areas when inundation occurs (Fan et al. 2017; Mark et al. 2004). Considering all the above, in the context of this master thesis, the problem under investigation was the estimation of the flood hazard maps triggered by torrential events with diverse return periods and the assessment of potential measures to mitigate the current and future flood problems in Jingan District, an urban area in the downtown of Shanghai. To achieve this, an additional problem was the development of a 2D urban flood model for the specific area of Shanghai, that would enable the production of the inundation maps.

1.2.2 Research objective

The research objective of this master thesis was to quantify the flood hazard and to investigate to what extent the proposed measure(s) could reduce the hazard due to pluvial flooding in the downtown area of Shanghai. The focus was mainly given in deriving the inundation characteristics (hazard maps) and proposing and implementing those measures that reduce in the most efficient way the inundation depths that are caused by rainfall events with diverse return periods.

To attain the main objective of the study, the analysis of the research problem was divided into subsections to have a better monitoring of the different tasks that arise during the study. Answering the questions of each subsections would lead gradually to the final objective. To that end, the following steps were followed:

- to develop a 2D model for the simulation of urban flooding in Jingan District by integrating the sewer system
- to produce the inundation maps for historical rainfall events and rainfall events with diverse return periods.
- to make recommendations on flood hazard reduction measures
- to evaluate the effectiveness of these measures

1.2.3 Scope

Although Shanghai is a city prone to three different types of flooding: coastal, fluvial and pluvial, the scope of this research was focused only on the rainfall induced flooding in the downtown area of the city.

1.2.4 Research strategy

The research strategy in this thesis was based on a sequence of steps representative of the tasks that led to the main objective. Firstly, to be able to simulate an urban flood event and obtain results close to the real situation, it is crucial to possess precise and up to date data. These are usually referring to digital surface model (DSM), land use map, drainage capacity, sewer (pipeline) system and recorded rainfall events. Within the context of this thesis a variety of data was provided. These are analyzed in chapter 4.

For the calculation of the flood hazard the hydrodynamic simulation program D-Flow Flexible Mesh (D-Flow FM) was used, which is part of the Delft3D Flexible Mesh Suite. This module is one of the numerous

modelling suites developed by Deltares¹ and enables the 1D, 2D and 3D computations in coastal, river and estuarine areas (Deltares 2019a). This module allows the combination of unstructured grids consisting of geometries from triangles to hexagons and leads to modelling the flow in a more realistic way. In the present study, an unstructured grid was created in DFM by combining curvilinear and triangular shapes to optimize the accuracy of the results.

The provided data were combined with the developed unstructured grid to simulate the flood. However, a preprocessing of these data was required before they could serve as inputs in DFM. To that end, the DSM was processed by using the QGIS and DFM software, while the flow in the pipeline system was simulated in SOBEK. SOBEK is also an integrated software package that was developed by Deltares and is suitable for river, urban and rural management (Deltares 2018). Regarding the rainfall events, different return periods were used for the generation of rainfall events from the Chicago hydrograph and three historical rainfall events were provided.

The obtained results from the model in DFM were geo-referenced and they were related with the DSM grid through a common coordinate system. The post processing of the results was performed in DFM. This enabled to visualize the results as inundation maps, based on the values of the water levels that were calculated by the simulation process.

According to these maps, the recommendation of some measures was made, structural and non-structural, to be implemented in locations that would mitigate the flood hazard of the most inundated areas. These measures were integrated in DFM and the simulation of the flood event followed the same steps, to reproduce the inundation maps that correspond to the specific return period of the rainfall event. A summary of the research strategy is presented in Table 1.

Table 1: Summary of research strategy

Phases	Tasks
1	<ul style="list-style-type: none"> <i>a.</i> Identification of research problem <i>b.</i> Formulation of research objectives and questions
2	<ul style="list-style-type: none"> <i>a.</i> Grid generation in DFM <i>b.</i> Preprocessing of data through QGIS, SOBEK, DFM <i>c.</i> Design of rainfall distribution due to return period
3	Production of inundation maps (flood hazard maps)
4	Proposal and implementation of flood hazard reduction measures in the 2D model
5	<ul style="list-style-type: none"> <i>a.</i> Study on the effectiveness of the measures <i>b.</i> Discussion of the results

¹ Deltares is an independent institute of applied research in the field of water and subsurface (Deltares 2018).

2 LITERATURE REVIEW

In this chapter, the literature review of this thesis is presented. The literature review consists in information regarding the hydrologic processes during an urban flood event, the types of flooding, the operation of the urban drainage system, the conditions of flooding and surcharge, the urban flood modelling, the digital surface models, the design of storms and the potential flood reduction measures.

2.1 Hydrologic processes during urban flooding

After a rainfall event, the water that falls on the surface has three possible routes to follow. In particular, the precipitated water can become underground by infiltrating into the soil, return to the atmosphere through the process of evaporation, be absorbed by the plants through transpiration or become runoff on the surface (Butler & Davies 2011). However, in urban areas the situation is more complex since the construction of roads and buildings makes the surface more impermeable than in the situation without human intervention. This can be translated as a decrease of the infiltration capacity of the surface and an increase in the water volume of the surface runoff (Butler & Davies 2011). During an urban flood event various hydrologic processes take place. These processes and the way they interact with each other are depicted in Figure 3 (Awakimjan, 2015).

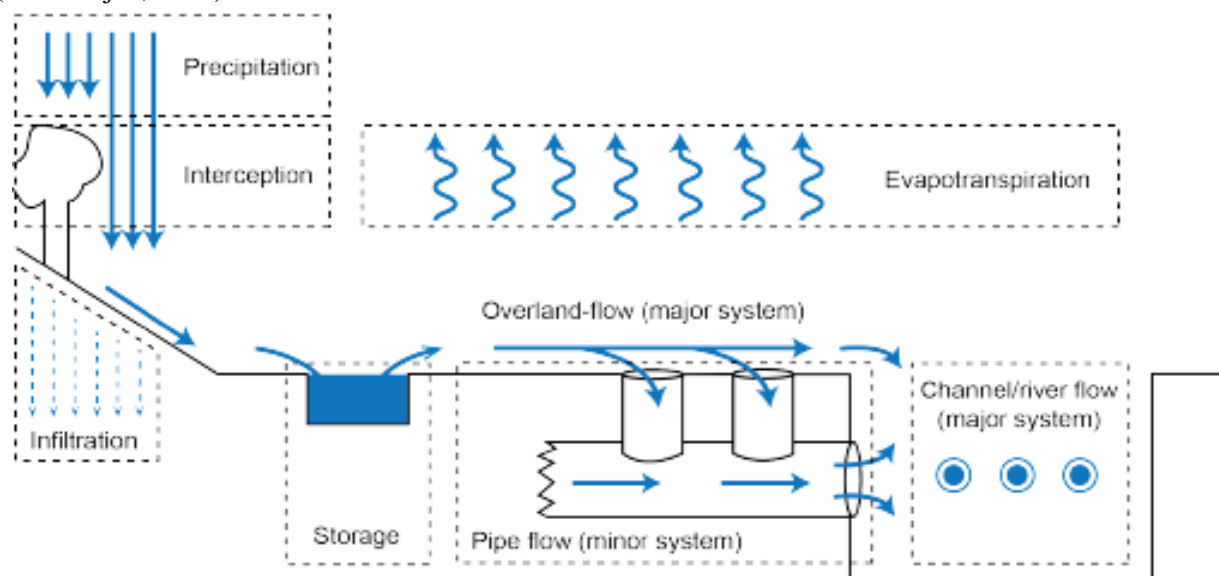


Figure 3: Hydrologic processes during an urban flood event (Awakimjan, 2015)

2.2 Types of flooding

The origins of flood events may be attributed to diverse reasons, but in this study the three more relevant types regarding the environment of urban areas are highlighted. These types of flooding are described shortly below:

Coastal flooding (Surge flood)

This type of flooding takes place in areas that are situated on the shoreline of an ocean, sea or other sizeable body of water. It is triggered by extreme conditions originated from severe weather conditions and its major cause is the storm surge which is usually associated with the high winds of hurricanes that pile water onshore. Also, this flood is related to situations where water intrudes into the low-lying inland areas and causes loss of life, loss of property and severe damage to the structures of the urban area (INTERMAP).

Fluvial flooding (River flood)

Fluvial flooding occurs when a torrential rainfall event lasts for a very long period causing the water level of a river or channel to rise over the crest of the river's bank. In other words, the river's capacity is exceeded. Other events that trigger fluvial flooding are ice jams and melt of heavy snow. Fluvial flooding in an upstream location of a river affects the more downstream rivers and causes breaking of dikes and dams. Also, it leads the water to spread and inundate the nearby low-lying dry lands. The degree to which a fluvial flood is severe is determined by a series of contributing factors such as the volume of the precipitated water in the area, the accumulation rate of the precipitation, the recent saturation of the soil and the nature of the terrain that the river system is surrounded by (INTERMAP).

Pluvial flooding (Surface flood)

Pluvial flooding or surface water flood occurs when an extreme rainfall event causes flood event irrespective of the overflowing body of water. One of the mistakes regarding flood risk events is that the level of risk is fully related to the distance from the body of water. However, pluvial flooding is a characteristic example of the opposite, since it can take place in urban areas that lie in higher elevations than the coastal or river low land areas. This type of flooding may be divided into two categories, according to the reason of their occurrence:

- A torrential rainfall exceeds the capacity of the urban drainage system, driving the water to flow out and inundate the streets and the nearby structures.
- A rainfall event occurs in an area of hillsides that reaches its infiltration capacity and the water starts runoff towards the urban area.

It is also common for pluvial flooding to occur together with events of riverine and coastal flooding and even though it may result in inundation depths of a few centimeters, it may cause considerable damage in properties (Figure 4) (INTERMAP).



Figure 4: Pluvial flooding due to torrential rain in the United Kingdom (summer of 2007) (INTERMAP)

Also, in urban areas it is quite common that the inlets of the drainage system may be clogged by trash and soil and eventually hamper the flow of the incoming water. In this way the pipe network becomes surcharged and therefore the flood events in the low-lying areas of the catchment become more and more intense.

2.3 Urban drainage system

The main purpose of the urban drainage systems is twofold. On one hand it is designed to gather the wastewater and stormwater and transport it out of the limits of the urban area, while on the other it act as a closed system that conveys efficiently and rapidly the excessive volume of the surface runoff of the urban area, contributing to the elimination of the phenomenon of ponding. Generally, the urban drainage systems may be divided into two categories. The one corresponds to the artificial systems that allow the storm water to be transported through a closed pipeline system (minor system). This system may or may not has the capacity to contain the wastewater coming from the urban areas. The other system (major system) consists in infiltration trenches and soak ways and corresponds to a more water sensitive and natural way of drainage. This system relies on the properties of semi-natural materials regarding their storage and infiltration capacities (Butler & Davies 2011). Also, the overland flow is considered part of the major system.

Overland flow or surface runoff (major system)

The overland flow or surface runoff is one of the most important components of the water cycle. It represents the excess storm water or melt water that flows over the surface of the earth. This flow originates in case of either the soil has reached its infiltration capacity, or the precipitation rate is higher than the ability of the soil to absorb the water. The latter is highly influenced by the existence of other impervious surfaces in the surrounding area such as pavements and roofs of the buildings that send their runoff to the adjacent soil surface. Also, the surface runoff is the primary factor that causes soil erosion (Beven 2004).

Sewer system (minor system)

In the category of the minor drainage system, the sewerage system possesses the primary place. This system is constituted by a network of pipes and conduits that collect water from the components of the urban area (houses, streets, parks). Later, this volume of water is transported to the elements of the major system like the rivers and the channels (Awakimjan, 2015).

The artificial drainage system or sewer system can be separated into two types depending on the source of water (Butler & Davies 2011). A short description of these types is presented below:

- Combined system: the flow of stormwater and wastewater takes place in a single pipeline network.
- Separate system: stormwater and wastewater flow in two distinct and separate pipeline networks.

Besides these two types of piped system, in some urban areas hybrid (partially separated) systems are used in which stormwater and wastewater flow in a system that part of the pipeline network is combined and part of it is separated. Also, hybrid systems may exist due to the inclusion of an old part of a combined system in a new separated system or due to wrong connections.

2.4 Flooding in urban drainage systems

As stated in European Standard EN 752 (2008), "flooding" is defined as the "condition where wastewater and/or surface water escapes from or cannot enter a drain or sewer system and either remains on the surface or enters buildings" (Schmitt et al. 2004). Flood events may take place in both rural and urban areas, however these events are of greater importance in urban areas. This is because the possibilities of more damages and loss of lives is higher since people tend to move in urban areas.

2.5 Surge in urban drainage systems

Contrary to the situation of flooding, "surcharge" is the "condition in which wastewater and/or surface water is held under pressure within a gravity drain or sewer system but does not escape to the surface to cause flooding" (Schmitt et al. 2004). In extreme cases the water level inside the sewer system rises to the

surface level. At this point the water either escapes to the surface or prevents the surface water to enter the sewer system. The stages of surcharge of the sewer system are illustrated in Figure 5 (Schmitt et al. 2004).

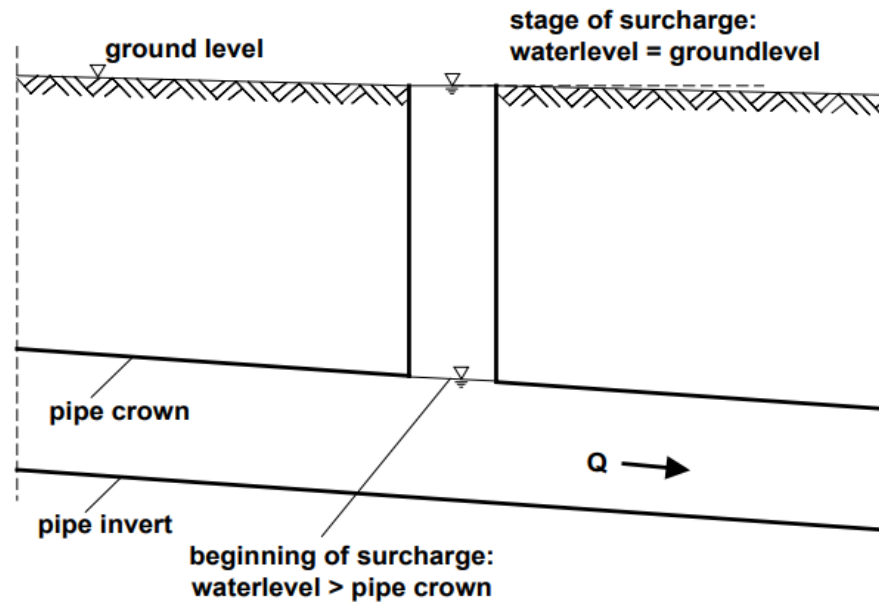


Figure 5: Sewer surcharge (Schmitt et al. 2004)

2.6 Simulation of urban flooding

Within the field of modelling the urban drainage system, the models that cover the hydrological and hydraulic features of the system are of great importance. The first concerns the estimation of the rainwater that represents the free surface flow on the streets and acts as an input rate for the sewer system, while the second focuses on the behavior of the water flow on the street and the sewerage pipe network regarding the depth and the flow rates (Butler & Davies 2011; Mark et al. 2004). When dealing with the modelling of urban drainage systems, there is a discrimination between the hydrological and hydraulic processes. An approach regarding the interaction between the two systems for a flooded drainage system in an urban area is depicted in Figure 6 (Mark et al. 2004).

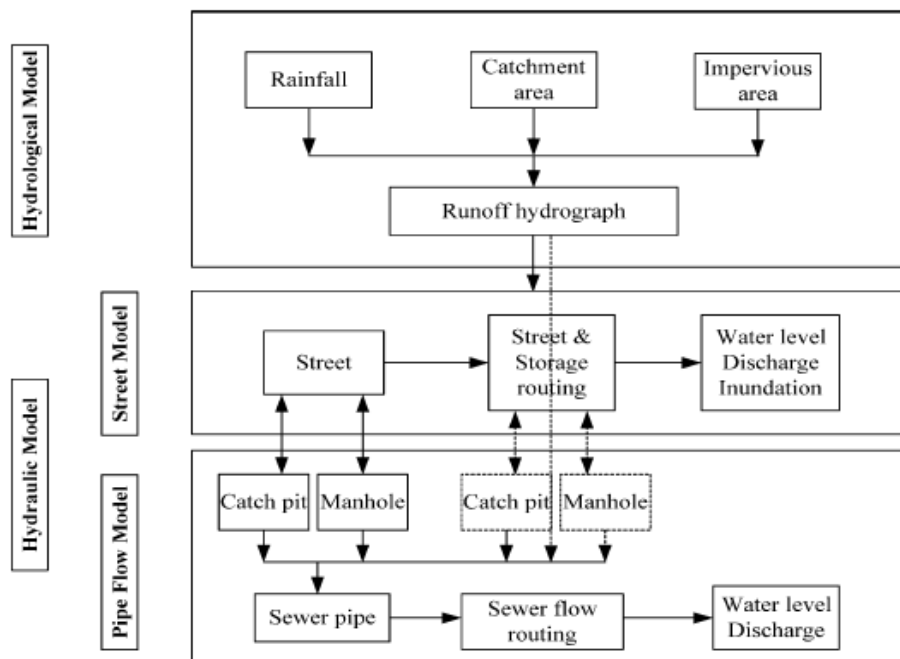


Figure 6: Approach for modelling a flooded urban drainage system (Mark et al. 2004)

2.6.1 Hydrological models

The main purpose of hydrological models is to convert the rainfall into runoff (Butler & Davies 2011). This can be accomplished by surface runoff models such as the linear reservoir model (Mark et al. 2004), which use a group of hydrological parameters to describe the features of a catchment area, compute the surface runoff hydrograph for each sub-catchment and quantify the volume of water that eventually enters the sewer system (Henonin et al. 2013; Mark et al. 2004).

The basis of these models is related to data and not physical processes (Henonin et al. 2013) and the resulted runoff hydrographs are usually used as an input in the hydrodynamic models for the simulation of the flow in the drainage network of an urban area, the street and pipe systems (Mark et al. 2004). Several software of hydrodynamic modelling provides the user with an option related to rainfall and runoff (Henonin et al. 2013).

2.6.2 Hydraulic model (dual drainage model)

The urban drainage system is modelled as two interlinked network systems that are dynamic. This model is called dual drainage system (Boonya-Aroonnet et al. 2007). The concept of dual drainage model means that the urban drainage system is composed by two separate components: the surface and the subsurface system (Schmitt et al. 2004). As stated earlier, the first is the 'major system' that includes the flow in the streets, ditches and in other artificial or natural channels, while the second system is named the 'minor system' and is referring to the flow through the sewer pipe network (Mark & Drordjević 2006). The flow interactions between the major and minor systems are depicted in Figure 7 (Chang et al. 2015).

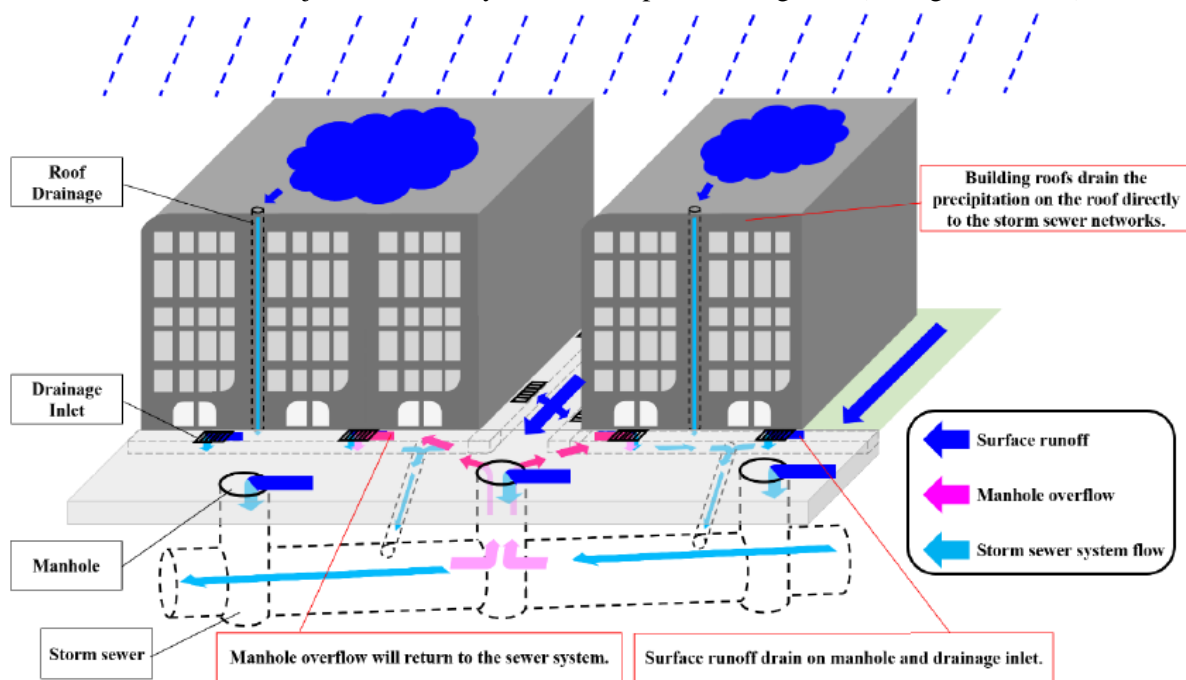


Figure 7: Flow interactions between the overland flow (surface flow) and the sewer system (subsurface flow) (Chang et al. 2015)

These two networks describe the path of the rainfall-runoff both on the surface and in the pipeline system. Flow exchanges between these two systems are achieved through the manholes. In particular, the water that flows on the surface of the street system can enter the pipe network by entering the manholes and gullies. Also, the opposite may occur, to wit, water can flow out of the pipe system and inundate the street network. The connection between a street and a pipe system through manholes or catch pits is illustrated in Figure 8 (Mark et al. 2004).

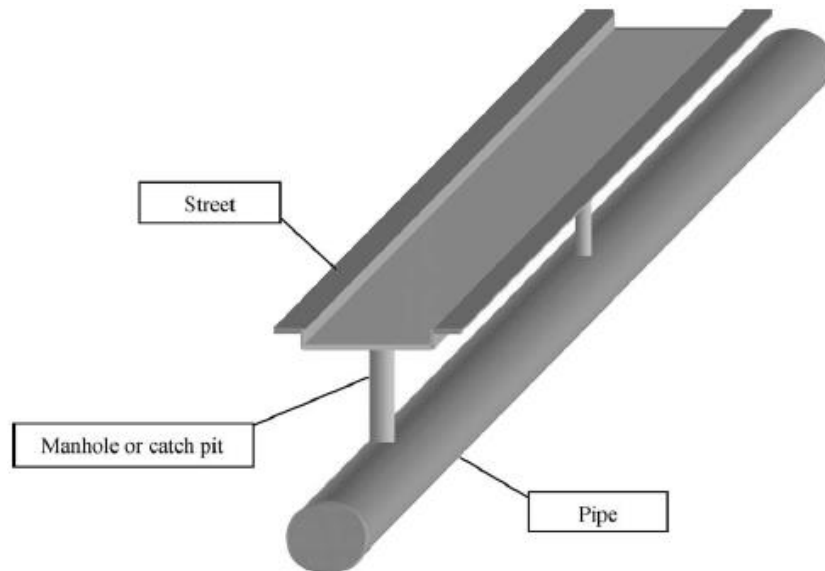


Figure 8: Connection between a street and a pipe system (Mark et al. 2004)

2.6.2.1 Saint-Venant equations

The behavior of the unsteady water flow is described by the Saint-Venant equations. However, these equations can be applied under the following assumptions (Deltares 2018; Butler & Davies 2011):

- one-dimensional flow: the velocity distribution at the cross section of the channel can be described by uniform flow and the water level is assumed horizontal
- hydrostatic pressure distribution: small streamline curvature and negligible vertical accelerations
- friction losses and effects of turbulence for equations of steady flow are valid in conditions of unsteady flow
- small slope of the channel bed

1D Saint-Venant equations

For the simulation of the hydrodynamic behavior of the flow in a piped drainage network (sewer system), the 1D model is considered the most suitable tool. This can be explained by the fact that for a channeled water flow situation, the 1D flow characteristics are relevant (Henonin et al. 2013). The Saint-Venant 1D flow equations are (Deltares 2018):

Continuity equation (1D):

$$\frac{\partial A_T}{\partial t} + \frac{\partial Q}{\partial x} = q_{lat}$$

where: A_T (m^2): total cross-sectional area of the channel (flow area plus storage area), Q (m^3/s): flow discharge, q_{lat} (m^2/s): lateral flow discharge per unit length (inflow conditions: $q_{lat} > 0$, outflow conditions $q_{lat} < 0$).

Momentum equation (1D):

$$\frac{\partial Q}{\partial t} + \frac{\partial}{\partial x} \left(\frac{Q^2}{A_F} \right) + g \cdot A_F \cdot \frac{\partial h}{\partial x} + \frac{g \cdot Q \cdot |Q|}{C^2 \cdot R \cdot A_F} - w_f \cdot \frac{\tau_{wind}}{\rho_w} = 0$$

where the terms describe:

- 1st term → inertia
- 2nd term → convection
- 3rd term → gradient of water level
- 4th term → bed friction
- 5th term → influence of wind force

and: Q (m^3/s): flow discharge; t (s): time; x (m): distance in the longitudinal direction of the channel; A_F (m^2): flow area; g (m/s^2): gravitational acceleration; h (m): water level; C ($m^{1/2}/s$): Chézy coefficient; R (m): hydraulic radius; w_f (m): width of water surface; τ_{wind} (N/m^2): shear stress of wind; ρ_w (kg/m^3): fresh water density

2D Saint-Venant equations

For the simulation of the overland flow, a 2D model is usually the most suitable tool to be applied since it solves the Saint-Venant 2D flow equations. The Saint-Venant 2D flow equations are (Deltares 2018):

Continuity equation (2D):

$$\frac{\partial h}{\partial t} + \frac{\partial(h \cdot u)}{\partial x} + \frac{\partial(h \cdot v)}{\partial y} = 0$$

where: u (m/s): velocity in the x direction; v (m/s): velocity in the y direction; h (m): water level; x (m): primary direction of the flow; y (m): direction of the flow perpendicular to x

Momentum equation (2D):

$$\begin{aligned} \frac{\partial u}{\partial t} + u \cdot \frac{\partial u}{\partial x} + v \cdot \frac{\partial u}{\partial y} + g \cdot \frac{\partial h}{\partial x} + g \cdot \frac{u \cdot |\vec{u}|}{C^2 \cdot h} + \alpha \cdot u \cdot |u| &= 0 \\ \frac{\partial v}{\partial t} + u \cdot \frac{\partial v}{\partial x} + v \cdot \frac{\partial v}{\partial y} + g \cdot \frac{\partial h}{\partial y} + g \cdot \frac{v \cdot |\vec{u}|}{C^2 \cdot h} + \alpha \cdot v \cdot |v| &= 0 \end{aligned}$$

where the terms describe:

- 1st terms → acceleration
- 2nd, 3rd → convection
- 4th → horizontal pressure gradient
- 5th → bottom friction
- 6th → wall friction

and: u (m/s): velocity in the x direction; v (m/s): velocity in the y direction; $|\vec{u}|$ (m/s): magnitude of velocity ($= \sqrt{u^2 + v^2}$); h (m): water level; x (m): primary direction of the flow; y (m): direction of the flow perpendicular to x ; C ($m^{1/2}/s$): Chézy coefficient; α ($1/m$): coefficient of wall friction

2.6.2.2 1D/1D and 1D/2D models

At present, there is a limited number of studies that deal with the modelling of urban flooding by combining the flow both in the pipe network system and on the surface (Mark et al. 2004). In general, the modelling of a dual drainage system can be described by two different combinations of model system. The first combines the use of a 1D model for the flow in the sewer network and a 1D model for the overland flow, whereas the second model combines the 1D model for the minor system, but it uses the 2D model for the simulation of the flow in the major system.

1D/1D model

According to 1D/1D model, the flow behavior in both the minor and the major system is described by the 1D Saint-Venant equations. In terms of a schematic configuration, this model can be understood as a 1D model that represents the path of the overland flow on top of a 1D model for the flow in the sewer network. The flow exchanges between these two systems are accomplished by interconnections such as manholes and catch pits (Henonin et al. 2013; Mark et al. 2004). One example of the 1D/1D approach of modelling an urban drainage system is depicted in Figure 9 (left panel) (Henonin et al. 2013).

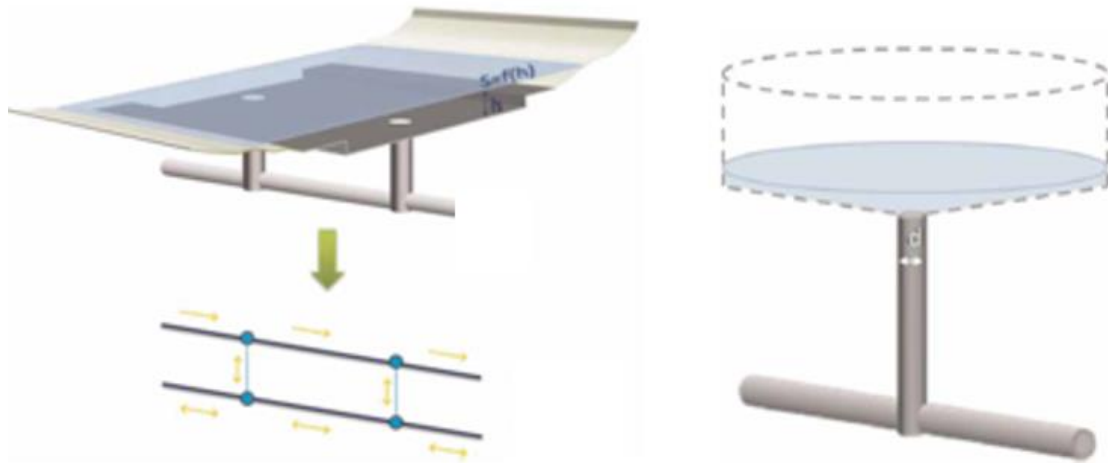


Figure 9: 1D-1D modelling approach (left panel), Virtual storage on top of a manhole using MOUSE Pipe Flow software (right panel), (Henonin et al. 2013)

Urban flooding has been treated as a one-dimensional (1D) problem by a few case studies. According to Mark et al. (2004), some of these studies are: Bangkok in Thailand (Boonya-Aroonnet et al. 2002), Dhaka in Bangladesh (Mark et al. 2001) and Playa de Gandia in Spain (Tomicic et al. 1999). Some examples of software that are used for building models of the drainage system are MOUSE, InfoWorks and MIKE.

However, there are limitations of the 1D/1D modelling approach. Firstly, the 1D model is a suitable tool for the representation of the flow in the streets when the flow is considered channeled. But, when the surface flow leaves out of the limits of the streets, then the flow stops being channeled and therefore this approach should not be used for the surface flow (Henonin et al. 2013; Allit et al. 2009). The amount of water that leaves the streets is modelled by using storage functions, but in this case, data is required regarding the land use and infiltration capacity of the terrain (Mark et al. 2004).

Also, as stated in a previous subchapter, the 1D/1D models are valid for the situation of an underground piped drainage system, but to deal with the problem of the overland flow a series of simplifications can be made. One example of this approach is the concept of virtual storage on the top of the manholes, as depicted in Figure 9 (right panel) (Henonin et al. 2013). However, even though this method can be used to estimate the location of potential overflow event, eventually it leads the researcher to an overestimation of the water depth of the overland flow (Boonya-Aroonnet et al. 2002; Mark et al. 2004).

1D/2D model

In contrast to the 1D/1D model, the 1D/2D model solves the 2D Saint-Venant equations for the overland flow. The concept of the 1D/2D modelling approach is depicted in Figure 10 (Henonin et al. 2013).

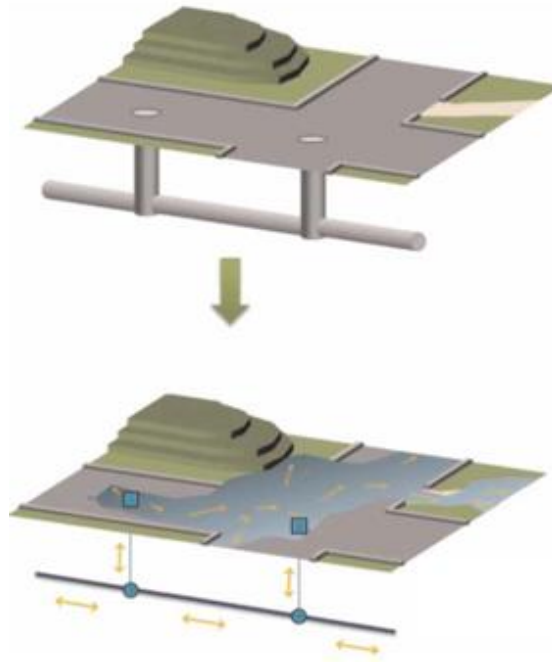


Figure 10: 1D-2D modelling approach (Henonin et al. 2013)

This approach enables the researcher to reproduce the surface topography of an urban area and to simulate the flow across the whole area of interest by giving results regarding the water depths and the velocities with components in two directions (Henonin et al. 2013). Examples of studies related to urban flood that use this coupling modelling approach have been conducted by Schmitt et al. (2004), Mark and Drordjević (2006) and Carr and Smith (2006) and the software packages that enable this are InfoWorks and MIKE FLOOD (Henonin et al. 2013).

This accuracy is highly dependent on the size of the model grid and the resolution of the available topographical data. Especially for applications in an urban environment the use of a fine 2D grid is necessary since a proper analysis would require information regarding the location of the buildings and trees. Apart from a detailed grid size, a high resolution of the topographical data is also important for the computation of the flood with an improved resolution. However, due to the fine grid and the high resolution the computational time becomes longer, making the 2D models useless for the simulation of real-time systems. Moreover, a 2D model allows the user to simulate rainfall events on a 2D grid, but it's not suitable for the representation of the flow in an underground piped drainage system (Henonin et al. 2013).

2.7 Digital Elevation Model (DEM)

Digital Elevation Models (DEMs) are raster grids that represent the earth's surface elevation referenced to a certain vertical datum such as the mean sea level. These models are created by measuring the earth's elevation at either regular or irregular points (PagerPower; GISGeography). Among the various areas of application, DEMs can be used for the modelling of the water flow which is investigated in this study. However, DEMs can be divided into Digital Surface Models (DSMs) and Digital Terrain Models (DTMs). The former is used for the representation of the earth's surface including all the objects placed on top of it like buildings, plants, etc., while the later represents the elevation of the bare ground. The difference between the two models is illustrated in Figure 11 (PagerPower).

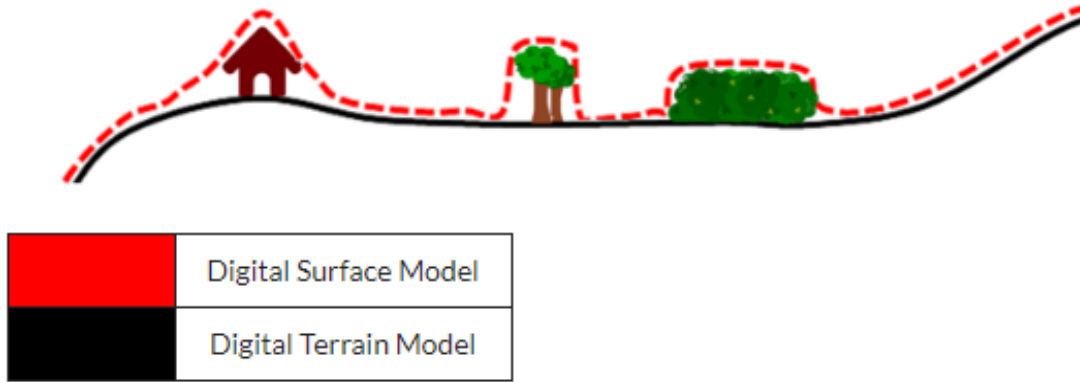


Figure 11: Digital Surface Model and Digital Terrain Model (PagerPower)

2.8 Design storms

The calculation of the designed flow for the pipeline network of a drainage system is based on the design of the rainfall hyetograph. This hyetograph represents graphically the distribution of the rainfall intensity as a function of time in the designed phase (Xie et al. 2017).

For the design of sewer systems, Chow and Kelfer introduced the Chicago design storm in 1957 (Van de Ven 2016). This method is based on a rainstorm intensity formula. For China, this equation is (Xie et al. 2017):

$$q = \frac{167 \cdot A_1 \cdot [1 + C \cdot \log(P)]}{(t_d + b)^n}$$

where: q ($L/s \text{ ha}$): rainfall intensity; P (–): return period of designed rainfall; t_d (min): rainfall duration; A_1, C, b and c : local parameters estimated by statistical method

For Shanghai, the proposed rainstorm intensity formula is based on maximum data taken from the meteorological stations in the downtown area of Shanghai in the past 64 years.

The local parameters are:

$$A_1 = 9.851, \quad C = 0.846, \quad b = 7.0 \quad \text{and} \quad n = 0.656$$

and the rainstorm intensity equation becomes:

$$q = \frac{1600 \cdot [1 + 0.846 \cdot \log(P)]}{(t_d + 7.0)^{0.656}}$$

Based on this rainstorm intensity formula, the rainfall depth-duration-frequency (DDF) curves can be generated. These curves describe the precipitation depth as a function of the duration of the rainfall event for different return periods.

For the calculation of the hydrograph, the following equations (Wang et al. 2018) are used:

$$i(t_b) = \frac{9.581 \cdot [1 + 0.846 \cdot \log(P)] \cdot \left[\frac{(1 - 0.656) \cdot t_b}{r} + 7.0 \right]}{\left(\frac{t_b}{r} + 7 \right)^{0.656+1}}$$

$$i(t_a) = \frac{9.581 \cdot [1 + 0.846 \cdot \log(P)] \cdot \left[\frac{(1 - 0.656) \cdot t_a}{1 - r} + 7.0 \right]}{\left(\frac{t_b}{1 - r} + 7 \right)^{0.656+1}}$$

where: $i(t_b)$ (mm/min): rainfall intensity before the peak; $i(t_a)$ (mm/min): rainfall intensity after the peak; t_b (min): duration before the peak; t_a (min): duration after the peak; P (–): return period of designed rainfall; $r = 0.405$: coefficient of rainstorm peak position

However, one disadvantage of these design storm events is that they don't include the rainfall that takes place before and after the extreme of the rainfall duration curve (Van de Ven 2016).

For this reason, Sifalda added a rainfall before and after the uniform part of precipitation quantity that was taken from a rainfall duration curve. The parts from which the rainstorm profile proposed by Sifalda is composed by are illustrated in Figure 12.

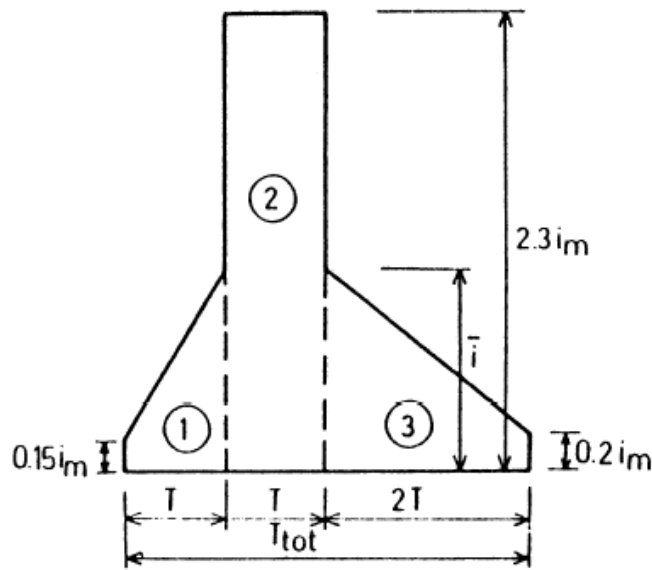


Figure 12: Rainstorm profile proposed by Sifalda (Van de Ven 2016)

2.9 Flood Management – Proposed flood reduction measures

2.9.1 Sustainable urban Drainage Systems (SuDS)

When dealing with flood mitigation and prevention, the Sustainable urban Drainage Systems (SuDS) is a key feature, since it forms a crucial role within the framework of integrated drainage design. The main objective of SuDS is to return the drainage system to nature-based processes capable to control large volumes of the surface runoff and increase the infiltration capacity of the surface by creating more permeable surfaces, and storage and retention elements. In this way, some additional benefits are achieved such as the improvement of the water quality, the enhancement of the aesthetics, the biodiversity and the amenities (Lashford et al. 2019). This can be achieved by the implementation of structures such as permeable and semipermeable pavements, infiltration trenches, gullies and wells, retention storage tanks, rooftop reservoirs, underground reservoirs and green roofing (Poletto and Tassi 2012).

2.9.2 Sponge Cities in China

The problems of pluvial flooding and lack of water that arise in China during the seasons of high rainfall and dry weather, respectively, led to the proposal of the Sponge City project as a solution in order to manage the urban water in a better way. This project is related to a sustainable way of managing water and is based on the infiltration, storage, drainage, use, cleaning and detention of water, making it an approach that is highly influenced from the Sustainable urban Drainage Systems (Lashford et al. 2019). The principles of the Sponge City model and the comparison with a conventional model of flood management are illustrated in Figure 13 (Lashford et al. 2019).

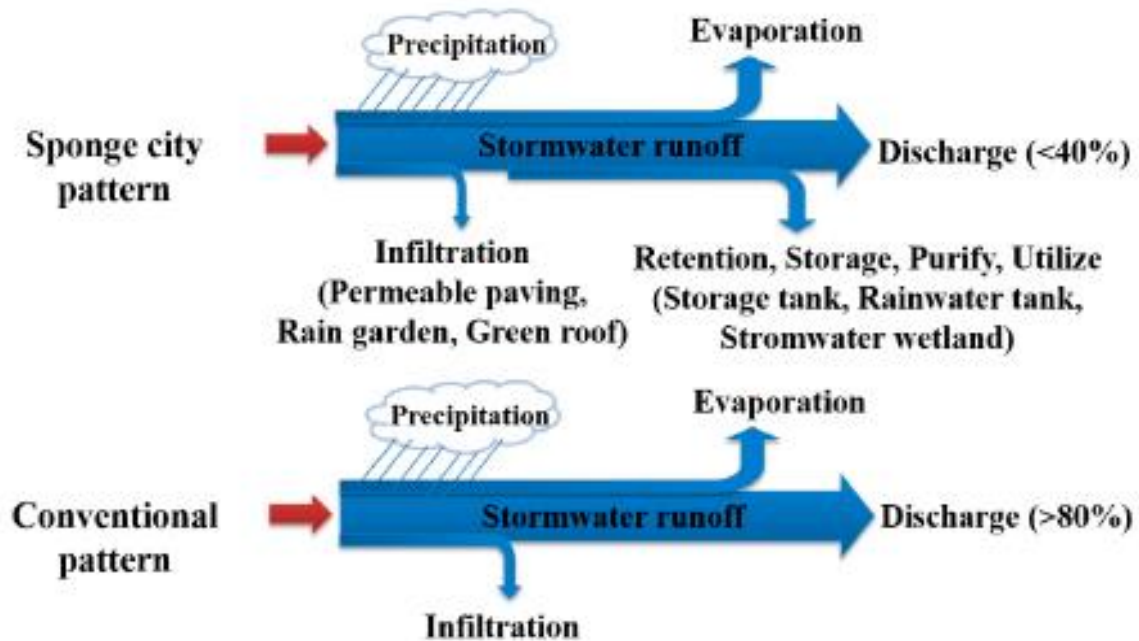


Figure 13: Patterns of Sponge City and conventional management of urban pluvial flooding (Lashford et al. 2019)

2.9.3 Upgrade of drainage system – Creation of water storage areas

Yuan et al. (2017) propose that the upgrade of the drainage system in an urban area and the increase or creation of water storage areas can be considered as potential countermeasures to prevent the occurrence of flood events triggered by torrential rainfall. For example, the length of the rivers in Shanghai decreased considerably since 1843 due to the effects of the urbanization and the deposition of sediment in the rivers. Consequently, the total area of the rivers decreased leading to decrease of the water storage area in general. In this case, to deal with urban pluvial flooding, actions should be taken such as deepening of the rivers and regular dredging of the riverbed.

An additional problem arises when the drainage system fails to discharge all the precipitated water in time. The origins of this problem may be found on the bad maintenance of the sewer system and the presence of debris and leaves in the gullies. By cleaning the entrances of the sewer system and fixing the parts of the system that have been damaged, the performance of the drainage system may be improved, reducing the possibilities of flood hazards (Yuan et al. 2017).

According to Van de Ven (2016) an alternative solution would be to delay the discharge through the sewer system and reduce the amount of water that enters the sewerage. This can be done by storing temporarily the precipitated water at the surface of the urban area and allowing more water to infiltrate into the soil. For a more gradual discharge of the water into the sewerage, temporary storage areas should be used such as roofs, rain barrels, ponds and ditches. To minimize the discharge in the sewer system, the infiltration into the paved surfaces should be maximized for example by using porous asphalt concrete. Also, the construction of spaces should be considered where the infiltration process is activated. These areas are usually referring to infiltration beds, basins and trenches. Finally, for the retention of storm water, the construction of green roofs is a solution with an increasing application in the last years because of their effectiveness on the runoff retention and the less problems regarding the quality of the water (Van de Ven 2016).

3 STUDY AREA AND METHODOLOGY

In this chapter, the study area is presented and the methods that were used for the accomplishment of the research objectives are described.

3.1 Study area

Jingan District is located in the downtown area of Shanghai. The district is composed of the old Jingan District and the Zhabei District that was merged into the rest district on November 2015 (Shanghai Daily). Jingan borders Baoshan District to the north, Putuo and Changning districts to the west, Huangpu district to the southeast and Hongkou district to the east. The maps that illustrate the location of Jingan District with respect to its adjacent districts and Shanghai city is presented in Figure 14.

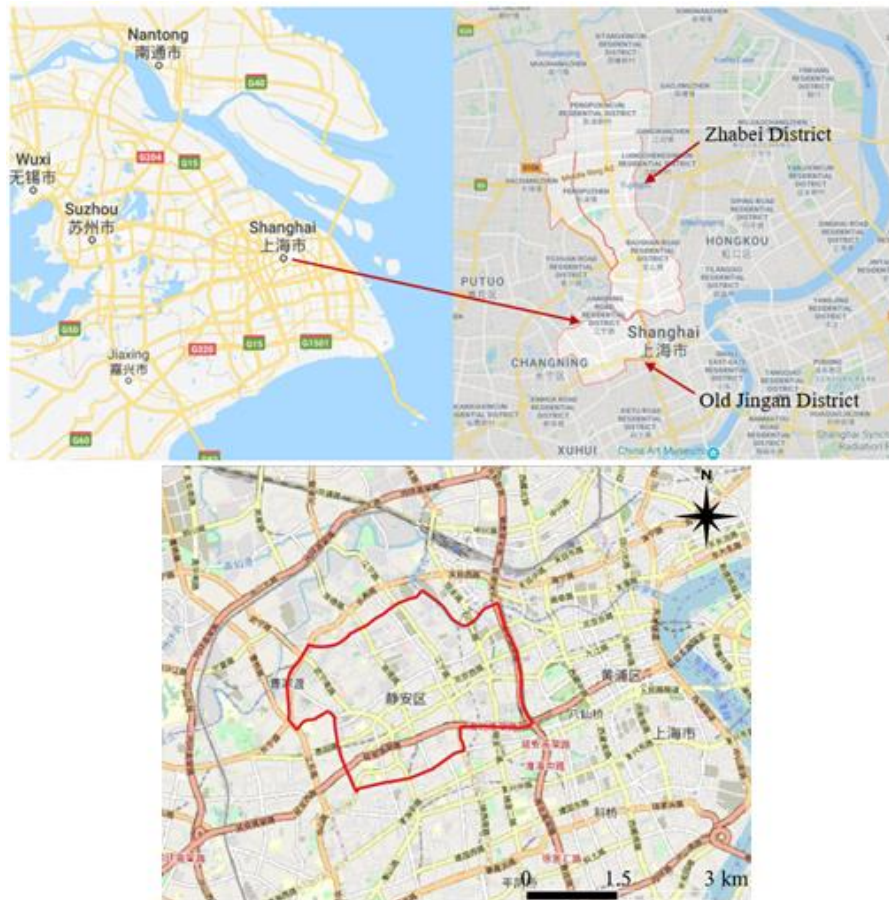


Figure 14: Location of Shanghai and Jingan District (upper panels) (Google Maps), area of interest (lower panel) (Open Street Map in QGIS)

However, in this research, the interest is confined to the old Jingan District Figure 14 (lower panel). The total coverage area of this district is 7.6 km² and the population is around 330,000 inhabitants (Shanghai Daily). This district is one of the most important Shanghai's districts with several commercial and business activities. Also, it is known for the many high office buildings, the shopping venues and the numerous large residential buildings.

3.2 Availability and quality of data

At the first stage of the research, an overview of the available and required data that would allow the development of the model to produce the flood hazard maps in Jingan District took place. After collecting

these data, a preliminary assessment of their quality was made to get a first idea about the accuracy of the expected results. Based on this, it was concluded that the available data were suitable for the development of the model, however, to achieve more accurate results that would correspond better to the real situation, further research of data and modifications of the already obtained data should take place. The available data and their pre-processing are described in chapter 4.

3.3 Flood hazard in Delft3D Flexible Mesh (Delft3D FM)

In this section an introduction is made to the main software that was used for the hydrodynamic simulation. Also, a description is made regarding the simulated rainfall events and the sensitivity analysis that was performed.

3.3.1 Delft3D Flexible Mesh (Delft3D FM)

The flood hazard model was developed by using the Dleft3D FM Suite (V. 2019 1.5.2). Delft3D FM is a robust modelling suite focusing mainly on coastal, river, estuarine, urban and rural environments. The selection of the specific software for the urban flood hazard was done since the same software was used for the coastal and river flood hazards. Hence, this would enable the merge of the pluvial, coastal and fluvial flooding models in the future.

Delft3D FM is composed of many modules, one of them is the D-Flow Flexible Mesh (D-Flow FM). The D-Flow FM solves the 2D (depth-averaged) or 3D non-linear shallow water equations which are derived from the three-dimensional Navier-Stokes equations under the assumption of incompressible free surface flow (Deltares 2019a). Among its several areas of application, D-Flow FM allows the modelling of rainfall runoff in urban environment. Also, this module enables the development of unstructured grids by allowing the flexible combination of diverse grid geometries such as curvilinear and triangles, leading to more realistic directions of the water flow and thus to a more accurate model.

Another module of Delft3D Flexible Mesh Suite is RGFGRID. This module allows the generation and manipulation of unstructured grids. One important factor for the accuracy of the grid is the orthogonality. This is the cosine of the created angle between a net and a flow link. The ideal value for the orthogonality of the grid is 0.01, with an upper limit of 0.5. Another property of the grid is the smoothness which is defined as the ratio between the surface area of two adjacent cells. The ideal value for the smoothness is 1, referring to two equal neighboring cells with respect to their surface area.

3.3.2 Simulation models and sensitivity analysis

To accomplish the objectives of the research, a series of models was considered. The development of these models was based on diverse simulated rainfall events and input data.

At first, the validation of the model was investigated by assessing its effectiveness to produce reliable flood hazard maps. For this reason, the rainfall event of August 2005 was simulated through model 1 and the results were compared with the results of a previous study by Meng et al. (2019).

After the validation, the model was tested for other two recorded historical rainfall events, referring to August 1997 and September 2013 of models 2 and 3, respectively. For these rainfall events, the data were available from the stations of Pudong and Longhua, which are located near Jingan District. The locations of Pudong and Longhua stations are shown in Figure 15. The rainfall distribution over time at Pudong and Longhua during the events of August 1997 and September 2013 are presented in Figure 48-Figure 51 in Appendix A. Also, the time series of the rainfall intensity for both events and for both stations are shown in Table 13 and Table 14 in Appendix A.

By observing the rainfall intensity values in Table 13 and Table 14, there are significant differences for some measurements between the two stations. This can also be realized by comparing the total storm volumes. For the rainfall event of August 1997, the storm volume in Pudong station was 146.2 mm against

94.3 mm in Longhua station, leading to a difference of 51.9 mm. For September 2013, the respective values were 141.0 mm and 71.4 mm, resulting in a higher storm volume difference of 69.6 mm.

However, in this study, for the simulation of the flood during the rainfall events of August 1997 and September 2013 only the data from Pudong station were considered, since based on the above analysis they would result in more severe flood events.

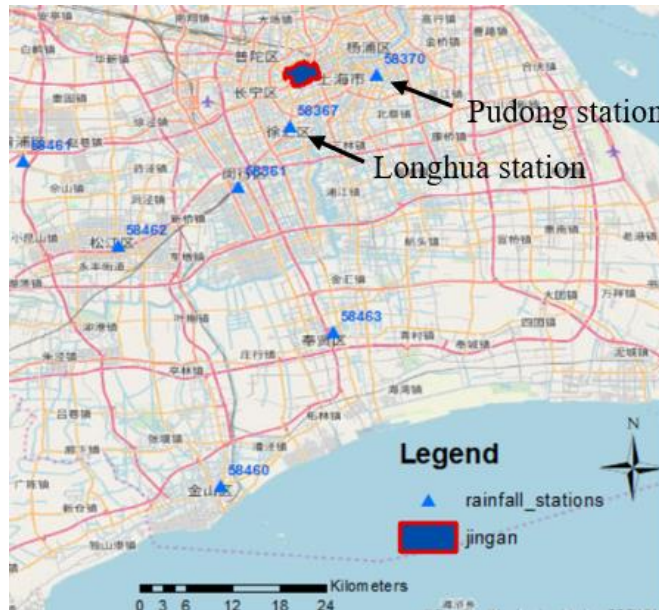


Figure 15: Location of Pudong and Longhua stations

For these three historical rainfall events, the simulation was performed by including the influence of the drainage system. An overview of these models is shown in Table 2.

Table 2: Overview of models for historical rainfall events

Model	Rainfall event	Drainage system
1	August 2005	YES
2	August 1997	YES
3	September 2013	YES

Later, the flood events triggered by rainfall events with diverse return periods were simulated. These rainfall events were generated by using the Chicago hydrograph for return periods of 1, 3, 5, 10 and 50 years and are integrated in the models 4, 5, 6, 7 and 8, respectively. These events are summarized in Table 3. By comparing the results of the models 4–8 that include the drainage system, the differences between rainfall events with diverse return periods can be realized.

Table 3: Overview of models for rainfall events generated by Chicago hydrograph

Model	Rainfall event (years of return period)	Drainage system
4	4a	NO
	4b	YES
5	5a	NO
	5b	YES
6	6a	NO
	6b	YES
7	7a	NO
	7b	YES
8	8a	NO
	8b	YES

Regarding the sensitivity analysis, one of the purposes was the assessment of the effectiveness of the drainage system. To reach this goal, models 4, 5, 6, 7 and 8 were divided into two cases, as shown in Table 3. Case a referred to the models that did not include the drainage system in the analysis, while case b considered the influence of the drainage system. By comparing the cases a and b for the models 4–8, the effectiveness of the drainage system of Jingan District was assessed.

Another objective of the sensitivity analysis was to assess the effectiveness of the implementation of potential flood reduction measures. The proposed measures were assessed by considering the rainfall event of 5 years return period. Four models were developed (models 9–12), and the resulted flood hazard maps were compared with the base model (model 6b) to assess their effectiveness. In models 9–12, the influence of the drainage system was considered. These models are described in Table 4.

Table 4: Overview of the models for flood reduction measures

Model	Rainfall event (years of return period)	Drainage system	Measure
9	5	YES	Water storage areas
10	5	YES	Increased drainage capacity in a single location
11	5	YES	Combination of models 9 and 10
12	5	YES	Increased drainage capacity in multiple locations

3.4 Additional software

A description of some of the additional software that were used for the preparation of the data is presented below:

3.4.1 SOBEK

SOBEK is a software package of Deltares. It is suitable for urban, rural or river management and it comprises seven interrelated modules for better understanding of the waterway systems. For obtaining

solutions regarding the overall water management of a specific area of interest, SOBEK offers an integrated framework that allows the link of canal, river and sewer systems (Deltares 2018).

3.4.2 Other software

In addition to the main software (SOBEK and Delft3D FM) that allow the hydrodynamic simulation of the 1D and 2D flow, some additional software was used for the pre- and pro-processing of the data and the results, respectively. Regarding the pre-processing of the data, QGIS and MATLAB were used. QGIS is a Geographical Information System software that allows the creation, editing, view and analysis of geospatial data. Also, it enables the composition and the export of graphical maps. It supports vector and raster layers and formats like shapefiles and coverages, while the integration of plugins allows to add new features and functions (QGIS).

4 DATA PREPROCESSING AND SIMULATION

An overview of the data that were used as input in DFM to create the flood hazard maps is presented in Table 5. The type, purpose, required format and software used for the preprocessing of these data are provided in this table.

Table 5: Overview of the input data

Type	Purpose	Format	Software
Grid	Numerical calculation	<i>.nc</i>	DFM
DSM	Surface elevation	<i>.xyz</i>	QGIS, MATLAB, DFM
Land use	Roughness	<i>.xyz</i>	DFM
Sinks/sources	Drainage	<i>.pli and .tim</i>	SOBEK, Excel, MATLAB
Rainfall events	Input data	<i>.tim</i>	Excel

In the following sections of this chapter, the procedure that was followed for the production or the preprocessing of the abovementioned data is presented.

4.1 Generation of unstructured grid in DFM

The unstructured grid for Jingan District was generated in the module RGFGRID of Delft3D Flexible Mesh. The grid comprised two parts. The first concerned the streets while the second considered the blocks where buildings, parks etc. are located. For the streets the curvilinear grid was adopted within polygons of splines while for the blocks an unstructured triangular grid system was chosen.

The purpose was to improve the unstructured grid of Sutter V. (2019). The resolution of this grid was 50 meters. However, to get more detailed and accurate results, the development of a new grid with 15 meters resolution was decided.

The development of the improved unstructured grid was based on the curvilinear grid for the streets that was created by Sutter V. (2019). This grid worked as a boundary for the generation of the triangular grids for the blocks that were in the inner zones of the street network. The triangular grids had a resolution of 15 meters.

In this way, the unstructured grid of Figure 16 was generated with a resolution of 15 meters. For the optimization of the grid the orthogonality was checked, and modifications were made where it was necessary. The maximum value of the orthogonality was 0.468, lower than the upper limit value 0.5, thus the orthogonality requirement was satisfied.

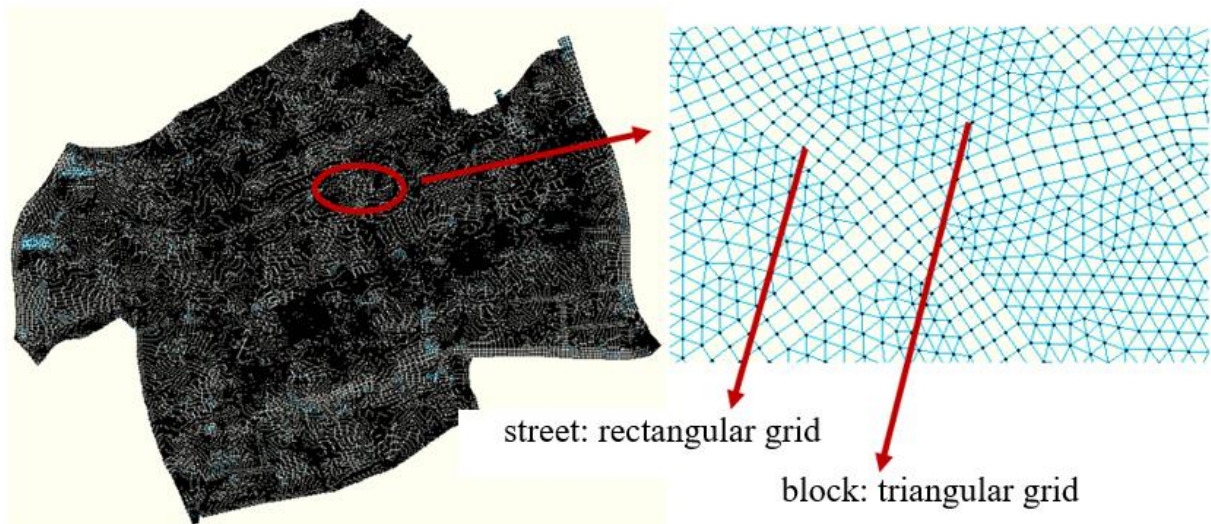


Figure 16: Unstructured grid for Jingan District (left), zoom in area to illustrate the connection between streets and blocks (right) – grid resolution: 15 meters

4.2 Digital Surface Model (DSM – 5 meters)

For the representation of the earth's surface elevation, a Digital Surface Model (DSM) was used. The initial DSM had a resolution of 5 meters (East China Normal University 2019). This means that the information regarding the surface elevation was provided in square pixels of 5 meters. This DSM is presented in Figure 17, however, due to some extreme negative values that were contained in this surface elevation map, the lower limit of the surface elevation values in the map of this figure is set to be 0. The DSM that was finally used for the hydrodynamic simulation in DFM had also a resolution of 5 meters, however modifications were made on it which are described below.

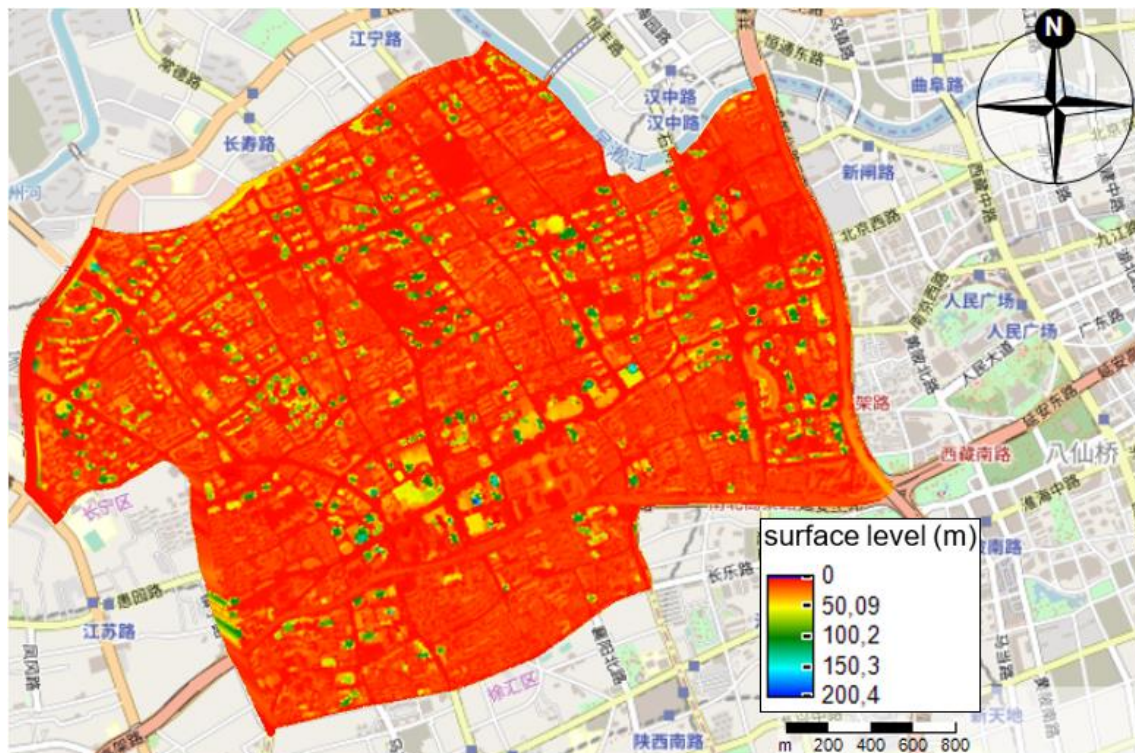


Figure 17: Initial DSM (5 meters) interpolated for the area of interest (without negative values)

Since the flow of the water takes place on the surface of the terrain, it was quite important to obtain a DSM with height information of the low-lying areas that represent the real conditions. In an urban district, these areas are mainly composed of the street system. The buildings are obstacles for the water flow and their real location should be included in the DSM. In Figure 17, the distinction between the streets and the blocks (buildings) is not clear. Thus, to achieve more accurate results, a preprocessing of this DSM took place before the hydrodynamic simulation.

The purpose of the preprocessing was twofold. Firstly, the location and the elevation of the streets were improved by assigning elevation values lower than in the rest map. The assignment of these values was based on the initial DSM of Figure 17 and the information provided by real maps of Jingan District.

Moreover, in order to allow a consistent connection between the 1D model and 2D model, the DSM should be modified in such a way that the precipitated water was collected on the surface of the streets. Then, the water could flow either on the surface of the street system or into the intakes of the sewer system. To achieve this, the areas covered by buildings (blocks) in DSM should become flat and elevation values higher than those of the roads should be assigned to them.

The reason of this modification in DSM had its ground on the way that the 1D model in SOBEK has been developed. Since all the intakes of the sewer system are located on top of the streets, then in order to allow runoff flow of the rainwater in the intakes of the sewer system, the surface area of each block was equally distributed to all the intakes that comprise the block. This means that all the amount of the precipitated water was collected on the streets, not allowing the creation of ponding or other water retaining areas in the block areas.

For the preprocessing of the DSM, the software QGIS, MATLAB and DFM were used. The MATLAB codes that were generated for the preprocessing of the DSM are included in Appendix D. The final DSM after preprocessing and interpolation is presented in Figure 18.

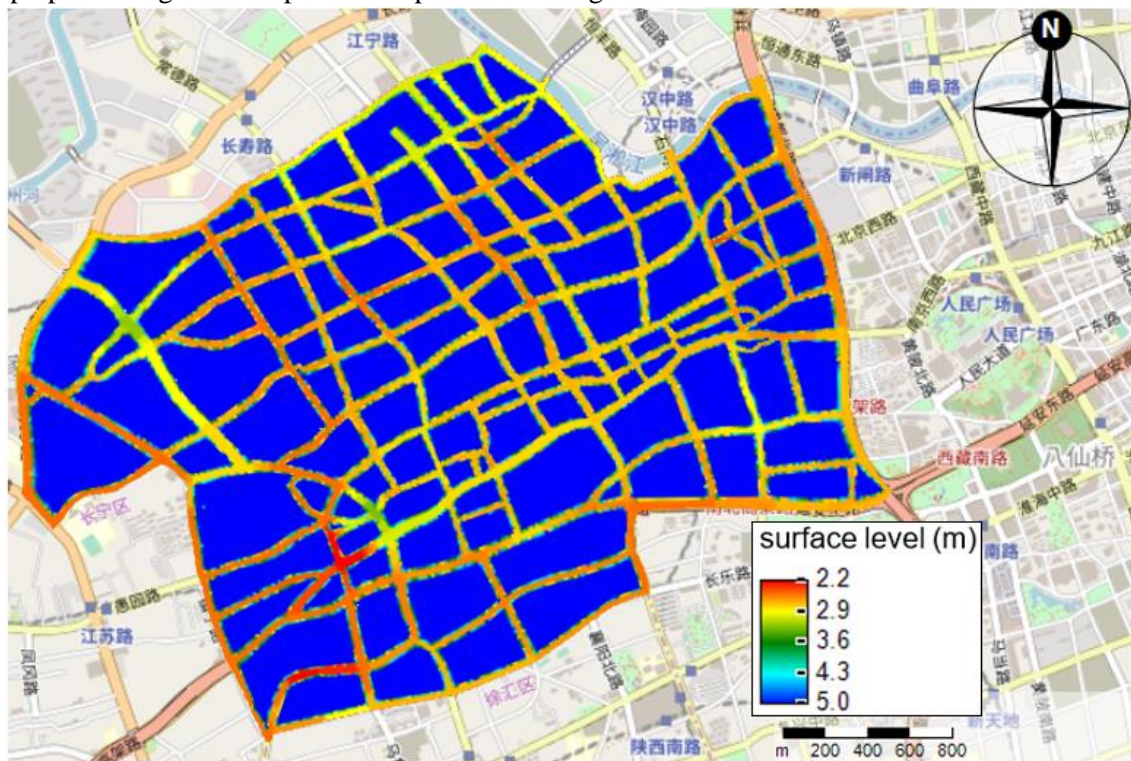


Figure 18: Final DSM (5 meters) interpolated for the area of interest

4.3 Sources and sinks

Sources (or intake facilities) and sinks (or outfall facilities) are used in Delft3D FM to add and extract a discharge to and from the model, respectively. Also, sources and sinks can be used to redistribute water and its properties like the temperature and the salinity within the model.

In the current 2D model, only sinks (outfall facilities) were considered. These are represented by the runoff discharges of the rainwater from the surface area to the intakes of the underground pipeline network. Sources were not used since no inflows from the sewer systems of the adjacent districts were considered. According to U.S. EPA (2003), in an urban environment with an impervious cover between 75–100 %, the surface runoff is estimated at 55% and the infiltration at 15%. However, since infiltration was not taken into account in the current study, the urban area was considered as impervious and the infiltration percentage was added to the surface runoff percentage, leading to 70%. This percentage was used for the calculation of the runoff discharges in SOBEK within the 1D flow simulation in the underground pipeline network. The set-up of the model in SOBEK is described in Appendix B.

The maps that illustrate the average values of the runoff discharges for Jingan District for all the considered rainfall events are presented in Figure 19. These maps illustrate the elements of the underground network of the sewer system (manholes and pipes). The information regarding the runoff discharges is attributed to the manholes since these are the connecting elements of the overland flow with the underground flow of the sewer system. To understand better the differences in the magnitude of the runoff discharges for all the models, the same range of values is used as shown in the legend. These values were taken from the model of the rainfall event of 50-years return period, since this was the model with the higher resulted runoff discharges. By comparing the maps of Figure 19, it can be observed that the runoff discharges become higher for increasing return period of the rainfall events. This is reasonable since the rainfall intensity increases. Also, the differences are small between the models for 3 and 5-years of return period and between the models for 5 and 10-years of return period.

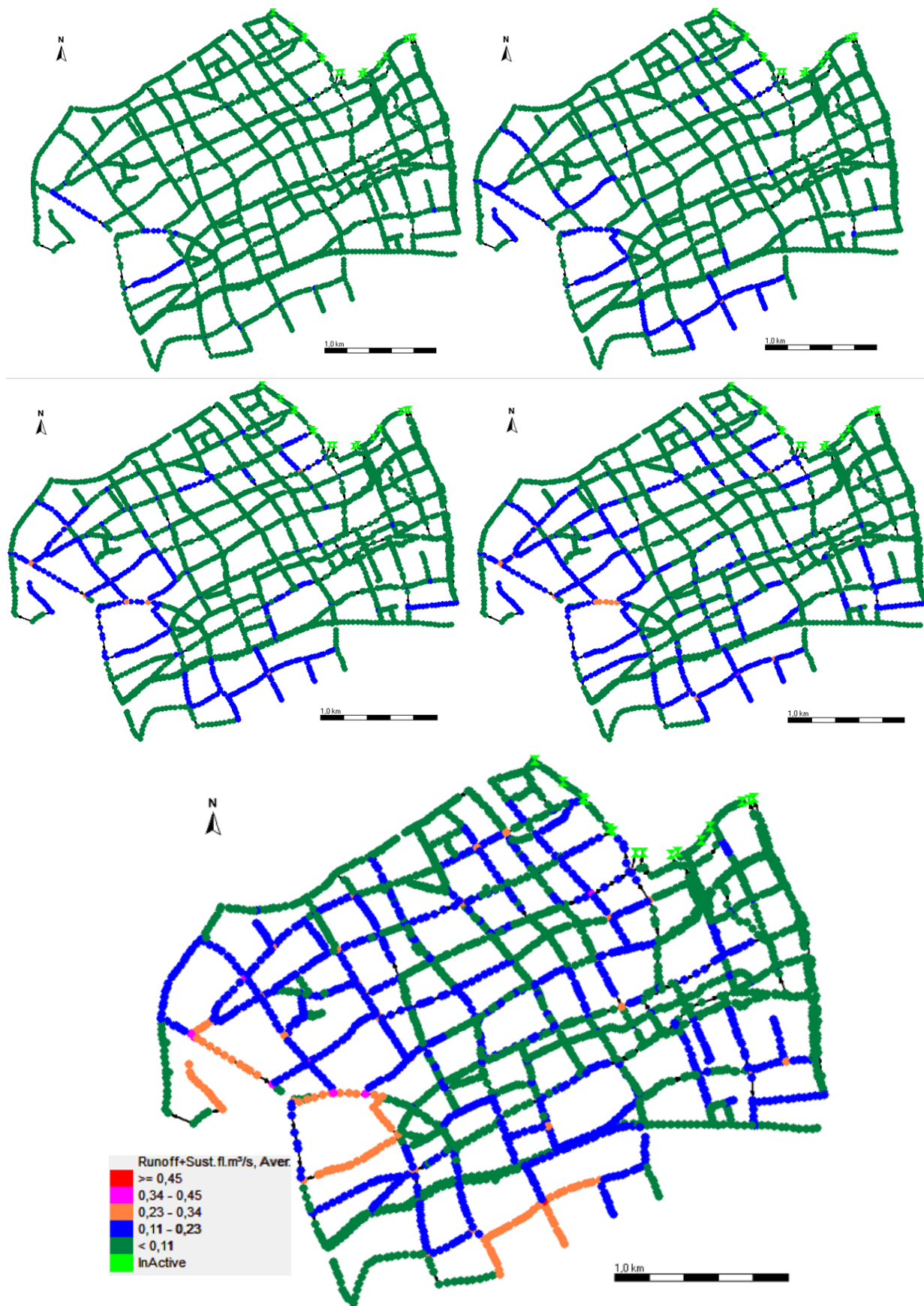


Figure 19: Average runoff discharges for rainfall events with return period of 1-year (top left), 3-years (top right), 5-years (middle left), 10-years (middle right) and 50-years (bottom)

4.4 Rainfall events

4.4.1 Rainfall events from Chicago design storm

For the simulation of the rainfall process, the Chicago rainfall hydrograph model was used. Based on this model and the rainstorm intensity formula for Shanghai that is mentioned in chapter 2.8, the rainfall depth-duration-frequency (DDF) curves were produced. The DDF curves for rainfall durations from 5 to 180 minutes were generated in MATLAB with codes provided by Dr. Qian Ke. The graph of these lines is presented in Figure 20.

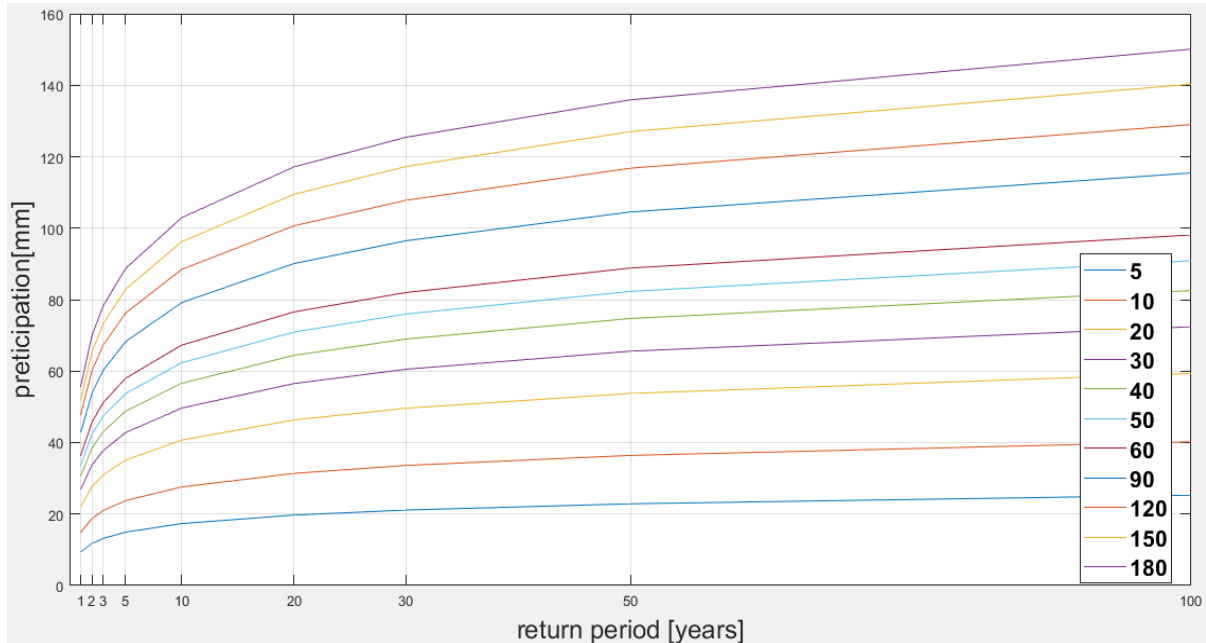


Figure 20: DDF curves for rainfall duration between 5 and 180 minutes

In this research, the duration of the rainfall was set as 3 hours and the return periods considered were 1, 3, 5, 10 and 50 years. The rainfall distribution over time under diverse rainfall return periods and a time step of 5 minutes is presented in Table 12 in Appendix A. The hydrographs for a rainfall duration of 3 hours and 1, 3, 5, 10 and 50 years return periods were generated in MATLAB with codes provided by Dr. Qian Ke and are shown in Figure 21.

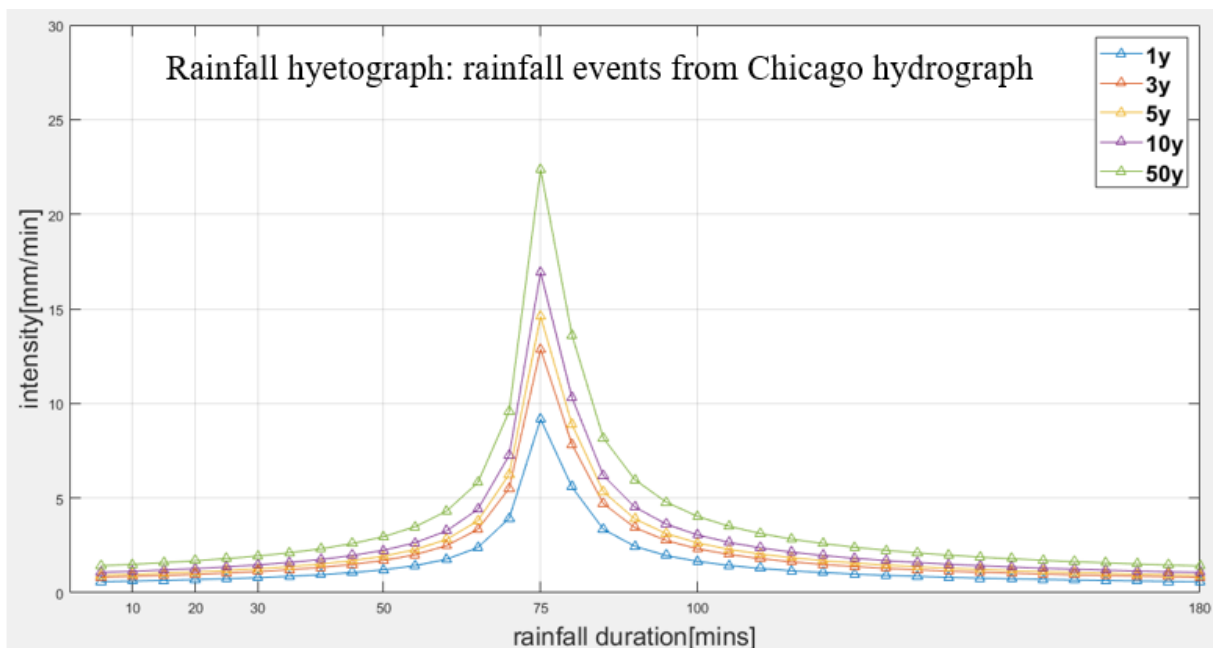


Figure 21: Hydrograph for rainfall duration of 3 hours and 1, 3, 5, 10 and 50 years return periods

4.4.2 Historical rainfall events

The developed model was also tested for three historical rainfall events. These are referring to the events of August 2005, August 1997 and September 2013 (Shanghai Climate Center 2019).

After preprocessing of these data in order to consider only the period that rainfall occurred, the dates and times of the start and end of each modified historical rainfall event are shown in Table 6.

Table 6: Start, end and duration (hours) of historical rainfall events

Historical rainfall event	Total storm volume (mm)	Start time	End time	Duration (hours)
August 2005	303.8	6/8 0:00	8/8 11:00	59
August 1997	146.2	18/8 18:00	20/8 11:00	41
September 2013	141.0	13/9 15:00	13/9 18:00	3

The data were provided in mm per hour. The corresponding hydrographs are presented in Figure 22-Figure 24.

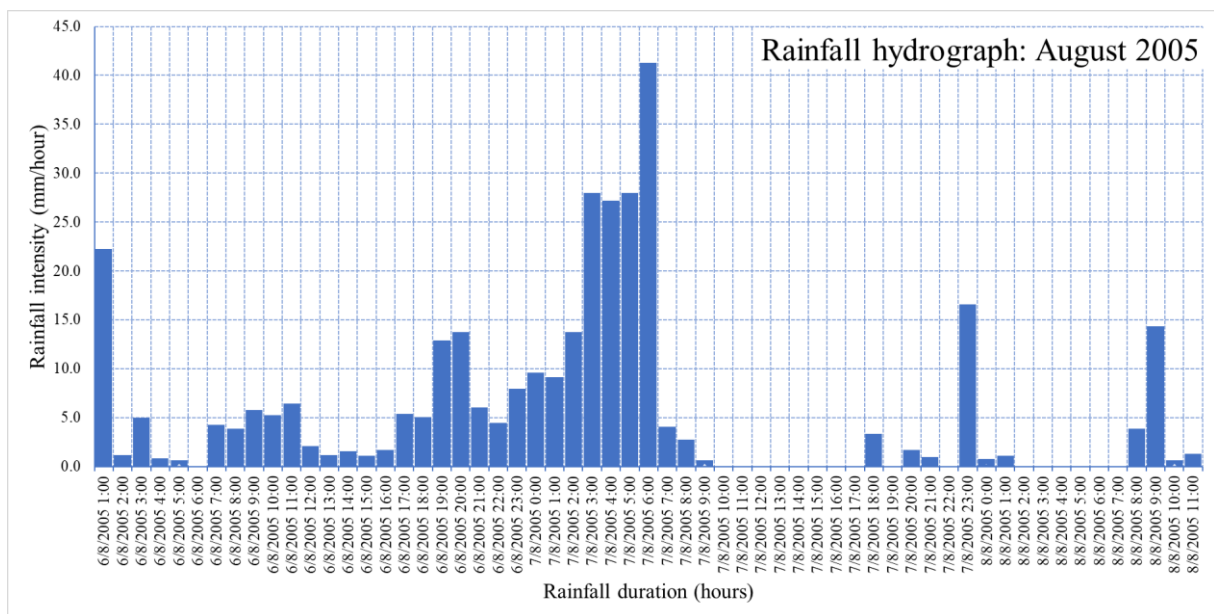


Figure 22: Rainfall hydrograph for August 2005, duration: 59 hours

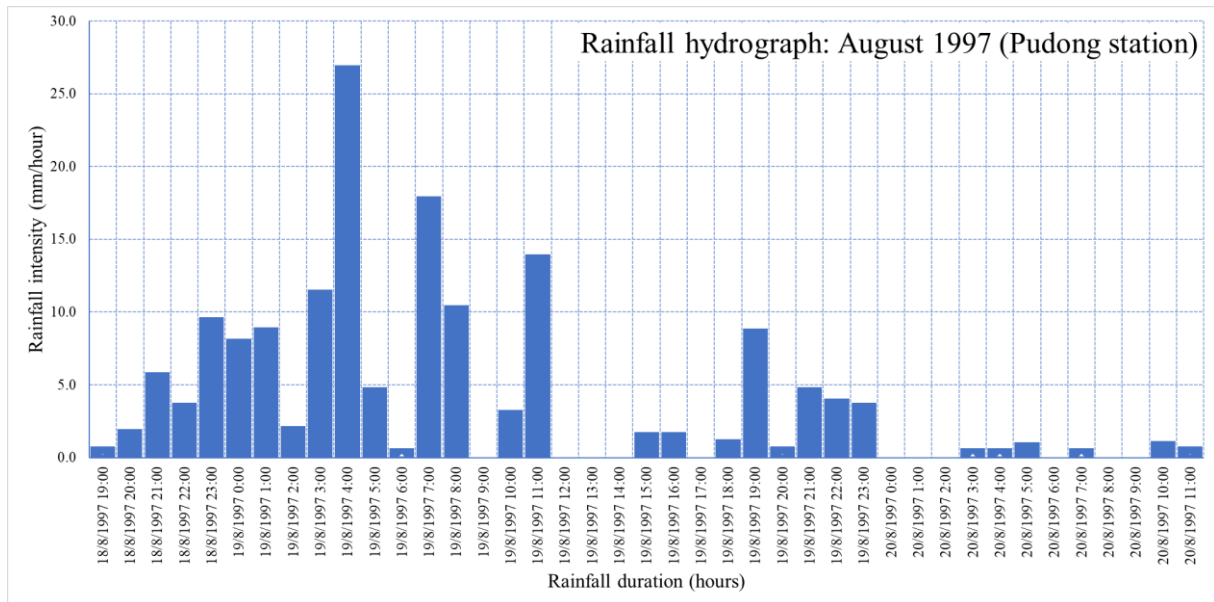


Figure 23: Rainfall hydrograph for August 1997, duration: 41 hours

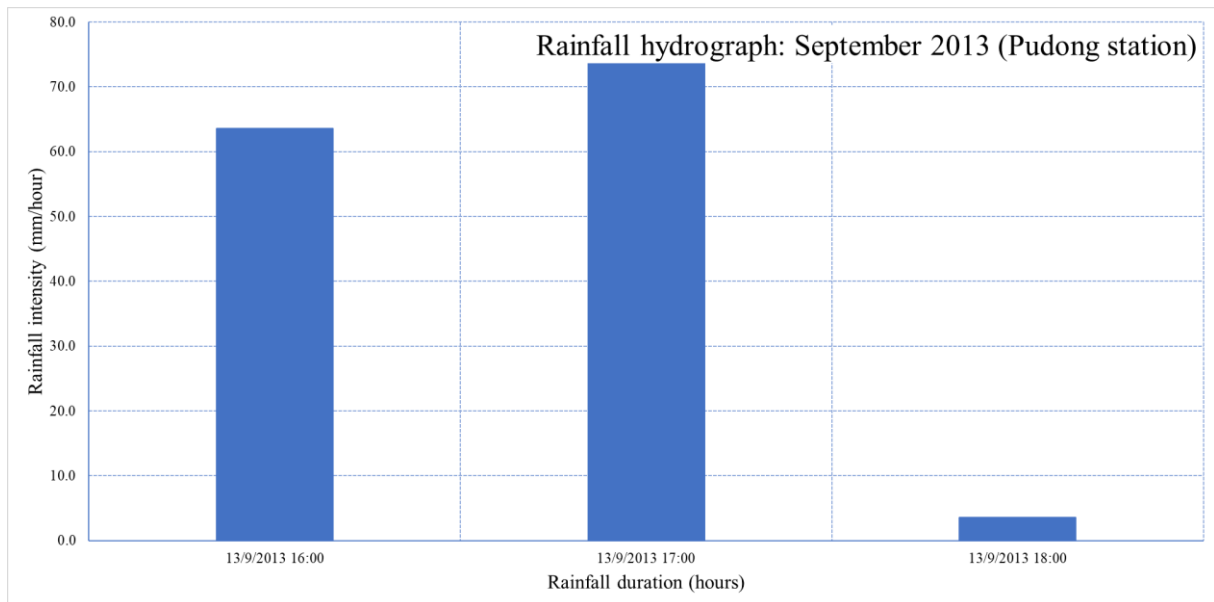


Figure 24: Rainfall hydrograph for September 2013, duration: 3 hours

4.5 Simulation

4.5.1 Set-up of flood hazard model

For the simulation of the abovementioned rainfall events, the determination of the flow model parameter settings took place at first. This is specified in the .mdu file. The values of the time and boundary parameters that were modified, are shown in Table 7 and Table 8, respectively. For the rest parameters, the default values provided by Deltares (2019a) were assigned. Since no underground water flow was considered, any negative water level value could be assigned in the parameters of water level boundary condition and water level initial condition.

Table 7: Set-up of time parameters

Time Parameters	Description	Rainfall events			
		Chicago hydrograph	Historical		
			Aug. 2005	Aug. 1997	Sep. 2013
RefDate	Start of event (yyyymmdd)	e.g. 20200101	20050806	19970818	20130913
DtUser	Timestep (external forcing/output map)	60 s	60 s	60 s	60 s
TStart	Start time w.r.t. RefDate	0 s	3600 s	68400 s	57600 s
TStop	Stop time w.r.t. RefDate	10800 s	212400 s	212400 s	79200 s
MapInterval	Map file output	300 s	3600 s	3600 s	3600 s

Table 8: Set-up of boundary conditions parameters

Boundary Parameters	Description	Rainfall events			
		Chicago hydrograph	Historical		
			Aug. 2005	Aug. 1997	Sep. 2013
Waterlevelbnd	Water level boundary condition	-5 m	-5 m	-5 m	-5 m
WaterLevelIni	Water level initial condition	-100 m	-100 m	-100 m	-100 m
Start time boundary condition		=RefDate (Table 7)	2005-06-08	1997-08-18	2013-09-13

The time step of the output maps was chosen according to the time step of the input data regarding the rainfall events. Since the intensity for the Chicago rainfall hydrograph events and the historical events were provided every 5 minutes and 1 hour respectively, then the timestep of the resulted maps was 5 minutes and 1 hour, respectively.

4.5.2 Limitations

Due to the limitation of the current version of DFM software regarding the number of the input files, it was not possible to produce the flood hazard maps for the whole Jingan District. For this reason, a smaller area of the district was considered. In contrast to the original plan that included 2785 inlets of the sewer system of Jingan District, the new area included only 1965 inlets. The grid and the DSM of 5 meters resolution for this area are presented in Figure 25 and Figure 26, respectively.

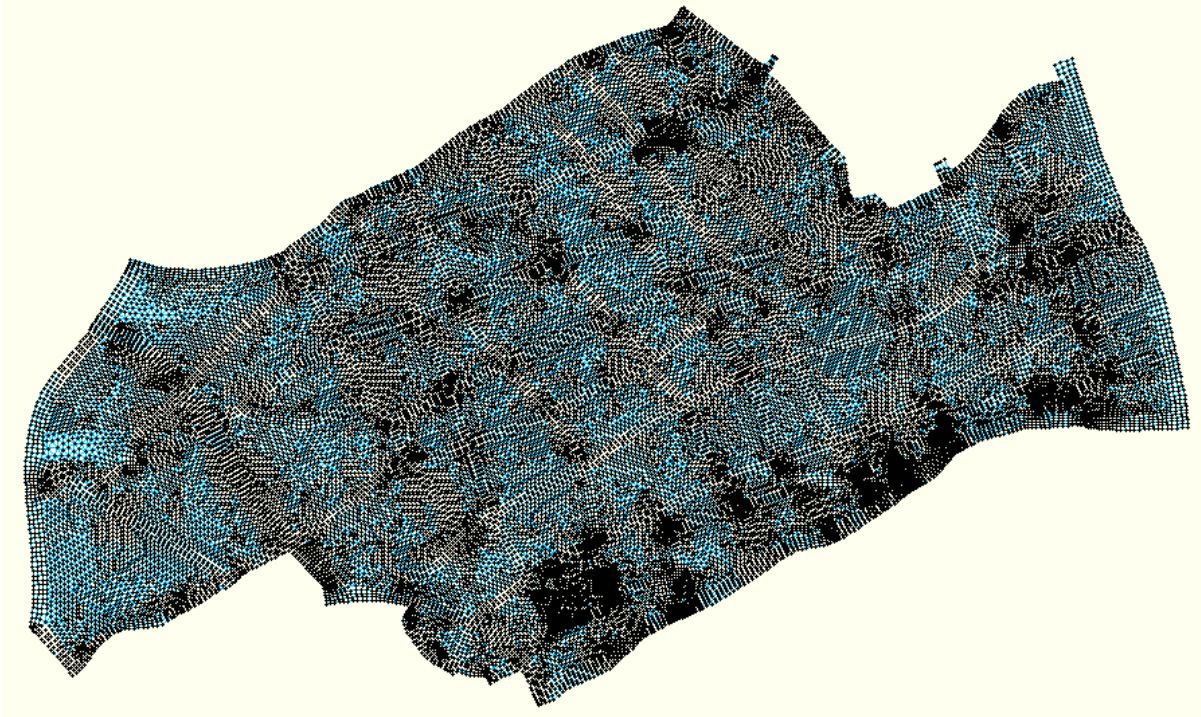


Figure 25: Unstructured grid with 15 meters resolution for Jingan District, used for the simulation

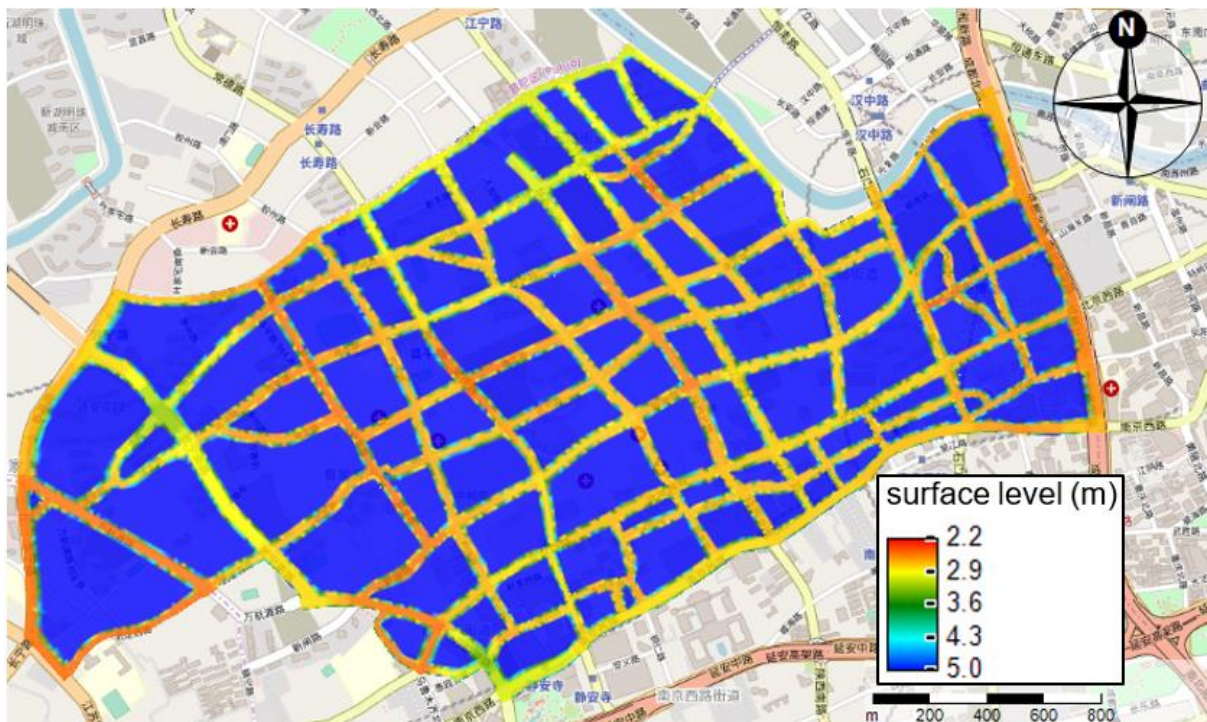


Figure 26: DSM with 5 meters resolution, used for the simulation

5 RESULTS AND ANALYSIS

In this chapter, the simulation results are presented for the models that were described in chapter 3.3.2. In section 5.1, the validation of the model is discussed by comparing the simulation results of the current model with the results of the model of a previous study. In section 5.2 and section 5.3, the resulted inundation maps are shown for the historical rainfall events and the rainfall events generated by the Chicago hydrograph, respectively. In section 5.4, the effectiveness of the drainage system is presented and in section 5.5 the comparison between the inundation maps in SOBEK and in DFM is presented. Finally, in section 5.6, the effectiveness of the proposed flood reduction measures is presented.

5.1 Validation - Model 1: Rainfall event of August 2005, including the drainage system

The performance of the model was evaluated by simulating the rainfall event of August 2005 and comparing the results with those of the model that was developed by Meng et al. (2019). The resulted inundation maps of the current study and the previous study are shown in Figure 27 and Figure 28, respectively. Also, Figure 28 contains information regarding the reported flood streets that are represented with red dotted lines. Both figures illustrate the inundation maps at the moments of the maximum inundation depths.



Figure 27: Maximum inundation depths for the rainfall event of August 2005 (07/08 at 10:00:00)

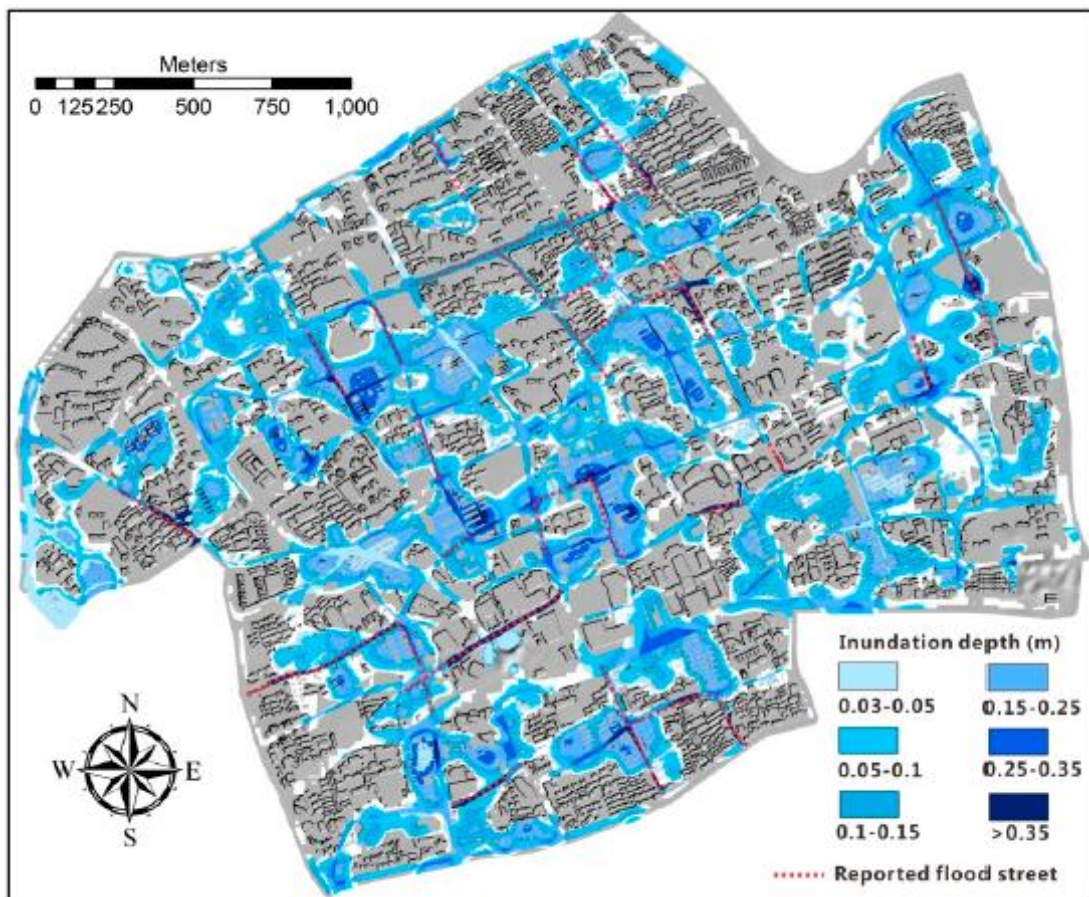


Figure 28: Maximum inundation depths for the rainfall event of August 2005 (Meng et al. 2019)

By comparing the two maps, it is observed that there is similarity regarding the range of the resulted water depth values and the maximum inundation depth value. For Figure 27, the maximum water depth is estimated to be 0.343 meters. Also, there is a partial agreement with regards to some of the locations that inundation occurs between the two models. The same remark can be done when the inundated streets of Figure 27 are compared with the reported flood streets of Figure 28.

On the other hand, in some areas of Figure 27, there is a shift of the inundation locations when they are compared with those of Figure 28. These differences may have their origins in the way that the current model was developed. Some of the assumptions of this model are mentioned below:

- The simulated area in this model (Figure 27) is smaller than the whole area of interest (Figure 28). This results from the limitation of the current version of the software regarding the number of the input data. Thus, depending on the surface slope in the connecting points between the simulated area and the rest area, this may prevent the water from flowing in or out of the simulated area. Consequently, this leads to lower or higher inundation depths, respectively.
- The surface elevation map that was used for the simulation has obvious differences when compared with the initial provided map. This results from the preprocessing of these data to obtain a map with a clear distinction between the street and block areas. Thus, the water flow on the streets of Figure 27 is performed without the existence of the obstacles that would occur due to the inaccurate values of the initial surface elevation map.
- In addition to the previous modification in the surface elevation map, the streets of Figure 27 are wider than those of Figure 28. This results from the orthogonality check in the generation of the grid for the numerical calculation. Consequently, this allows more water to flow on the streets of Figure 27.
- Also, for all the block areas of Figure 27, the same surface elevation value has been assigned so that they are considered as elevated flat areas, in other words each block was considered as a building. However, the real location of the buildings was used for Figure 28. This simplification for Figure 27

was done to achieve a consistent connection between the model for the water flow in the underground pipeline system and the model for the overland flow.

By considering all the above it can be argued that the validation of the current model cannot be proved. However, this model can be used as a base for future researches in which more precise and updated data will be added in the model.

5.2 Historical rainfall events

5.2.1 Model 2: Rainfall event of August 1997, including the drainage system

The rainfall hydrograph for the rainfall event of August 1997 is shown in Figure 23. The total storm volume is 146.2 mm. The moment of the maximum water depths coincides with the moment of the most inundated areas. The inundation map for this moment is shown in Figure 29. For completeness, the hydrograph of August 1997 is presented in the top left part of this figure.



Figure 29: Maximum inundation depths and most inundated areas for the rainfall event of August 1997 (19/08 at 9:00:00)

As mentioned in Figure 29, the maximum inundation depths and the most inundated areas are observed on 19/08 at 9:00:00. Considering the rainfall hydrograph of Figure 23, these conditions occur 15 hours after the start of the rainfall event and 5 hours after the highest peak of the hydrograph. The maximum water depth is 0.238 meters. By setting as a lower limit of the water depth the 15 cm, the inundation period starts on 19/08 at 6:00:00 and ends on 20/08 at 7:00:00. The total duration of the inundation is 25 hours.

5.2.2 Model 3: Rainfall event of September 2013, including the drainage system

The rainfall hydrograph for the rainfall event of September 2013 is shown in Figure 24. The total storm volume is 141.0 mm. Like in the case of August 1997, the maximum water depths and the most inundated areas occur at the same moment. The inundation map is shown in Figure 30. The hydrograph of September 2013 is presented in the top left part of the figure.



Figure 30: Maximum inundation depths and most inundated areas for the rainfall event of September 2013 (13/09 at 18:00:00)

As mentioned in Figure 30, this situation is observed on 13/09 at 18:00:00. Considering the hydrograph of Figure 24, these conditions occur 3 hours after the beginning of the rainfall event and 1 hour after the peak of the rainfall hydrograph. The maximum observed water depth is 0.376 meters while the inundation period starts on 13/09 at 17:00:00. Even though the simulation was extended for 5 hours after the end of the rainfall event, there is still inundation at the end of the simulation period. This means that it would take a few more hours for the remaining water level to reduce below the limit of the 15 cm. Based on the simulation period, the total duration of the inundation is 6 hours.

5.3 Rainfall events from Chicago hydrograph

To compare the results of the models that simulate the rainfall events of 1, 3, 5, 10 and 50 years return period, Figure 31, Figure 33, Figure 35, Figure 37 and Figure 39, are used respectively. These figures show the inundation maps the moment of the maximum water depths. To be able to compare the context of these maps, the range of the water depth values, that is used in the legend of all the models, is based on the model of the rainfall event of 50 years return period.

To compare the moments of maximum water depths and most inundated areas, Figure 32, Figure 34, Figure 36, Figure 38 and Figure 40, are considered. In the left panels, the maximum inundation depths are presented, while in the right panels, the most inundated areas are illustrated. The range of water depth values in the legends of each map is based on the resulted inundation depths of the corresponding model. The rainfall hydrographs for the rainfall events of 1, 3, 5, 10 and 50 years return period are shown in Figure 21 with storm volumes of 278.8 mm, 391.4 mm, 443.7 mm, 514.7 mm and 679.6 mm, respectively. For completeness, the hydrographs of these events are presented in the top left part of each inundation map in Figure 31-Figure 40.

All the inundation maps that are presented in this chapter are products of the analysis that integrated the effect of the underground pipeline drainage network. In other words, these are the results of the models 4b, 5b, 6b, 7b and 8b, as mentioned in Table 3.

5.3.1 Model 4b: Rainfall event of 1-year return period, including the drainage system

In model 4b, the maximum inundation depth is 0.521 meters. The moment of the maximum water depths coincides with the end of the rainfall event, that is the same with the end of the simulation period. Due to this, the actual maximum water depth may be slightly larger than the abovementioned value.

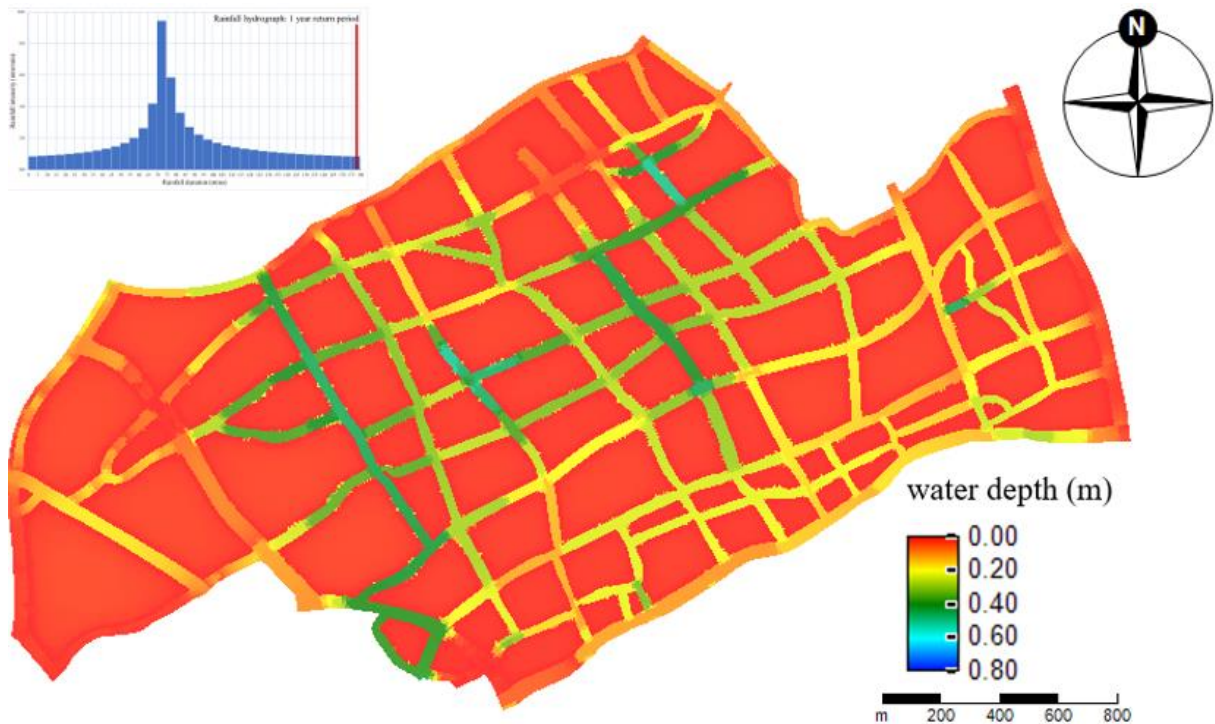


Figure 31: Maximum inundation depth for the rainfall event of 1-year return period at 3:00:00 (including drainage system)

The condition of the most inundated areas occurs 2 hours after the start of the rainfall event. It is estimated that the inundation period starts at 1:05:00 and ends at 3:00:00. Consequently, the duration of the inundation period is 1 hour and 55 minutes.

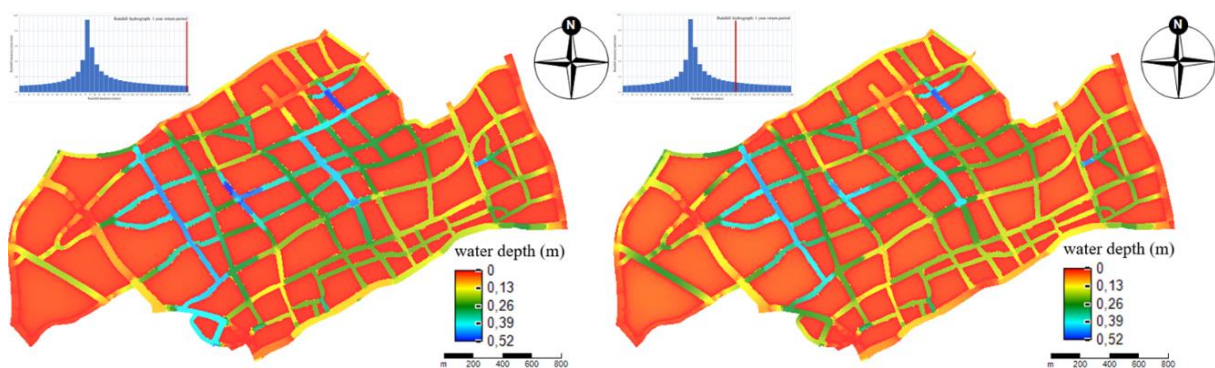


Figure 32: Maximum inundation depth at 3:00:00 (left panel) and most inundated areas 2:00:00 (right panel) for the rainfall event of 1-year return period (including drainage system)

5.3.2 Model 5b: Rainfall event of 3-years return period, including the drainage system

In model 5b, the maximum water depth is 0.611 meters. This occurs 2 hours and 55 minutes after the start of the rainfall event and 1 hour and 45 minutes after the peak of the hydrograph.

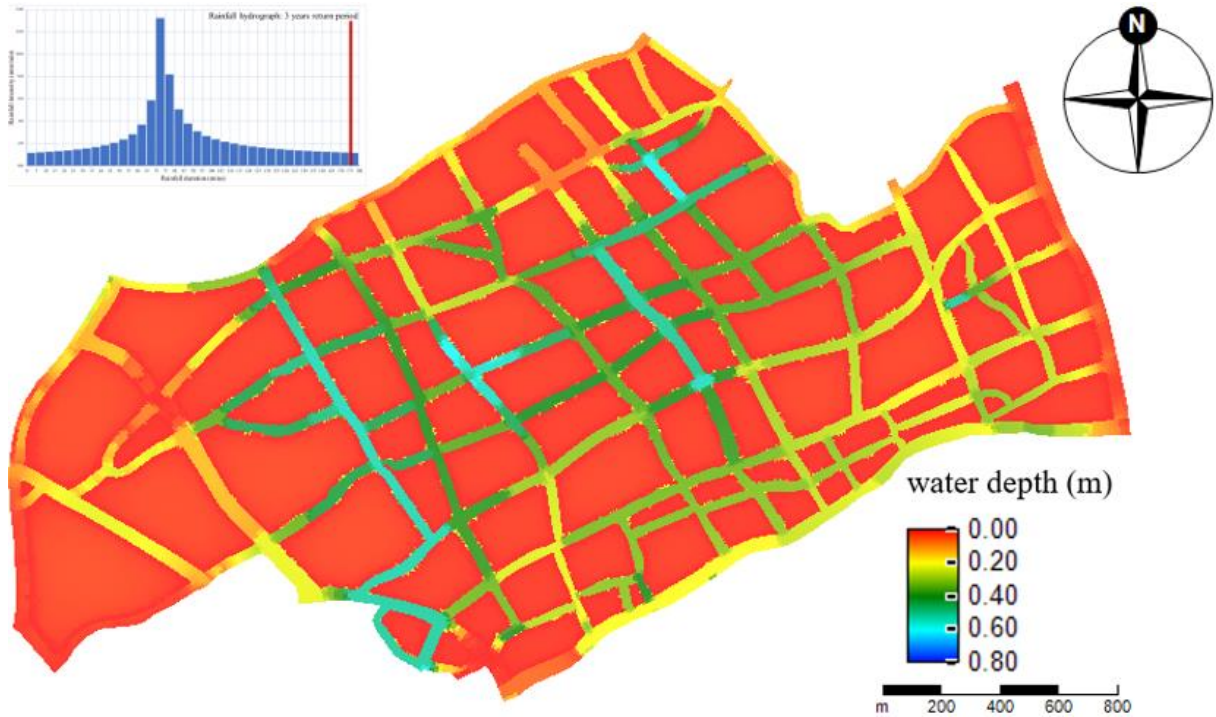


Figure 33: Maximum inundation depth for the rainfall event of 3-years return period at 2:55:00 (including drainage system)

The moment of most inundated areas occurs 1 hour and 45 minutes after the start of the rainfall event. The inundation period starts at 00:55:00 and ends at 3:00:00 and the duration is 2 hours and 5 minutes.

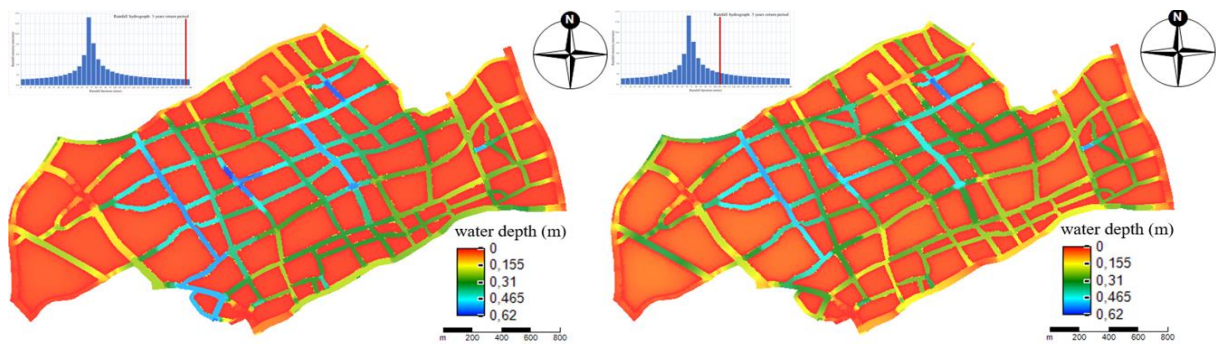


Figure 34: Maximum inundation depth at 2:55:00 (left panel) and most inundated areas 1:45:00 (right panel) for the rainfall event of 3-years return period (including drainage system)

5.3.3 Model 6b: Rainfall event of 5-years return period, including the drainage system

In model 6b, the value of the maximum water depth is 0.648 meters and appears 2 hours and 40 minutes after the beginning of the event and 1 hour and 25 minutes after the peak of the hydrograph.

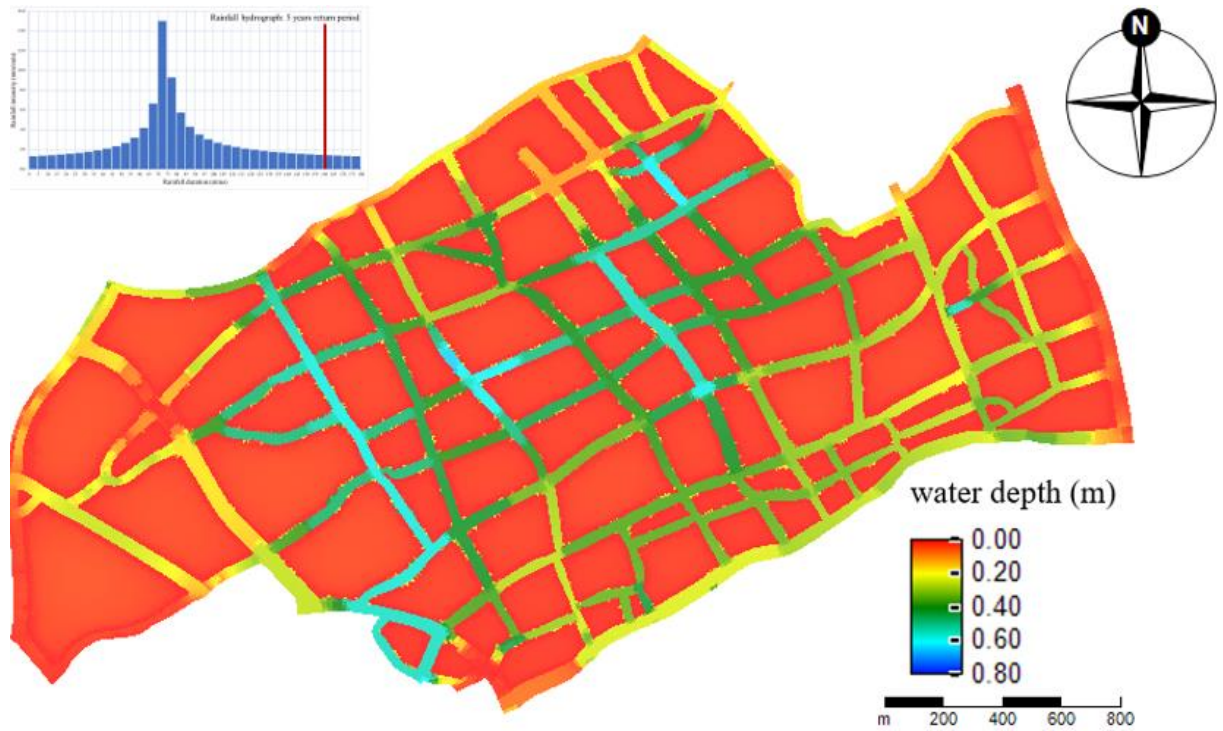


Figure 35: Maximum inundation depth for the rainfall event of 5-years return period at 2:40:00 (including drainage system)

The most inundated areas occur 1 hour and 40 minutes after the beginning of the rainfall event. The inundation period starts at 00:50:00 and ends at 3:00:00 with a duration of 2 hours and 10 minutes.

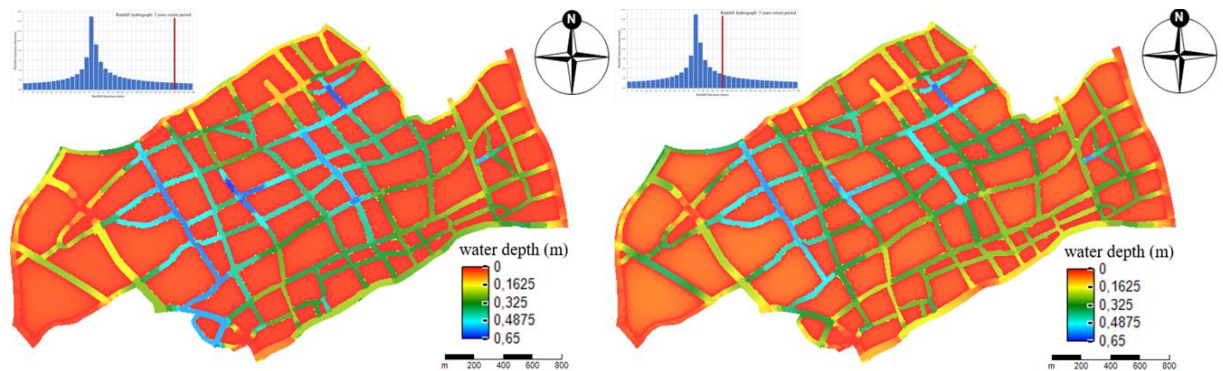


Figure 36: Maximum inundation depth at 2:40:00 (left panel) and most inundated areas 1:40:00 (right panel) for the rainfall event of 5-years return period (including drainage system)

5.3.4 Model 7b: Rainfall event of 10-years return period, including the drainage system

In model 7b, the maximum inundation depth is 0.695 meters. The moment of the maximum water depths occurs 2 hours and 25 minutes after the start of the rainfall event and 1 hour and 10 minutes after the peak of the rainfall hydrograph.

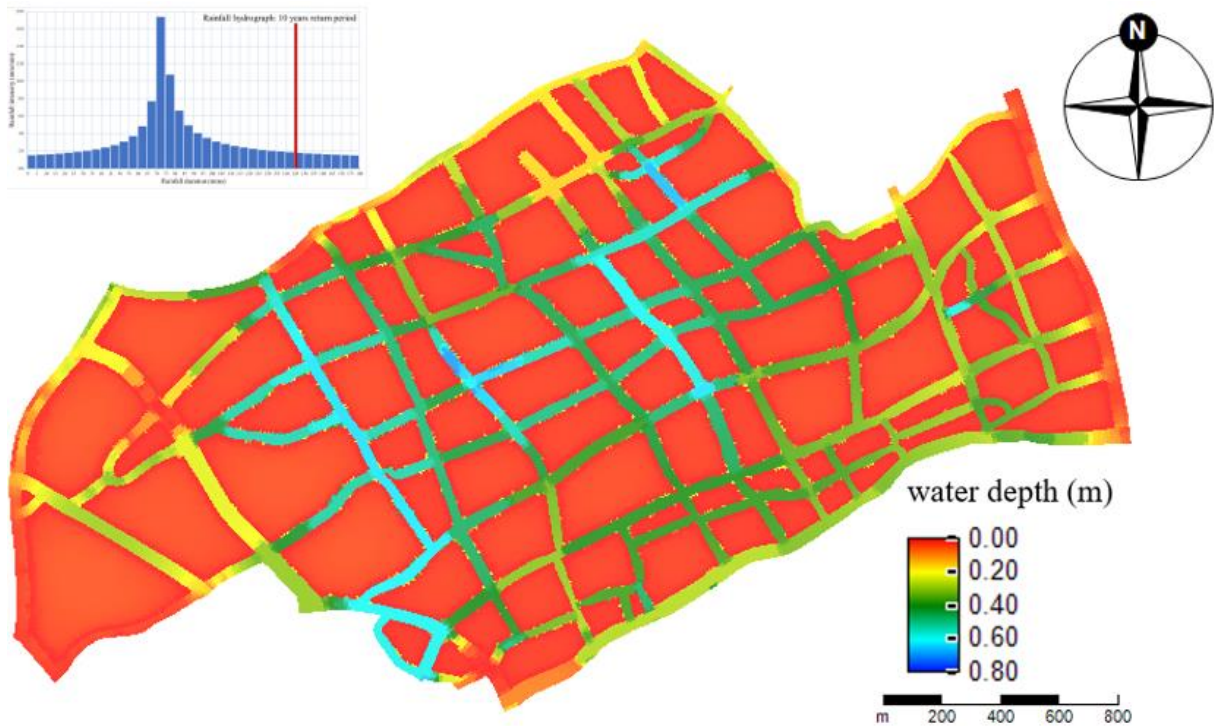


Figure 37: Maximum inundation depth for the rainfall event of 10-years return period at 2:25:00 (including drainage system)

The condition of the most inundated areas occurs 1 hour and 30 minutes after the start of the rainfall event. It is estimated that the inundation period starts at 00:45:00 and ends at 3:00:00. Thus, the duration of the inundation is 2 hours and 15 minutes.

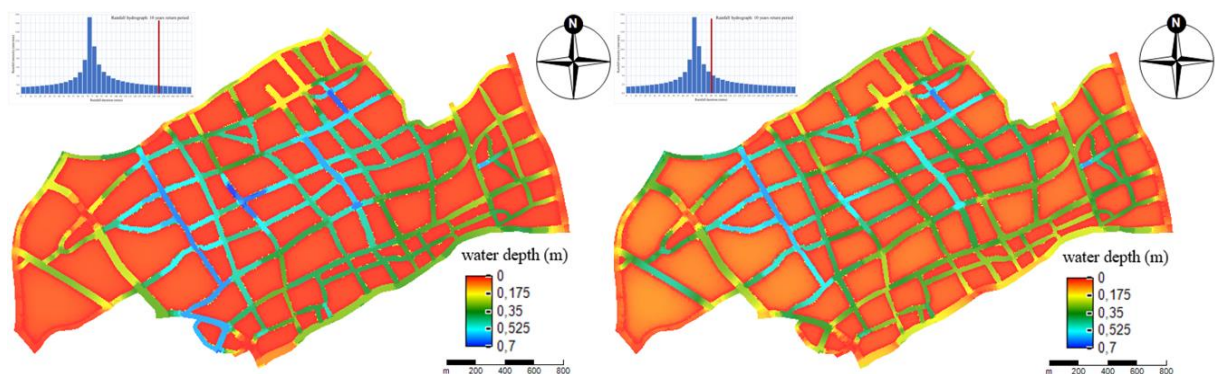


Figure 38: Maximum inundation depth at 2:25:00 (left panel) and most inundated areas 1:30:00 (right panel) for the rainfall event of 10-years return period (including drainage system)

5.3.5 Model 8b: Rainfall event of 50-years return period, including the drainage system

In model 8b, the maximum inundation depth is 0.796 meters. The maximum water depths appear 2 hours and 45 minutes compared to the moments of the beginning of the rainfall event and the peak of the hydrograph, respectively.

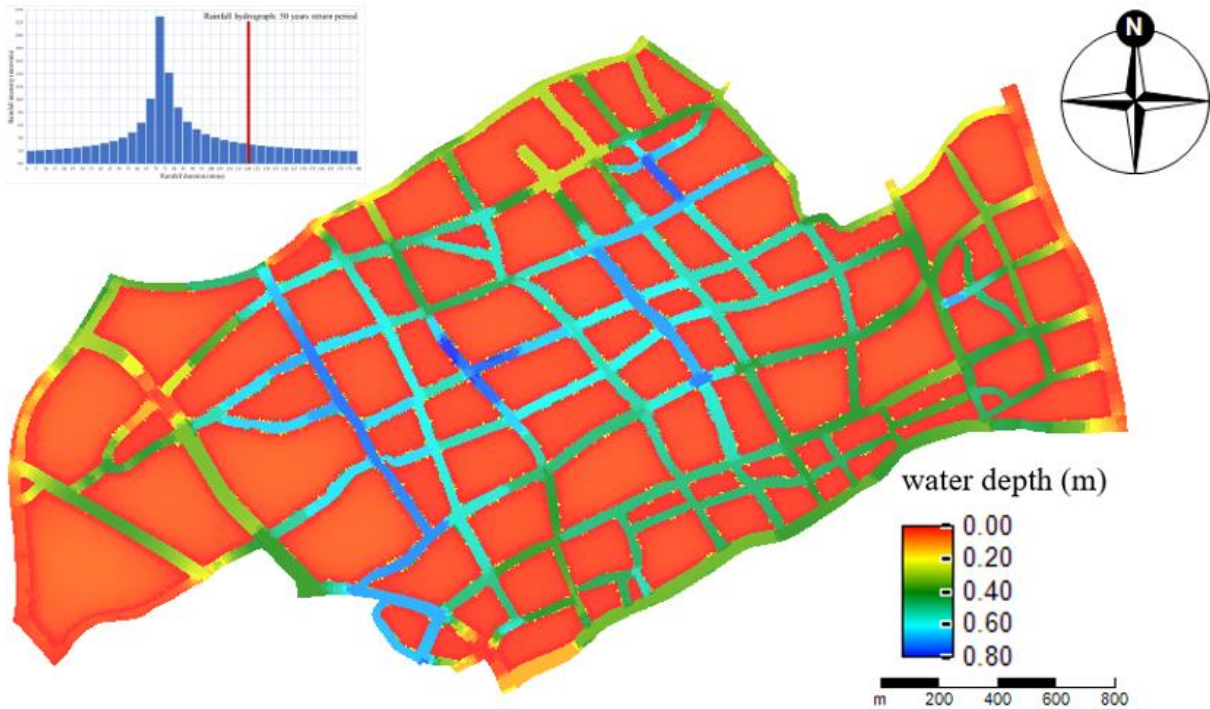


Figure 39: Maximum inundation depth for the rainfall event of 50-years return period at 2:00:00 (including drainage system)

The most inundated areas are observed 1 hour and 25 minutes after the start of the rainfall event. The inundation period starts at 00:40:00 and ends at 3:00:00. So, the inundation duration is 2 hours and 20 minutes.

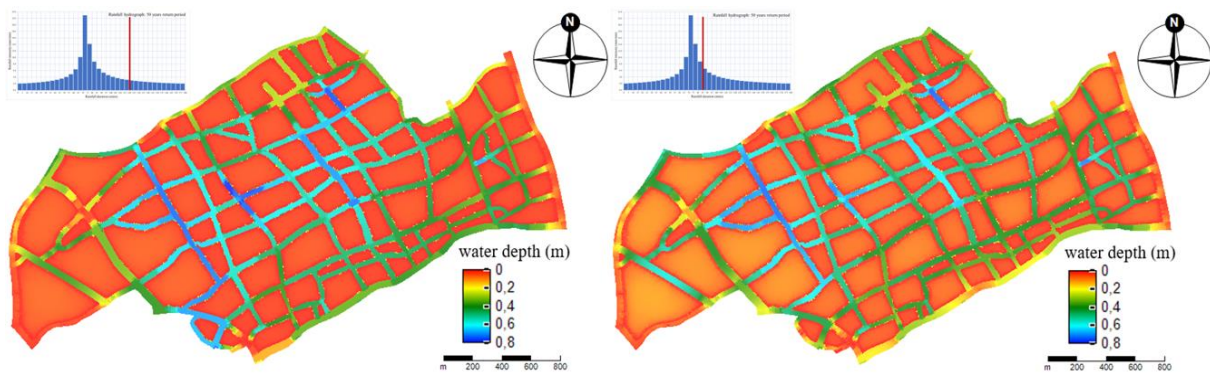


Figure 40: Maximum inundation depth at 2:00:00 (left panel) and most inundated areas 1:25:00 (right panel) for the rainfall event of 50-years return period (including drainage system)

A summary of the results of the above analysis is presented in Table 9.

Table 9: Summarized results for models 4-8, including the drainage system

Model	Return period of rainfall event (years)	Inundation (>15cm)			Maximum water depth		
		Start	End	Duration	Time of most inundated areas	Value (m)	Time
4	1	1:05:00	3:00:00	1 hour 55 mins	2:00:00	0.521	3:00:00
5	3	00:55:00	3:00:00	2 hours 5 mins	1:45:00	0.611	2:55:00
6	5	00:50:00	3:00:00	2 hours 10 mins	1:40:00	0.648	2:40:00
7	10	00:45:00	3:00:00	2 hours 15 mins	1:30:00	0.695	2:25:00
8	50	00:40:00	3:00:00	2 hours 20 mins	1:25:00	0.796	2:00:00

From Table 9, it can be concluded that there is still inundation for all the models at the end of the simulation period. Thus, the inundation duration is calculated until the end of the simulation. However, in reality a few more minutes are needed for the water level to drop below the 15 cm, leading to longer inundation periods. In addition to the information provided in Table 9, it should be mentioned that the water depth at the end of the simulation period is higher for increasing return period of the rainfall event. Also, the following conclusions can be made:

- Inundation conditions start earlier with increasing return period of the rainfall event.
- Inundation duration increases with increasing return period of the rainfall event.
- Conditions of most inundated areas occur earlier with increasing return period of the rainfall event.
- Maximum water depths increase with increasing return period of the rainfall event.
- Maximum water depths occur earlier with increasing return period of the rainfall event.

5.4 Effectiveness of the drainage system

To assess the effectiveness of the drainage system, the simulation results are compared between the cases a and b for the models 4-8. As mentioned in Table 3, case a is referring to the analysis that neglects the influence of the drainage system, while case b includes the effect of the drainage system. The inundation maps for all these models the moment of the maximum water depths are presented in Figure 57-Figure 61 in Appendix C.

By analyzing the resulted inundation maps of each model, for the case that the drainage system is not considered, the following information can be summarized.

Table 10: Summarized results for models 4-8, without including the drainage system

Model	Return period of rainfall event	Inundation (>15cm)				Maximum water depth	
		Start	End	Duration	Time of most inundated areas	Value (m)	Time
4	1	00:40:00	3:00:00	2 hours 20 mins	2:35:00	0.913	2:30:00
5	3	00:30:00	3:00:00	2 hours 30 mins	1:35:00	1.093	2:05:00
6	5	00:30:00	3:00:00	2 hours 30 mins	1:30:00	1.171	1:55:00
7	10	00:25:00	3:00:00	2 hours 35 mins	1:25:00	1.272	1:50:00
8	50	00:25:00	3:00:00	2 hours 35 mins	1:20:00	1.489	1:40:00

For Table 10, the same conclusions can be made as for Table 9.

When comparing the cases a and b for each model or the information provided in Table 9 and Table 10, the following conclusions can be made.

- Inundation conditions start later when the drainage system is included.
- Inundation conditions still exist at the end of the simulation period for both cases.
- Inundation duration decreases by around 14.1% when the drainage system is included.
- Maximum water depths decrease by around 44.7% when the drainage system is included.
- Maximum water depths occur later when the drainage system is included.

5.5 Comparison of inundation maps after simulation in SOBEK and DFM

To compare the resulted inundation maps from SOBEK and DFM, the rainfall event of 5 years return period was chosen for the simulation. The inundation maps after the simulation of this rainfall event in SOBEK and DFM are illustrated in Figure 41 and Figure 42, respectively. To compare the two maps the legend values of the resulted map from SOBEK were adjusted to those of the resulted map from DFM. The results from SOBEK include the whole Jingan District, while the results from DFM represent only the area that could be simulated due to the limitation of the software regarding the number of the input data.

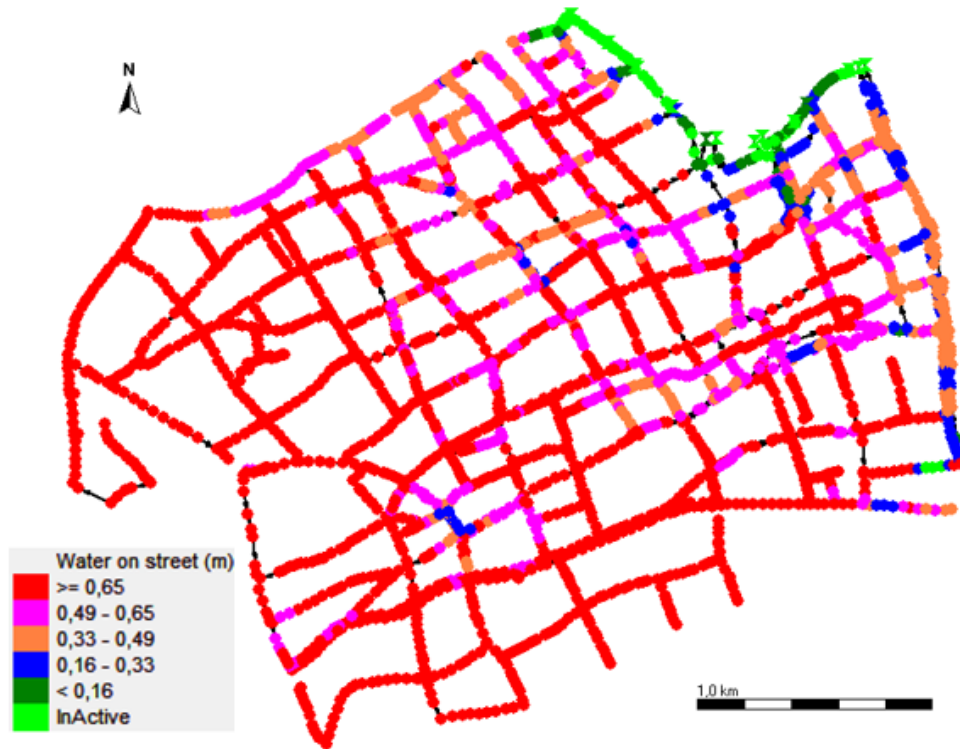


Figure 41: Water on street for the rainfall event of 5-years return period after the simulation in SOBEK

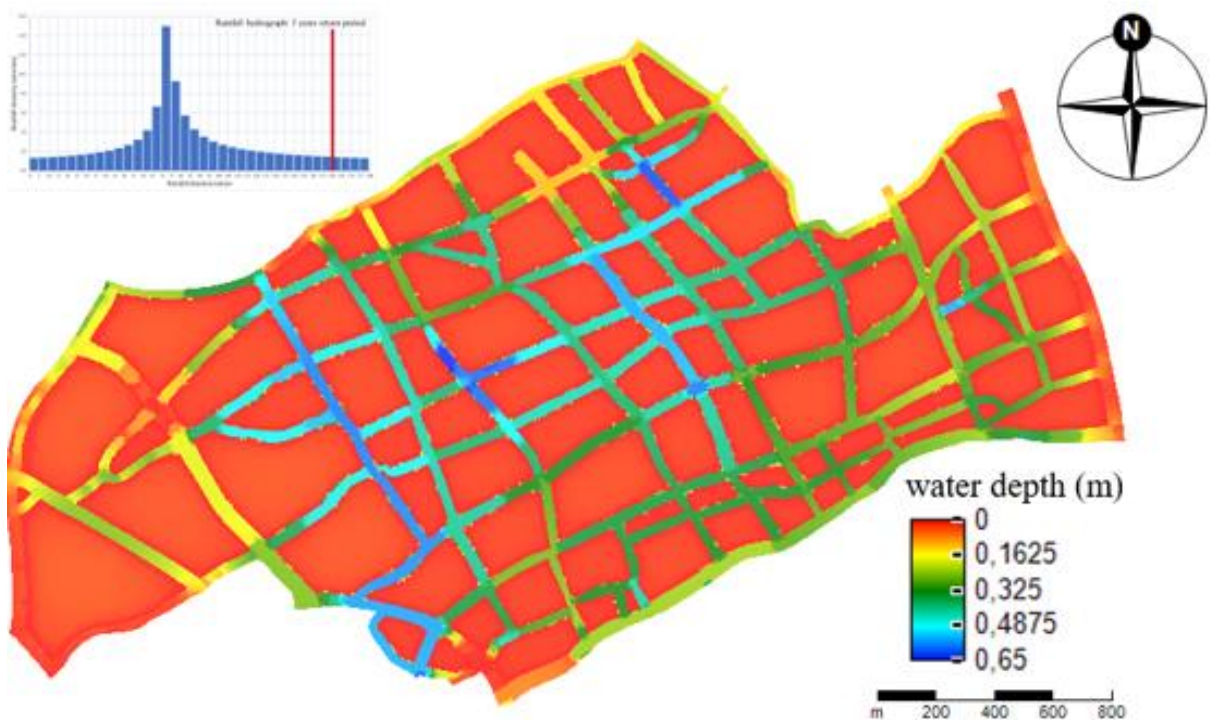


Figure 42: Maximum inundation depths for the rainfall event of 5-years return period, including the drainage system after the simulation in DFM

By comparing these maps, it can be observed that the inundation area in SOBEK (Figure 41) is larger than in DFM (Figure 42). Also, there are considerable differences regarding the maximum inundation depths. For the simulation in SOBEK, the resulted maximum water depth is around 2 meters while for the simulation in DFM it is 0.65 meters.

However, there are obvious reasons for this inconsistency in the results of the two models. Some of them are presented below:

- The results in DFM cover the whole surface of the street network, while the results in SOBEK are illustrated in points, representative of the location of the manholes of the sewer system.
- Due to the above, for the results in DFM there is a continuous water flow on the surface of the streets, while in SOBEK the water on the street is stored as is the case in reservoirs.
- The simulation in SOBEK considers the whole sewer system of Jingan District, while the simulation in DFM takes into account only around the 70% of the drainage system.

5.6 Effectiveness of the proposed flood reduction measures

In this section, the study is focused on the assessment of the effectiveness of some potential flood reduction measures. More specific, four different cases were investigated. The considered measures are mentioned below:

- i. Development of water storage areas in the block areas → model 9
- ii. Increase of drainage capacity in a single location → model 10
- iii. Combination of i and ii → model 11
- iv. Increase of drainage capacity in multiple locations → model 12

In the models that involve the increase of the drainage capacity, this measure is implemented only in a specific area of Jingan District due to the long simulation period needed. However, the analysis of the resulted inundation maps may provide sufficient information regarding the potential locations of implementation of the same measure in future studies.

The implementation of measures i-iv was applied on the model that simulates the rainfall event of 5-years return period and includes the drainage system, model 6b.

The resulted inundation maps for the models 9-12 are presented in the lower panels of Figure 44, Figure 45, Figure 46 and Figure 47, respectively. For easy comparison of these results with that of model 6b, the inundation map of this model is presented in the upper panels of these figures. Also, the range of the water depth values for all the maps is set the same with that of model 6b.

5.6.1 Model 9: Rainfall event of 5-years return period including the drainage system and the development of water storage areas

In this model, the creation of water storage areas is studied. These areas are applied in the blocks next to the most inundated locations of the street network. This is done by modifying the DSM of 5 meters resolution of Figure 26. The modified DSM that is used in model 9 is shown in Figure 43.

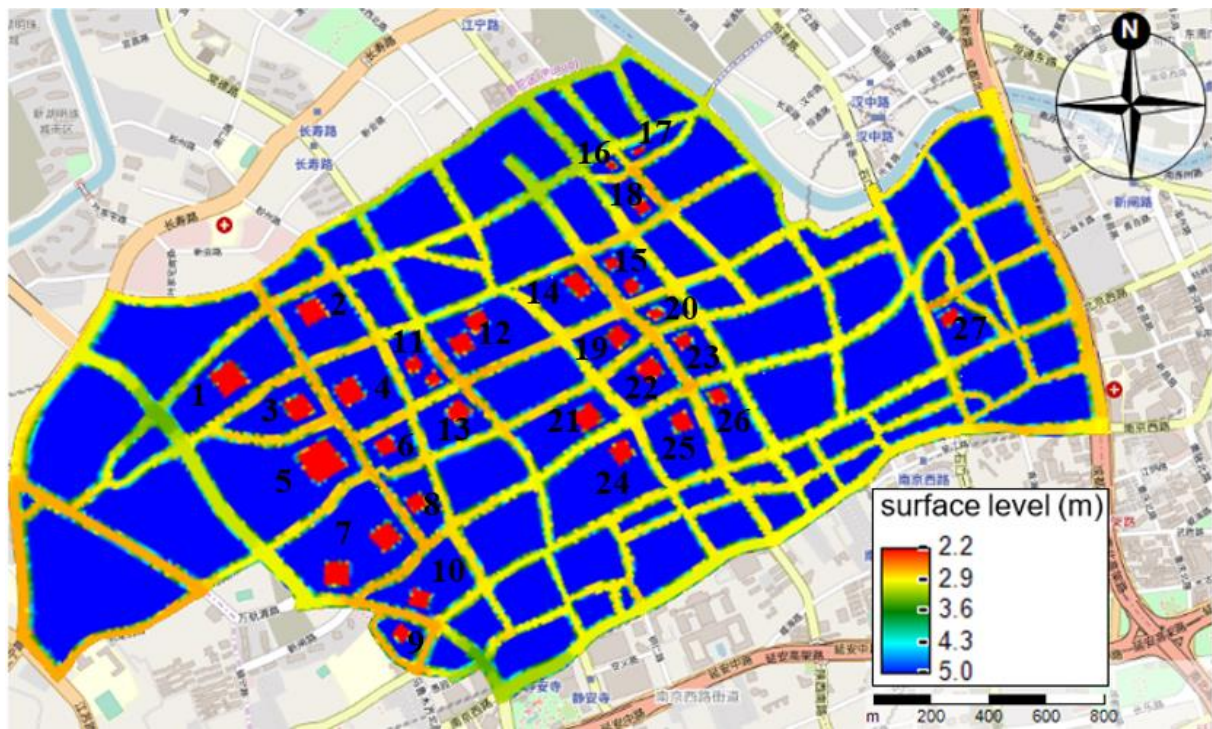


Figure 43: Modified DSM for model 9 including the water storage areas in the blocks

In Figure 43 the water storage areas are shown in red color. The new elevation value that was assigned in these areas was 2 meters. The specific locations were chosen based on the location of the most inundated streets and the availability of free space in the blocks due to the presence of buildings according to the Open Street Map in DFM. The surface of these areas is approximately 10%, or less, of the total surface area of the block that they are located. The total surface area of the blocks was estimated in QGIS. For the water storage areas, rectangular shapes were selected because it was easier to estimate their surface area. The surface area of these water storage areas was estimated in DFM and their values are shown in Table 15. The resulted inundation map of model 9 is presented in the lower panel of Figure 44.

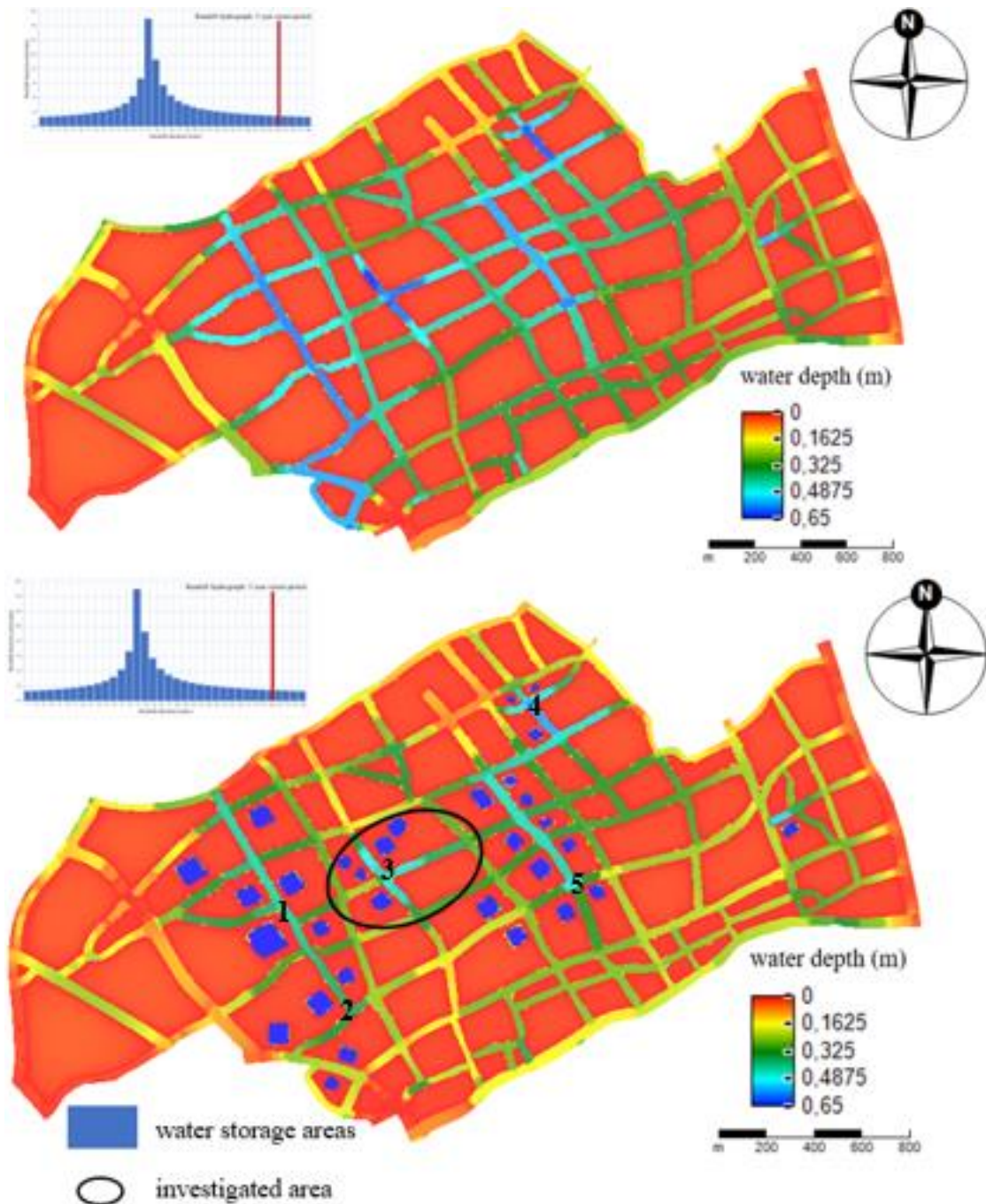


Figure 44: Maximum inundation depth for the rainfall event of 5-years return period including the drainage system, without the water storage areas at 2:40:00 (upper panel) and with the water storage areas at 3:00:00 (lower panel)

The effectiveness of this measure is assessed by selecting some points of the street network, that are located near the water storage areas, and comparing their maximum water depth in the lower panel with that in the upper panel of Figure 44. These points are illustrated in the lower panel of Figure 44 with numbers (1 - 5). The comparison of the maximum water depth for these points is presented in Table 11. The closed investigated area that is illustrated in Figure 44 is used for the comparison with the models 10, 11 and 12.

Table 11: Reduction of maximum water depth in specific points

Point	Max. water depth without measure (upper panel) (m)	Max. water depth with measure (lower panel) (m)	Difference (m)	Reduction percentage (%)
1	0.578	0.425	0.153	26.5
2	0.569	0.372	0.197	34.6
3	0.648	0.502	0.146	22.5
4	0.613	0.559	0.054	8.8
5	0.577	0.472	0.105	18.2

It is observed that the reduction in the maximum water depth is not the same for all the selected points. This is reasonable due to the different acreage of the water storage areas. As expected, the maximum reduction is observed close to the locations where the larger water storage areas were developed. Also, in general there is a reduction of the water depth in the whole map, however inundation (water depth > 15cm) is still present in almost all the streets. By comparing the upper and lower panels of Figure 44, it is estimated that in approximately 1607 meters of street length the water depth decreased to a value lower than 15 cm. Regarding the duration of the inundation, there is not significant difference between the two cases. By setting the 15 cm of water depth as the start of the inundation, the inundation period for the case that the water storage areas are included starts 5 minutes after that of the case without the measure.

5.6.2 Model 10: Rainfall event of 5-years return period including the drainage system and the increased drainage capacity in a single location

In this model a different approach is followed in which the capacity of the drainage system is modified to allow more water to escape from the surface of the streets. This is done by increasing the drainage capacity in the sinks (outfall facilities). In this case a single location with high water depths is chosen for the implementation of this measure as shown in the lower panel of Figure 45 in black circle. This location is the same with the location 3 as illustrated in the lower panel of Figure 44. In total 6 sinks (outfall facilities) were modified by assigning a discharge of 1 m³/s. The average of the maximum calculated drainage capacities in these sinks was 0.27 m³/s. The resulted inundation map of model 10 is presented in the lower panel of Figure 45.

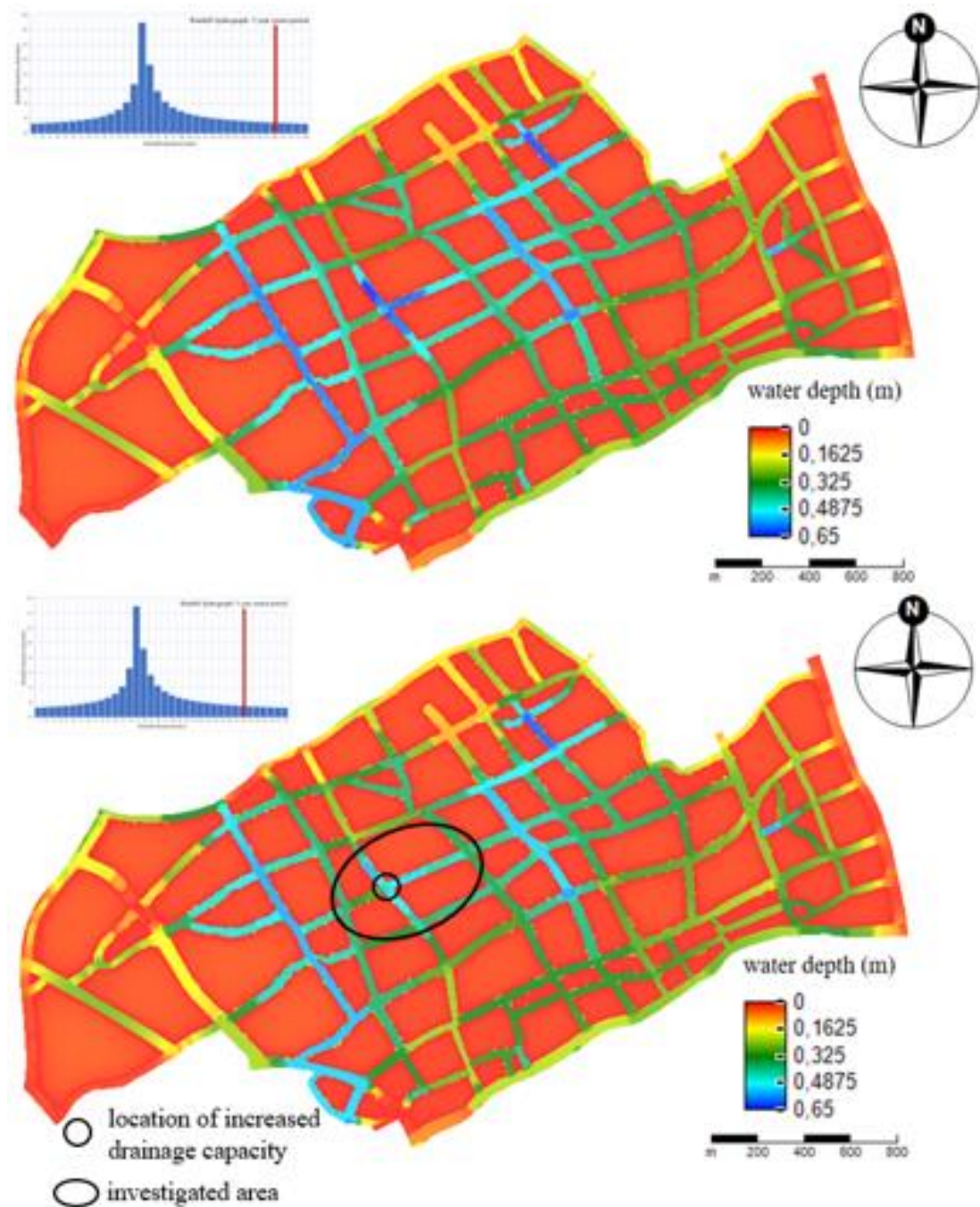


Figure 45: Maximum inundation depth for the rainfall event of 5-years return period including the drainage system, without the increased drainage capacity at 2:40:00 (upper panel) and with the increased drainage capacity at 2:30:00 (lower panel)

For the assessment of the effectiveness of this measure, the magnitude of the maximum inundation depth is examined, in the area of the implementation of the increased drainage capacity. In the base model of the upper panel, the maximum water depth in this area is 0.648 meters, while in the lower panel the value is 0.545 meters, leading to a reduction percentage of 15.9%.

The inundation period is the same for both models since only a single location of the system was modified. Also, a slight flood reduction is observed in the streets around the location of the implementation of the measure, but there are no differences regarding the length of the inundated streets. However, in a future scenario, the same approach could be applied for more locations of the street network. This may lead to shorter inundation period, lower water depth values and larger area of flood reduction.

5.6.3 Model 11: Rainfall event of 5-years return period including the drainage system, the development of water storage areas and the increased drainage capacity in a single location

In this model, the combination of the solutions that were proposed in models 9 and 10 is studied. The resulted inundation map of model 11 is presented in the lower panel of Figure 46.

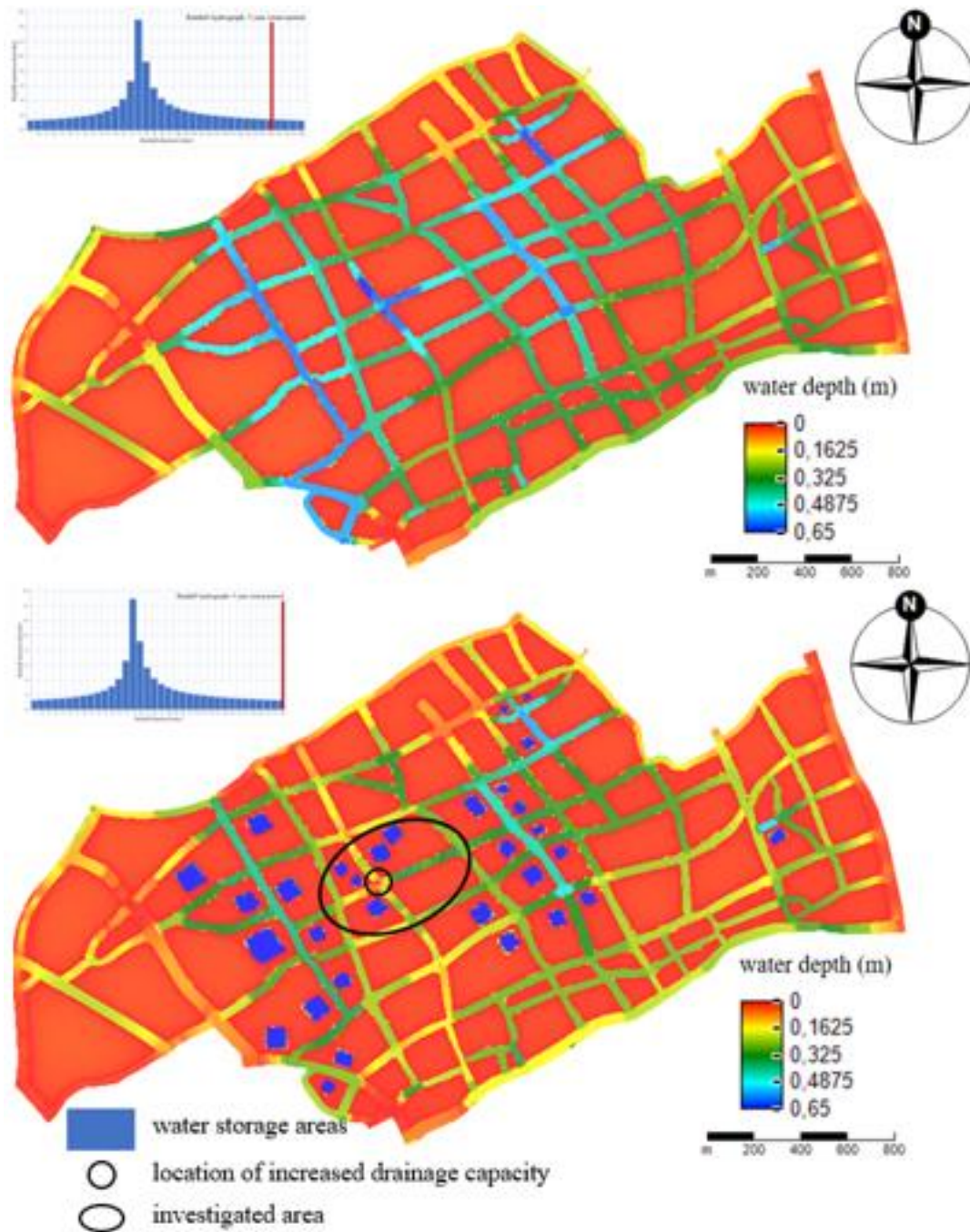


Figure 46: Maximum inundation depth for the rainfall event of 5-years return period including the drainage system, without the water storage areas and the increased drainage capacity at 2:40:00 (upper panel) and with the water storage areas and the increased drainage capacity at 3:00:00 (lower panel)

In this model, the maximum inundation depth in the area close to the implementation of the measure is estimated to be 0.372 meters. Compared with the results of model 6b, model 9 and model 10, the percentage of water depth reduction is 42.6%, 25.9% and 31.7%, respectively. Also, by comparing the lower panels of Figure 44, Figure 45 and Figure 46, it is observed that model 11 results in more considerable reduction of the water depth not only close to the area of the implementation of the increased drainage capacity but also

for the adjacent areas. It is estimated that the total street length that experienced water depth reduction below 15 cm compared to the inundation map of the upper panel is 2362 meters.

5.6.4 Model 12: Rainfall event of 5-years return period including the drainage system and the increased drainage capacity in multiple locations

In this model, the location 3 is studied again. However, the increase of the drainage capacity is investigated in multiple locations near the area of interest. In total 25 sinks were modified by assigning a discharge of 1 m³/s. The locations where the drainage capacity increased are illustrated in the lower panel of Figure 47.

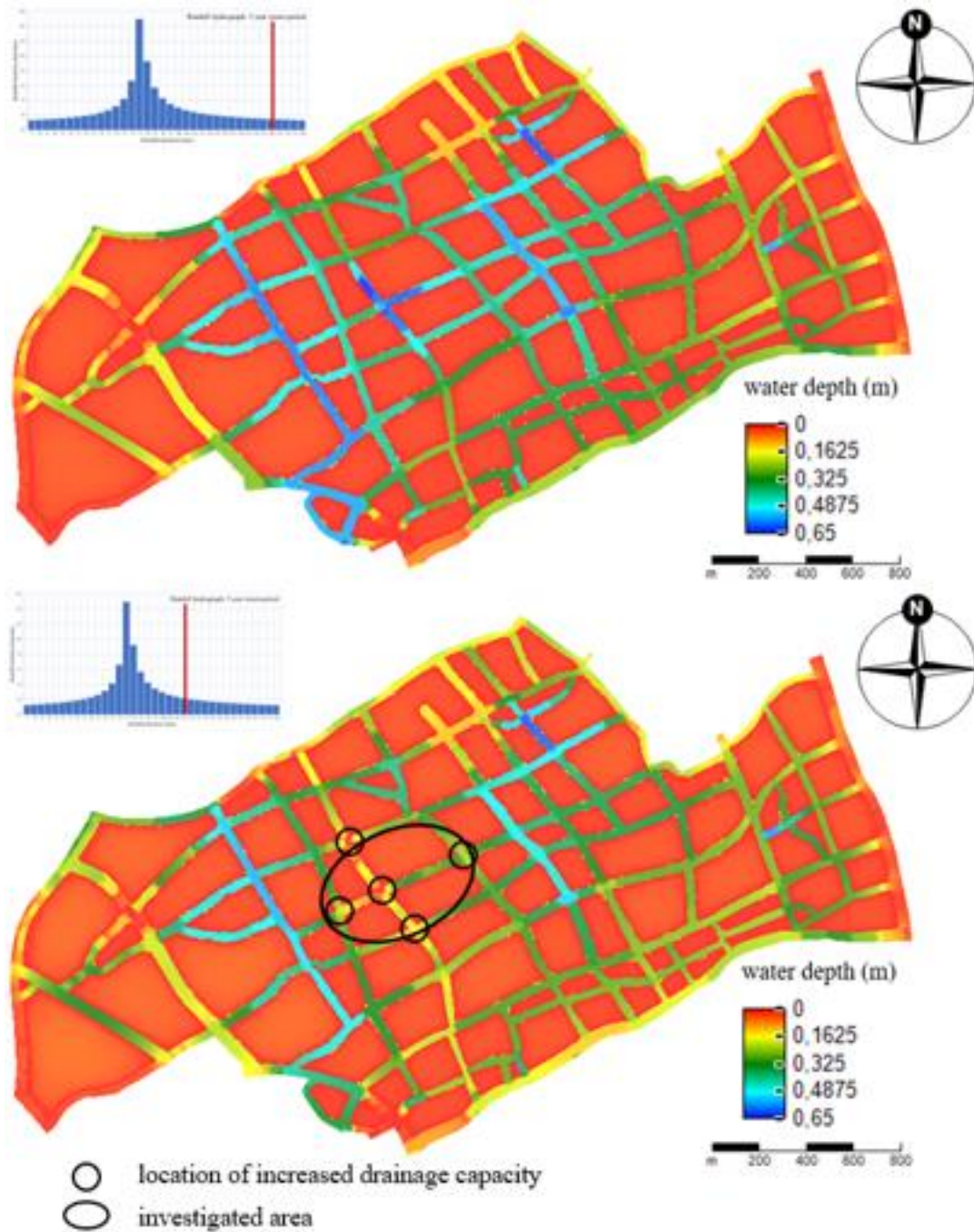


Figure 47: Maximum inundation depth for the rainfall event of 5-years return period including the drainage system, without the increased drainage capacity at 2:40:00 (upper panel) and with the increased drainage capacity at 1:55:00 (lower panel)

By comparing the maps of Figure 47, it is observed that the maximum water depth is 0.648 meters for model 6b and 0.353 meters for model 13. Thus, there is a 45.5% reduction of the maximum water depth. However, the reduction of the water depth out of the investigated area of Figure 47 is not significant. The total street length in which the water depth decreased below 15 cm is 467 meters and is located only inside the investigated area of the map. This is reasonable due to the initial large water depths in this area.

6 DISCUSSION

6.1 Input data

In this section, the quality and the accuracy of the input data are discussed in order to have a better understanding with regards to the uncertainties and the weaknesses of the model that was developed.

Firstly, for the numerical calculation of the water flow, the development of the grid included the main streets of Jingan District. However, a few secondary streets, where water can flow in real situations, were ignored. Also, due to the check of the grid's orthogonality, the width of the streets became larger than reality, causing more water to flow on the streets. Since the streets were wider, this means that the surface area of the building blocks decreased, leading to less water volume in these areas.

Regarding the representation of the surface elevation, the initial provided surface elevation map of 5 meters resolution was not used. Since the interest of the research was based on the water flow on the surface of the streets, the surface elevation map was modified according to the simplifications that were described in chapter 4.2. This was done in order to achieve consistency between the 1D model in SOBEK and the 2D model in DFM and between the grid and the surface elevation map. Thus, the surface elevation map that was finally used provides just an approximation of the elevation of the streets. These simplifications add uncertainties in the results of the model compared to the situation where the real location and elevation of the buildings are considered.

In addition, in the current 2D model, only sinks were considered that are referred to the locations of the gullies on the streets. The flow characteristics in these locations were calculated in the 1D model for the sewer system in SOBEK. Also, since there were no data regarding the number and the location of the outfall facilities across the river, some reasonable assumptions were made as described in Appendix B. Moreover, for the calculation of the runoff area for each gully, a simplified approach was adopted in which the surface area of each block was equally distributed to the gullies. However, a more detailed calculation is needed since the distance between the gullies is not constant. This would lead to more accurate calculation of the runoff discharges.

In addition, water discharges can flow into the area of interest from the adjacent districts contributing to the increase of the flood characteristics. However, in this study, the flow conditions in the borders with the adjacent districts were unknown. For a proper analysis and assessment of the model, sources should also be included with known water flow conditions in these areas. Also, the infiltration of the soil should be included in the input data since this is part of the hydrological cycle in an urban area.

Furthermore, the surface elevation of the urban area is represented in the model of the sewer system with the parameter of the street level. In order to achieve consistency between this model with the 2D model of the overland flow, the surface elevation values should be the same with the street level parameter. However, since the sources of the data for the sewer system and the surface elevation were different, their values were not the same.

Uncertainties about the results of the developed model arise regarding the hydrographs of the rainfall events that were used for the simulation. Considering the historical rainfall events, the data were taken from the stations of Longhua and Pudong, which are out of the limits of Jingan District. This may contribute to a deviation of the simulation results from the flood characteristics of the real flood event in Jingan District. Also, for all the simulated historical rainfall events the time step for the measurements was 1 hour. However, a time step of 1 hour is not suitable for the hydraulic modelling of flooding, leading to less reliable inundation maps. Since the flooding is much more of a flash-flood type, a time step between 5-10 minutes is more reasonable. Regarding the rainfall events with diverse return periods that were generated from the Chicago hydrograph, their duration was 3 hours. However, a more detailed analysis should be performed in which rainfall events with diverse rainfall durations should be simulated in order to find the event that corresponds to the local system. In addition, the type of these hydrographs includes only that part of the rainfall event with the peak rainfall intensity. But, in a real situation, rainfall events with lower

intensities may occur before and after this peak. These rainfall periods should be included in the analysis since they add water in the system and influence the way that the area of interest is flooded and relieved. An additional issue occurs when thinking about the reliability of the data for the drainage system of the area. The data for the dimensions of the system, such as the diameters of the pipes, were used without checking for divergences from the real situation. Also, there were not data about the maintenance status of the system. Since the local drainage system is old and includes both large and small pipe diameters, clogging events in some small pipes could be possible.

6.2 Flood hazard maps

In this section, the discussion is focused on the flood hazard maps with regards to the differences between the rainfall events with diverse return periods, the drainage system, and the flood reduction measures.

Firstly, in this study, due to the limitation of the current version of DFM regarding the number of the input data, it was not possible to include the sewer system of the whole Jingan District. Thus, only a part of Jingan District was simulated. With an updated version of DFM, the simulation of the whole Jingan District would be possible in future researches.

The flood hazard maps for the rainfall events of 1, 3, 5, 10 and 50 years return period were discussed in chapter 5.3 and 5.4. As it was expected, the characteristics of the flood events (water depth and duration) are more severe for increasing return period of the rainfall event. From the estimation of the inundation period, it can be argued that the simulation period should be chosen longer than the period of the rainfall event since at the end of the simulation there is a considerable acreage of land that is still inundated. Also, for the rainfall event of 1-year return period it was observed that the maximum inundation depth occurs at the end of the simulation period. This is an additional reason for the prolongation of the simulation period since a higher water depth may be present after the end of the current simulation period.

Regarding the assessment of the drainage system, the comparison between the inundation maps of cases a and b for models 4–8, showed that there is a considerable reduction in the inundation duration and maximum water depth, pointing out the significant place that the drainage system possesses in the study of urban flooding.

Even though for the flood reduction measures only two possible solutions were investigated: creation of water storage areas and increase of drainage capacity, the results showed that with a proper combination of measures a significant flood reduction can be achieved. Regarding the consideration of water storage areas, the available space for the implementation of this measure was only the 10% of each block, based on the Open Street Map. However, since it is common for urban areas to change fast, more recent and updated maps should be used in order to avoid the situation in which the proposed storage areas coincide with the location of existing buildings. Regarding the increase of the drainage capacity, the value of $1 \text{ m}^3/\text{s}$ was selected in the models 10, 11 and 12. Also, the number of the modified sinks was based on the number of the sinks that are located in the intersections of the streets as shown in the inundation maps of these models. However, both the value of the increased drainage capacity and the number and location of the sinks can be improved in order to achieve better flood reduction results. For example, a lower value than $1 \text{ m}^3/\text{s}$ can be used for the drainage capacity, but more locations of implementation of the measure can be considered.

7 CONCLUSIONS AND RECOMMENDATIONS

7.1 Conclusions

7.1.1 Validation of model

For the assessment of the model numerous factors were considered. By analyzing the input data and the results of the model, it can be argued that the created model in DFM can simulate some processes, however the validation of the model is not yet achieved due to the simplifications that were made in the model and the lack of up to date and precise data. For example, the surface elevation map that includes the real location and elevation of the buildings should be considered instead of the simplified version that was used where the same elevation was assigned in the building block areas. Also, there were not available reported flood levels to perform a proper validation and the results were compared with the results of another study and the reported flood streets as shown in Figure 28. However, it would be more reasonable to validate the results of the model with monitored data regarding the characteristics of the real flood such as the water depth and the inundation period.

7.1.2 Flood hazard maps and DSM

By observing the inundation maps of all the simulated rainfall events (Figure 27, Figure 29, Figure 30, Figure 31, Figure 33, Figure 35, Figure 37 and Figure 39) and the surface elevation map of Figure 26, it can be argued that the water is accumulated in the low-lying areas of the urban area, leading to higher water depths in these locations. The extent of the inundated areas depends on the magnitude and the distribution of the rainfall intensity over time which is shown in the hydrograph of the respective rainfall event.

7.1.3 Flood hazard maps for the historical rainfall events

By comparing the hydrographs for the rainfall events of August 1997 (Figure 23) and September 2013 (Figure 24), it is observed that the storm volume for the rainfall event of August 1997 is higher than that of September 2013. More specific the volume expressed in mm is 146.2 mm for August 1997 and 141.0 mm for September 2013. However, the maximum inundation depth for September 2013 is around 0.38 meters, while for August 1997 is around 0.24 meters. This can be justified by the effect of the combination of the rainfall duration and rainfall intensity of the two events. For August 1997 the rainfall duration is 41 hours and the maximum rainfall intensity is 26.4 mm/hour, while for September 2013 the rainfall duration is 3 hours and the maximum rainfall intensity is 73.8 mm/hour. This means that for the event of August 1997 the precipitated water volume is distributed over a longer rainfall period than that of September 2013, giving time for the drainage system to absorb the rainwater, reducing the inundation depth.

Also, by comparing the inundation maps in Figure 27, Figure 29 and Figure 30 for August 2005, August 1997 and September 2013, respectively, it is observed that the most severe flood event regarding the maximum water depth is that of September 2013, followed by August 2005 and August 1997. However, this was not verified with recorded field data during these rainfall events. Regarding the inundation duration, the event of August 2005 (32 hours) lasted more than that of August 1997 (25 hours) and September 2013 (6 hours). However, the estimation of the inundation duration for the events of August 2005 and September 2013 was based on the end of the simulation period, since there was still inundation at that moment.

7.1.4 Comparison of 1D and 2D inundation model simulation

Furthermore, a comparison between the inundation maps of SOBEK and DFM was tried. However, SOBEK illustrates only the nodes (gullies) and the pipelines of the sewer network and not the connection of the gullies on the surface. This means that the water flow on the street surface is not possible. This leads to the conclusion that the results of the models cannot be compared. Even though both models use the same

rainfall events for the simulation of the flood event, SOBEK simulates the flow of the water in the pipeline network and shows the remaining water as storage water on the surface of each gully. On the other hand, DFM simulates the overland flow in which there is a continuous flow of water on the surface of the simulated area.

7.1.5 Effectiveness of drainage system

Regarding the assessment of the effectiveness of the drainage system, the rainfall events were simulated with and without the inclusion of the drainage system. The results showed that the inclusion of the drainage system in the model plays an important role in the flood reduction, since it is observed that the flood characteristics such as the duration and the maximum water depth decrease by around 14.1% and 44.7%, respectively. Thus, it is critical to mention that due to their considerable contribution in the relief of the flooded area, the simulation of the flood events in general should be performed by considering the influence of the local drainage systems.

7.1.6 Effectiveness of flood reduction measures

As flood reduction measures, four cases were investigated: i) creation of water storage areas, ii) increase of drainage capacity in one location, iii) combination of i and ii, and iv) increase of drainage capacity in multiple locations. All these measures were implemented in the model that considers the rainfall event with 5-years return period. The analysis of the results showed that it is possible to reduce the flood depth by a percentage that depends on the considered measure and the location on the map.

More specific, an investigation area was selected as shown in the lower panels of Figure 44, Figure 45, Figure 46 and Figure 47 and the water depth reduction was studied compared to the base model without the inclusion of the measures. For measures i, ii, iii and iv the percentage of flood depth reduction was 22.5%, 15.9%, 42.6% and 45.5%, respectively. This means that by increasing the drainage capacity in several locations inside the investigation area, the water depth reduces by a higher percentage compared to the other measures. However, in this case, additional problems arise regarding the availability of water storage space or the way that the water flow is drained towards the receiving water body. Also, the capability of the receiving water body to handle the additional amount of water without causing problems downstream is a determining factor for the implementation of this measure. The same concerns apply for the measures ii and iii that include increased drainage capacity, but the less points of the modified drainage capacity make these measures more attractive than measure iv. Finally, the created water storage areas of measure i and iii cover around 10%, or less, of the building blocks that were located near the areas with the maximum water depth. Also, only the blocks with available free space were considered. However, this percentage may be lower since less space may be available in the current state of the urban area. Besides the reduction in the maximum water depth, it was found that for measures i-iv the total length of the streets that were no longer inundated compared to the base model situation is 1607, 0, 2362 and 467 meters, respectively.

7.2 Recommendations

In this section, a list is presented of the most important aspects that could be considered in a future research. The inclusion of these factors in the development of the model may lead to more realistic and accurate results. This list is presented below:

- develop a grid based on more updated and detailed maps that illustrate the current state of the urban area regarding the exact location of the building blocks and the width of the streets. Also, a grid finer than 15 meters would be a more useful tool.
- use a surface elevation map that includes the real elevation and location of the buildings. In this way, ponding phenomena would take place inside the building blocks which is realistic in urban areas.

- improve the 1D model for the sewer system by including the real number, the location and the prevailing water flow conditions in a) the outfall facilities of the system across the river and b) the connecting points with the sewer systems of the adjacent districts.
- perform a more detailed analysis in the calculation of the block surface area that corresponds to each manhole of the sewer system by taking into account the geometry of the blocks and the distances between the nodes of the network.
- make the street level parameter of each node in the model sewer system consistent with the surface elevation values.
- perform the flood simulations for the whole Jingan District by using an updated version of DFM. In this way, all the 2785 outfall facilities to the sewer system would be included in the analysis.
- simulate the flood events for recorded historical rainfall intensities with a timestep lower than 1 hour to achieve more detailed results.
- obtain monitored water levels in the flood prone areas in order to be used for the validation of the models.
- consider and assess additional measures such as underground tunnels, pumping stations and green areas.

BIBLIOGRAPHY

- Allit, R., Blanksby, J., Djordjevic, S., Maksimovic, Č. & Stewart, D. (2009) Investigations into 1D-1D and 1D-2D Urban Flood Modelling. *WaPUG Autumn Conference n.25*, November 2009, Blackpool, UK.
- Awakimjan, I. (2015). Urban Flood Modelling. Recommendations for Ciudad Del Plata. *Bachelor Thesis*. Faculty of Engineering Technology (CEM). University of Twente.
- Beven, K. (2004). Robert E. Horton's perceptual model of infiltration processes. *Hydrological Processes*, 18, 3447-3460.
- Boonya-Aroonnet, S., Weesakul, S., & Mark, O. (2002). Modelling of Urban Flooding in Bangkok. *Ninth International Conference on Urban Drainage*, Portland, Oregon, USA.
- Boonya-Aroonnet, S., Maksimović, Č., Prodanović, D., & Djordjević, S. (2007). Urban pluvial flooding: development of GIS based pathway model for surface flooding and interface with surcharged sewer model. *Novatech 6th Conference of Sustainable Techniques and Strategies in Urban Water Management*, 25-27 June 2007, Lyon, France.
- Butler, D., & Davies, J. W. (2011). *Urban Drainage* (Third Edition). Oxon, *Spon Press*.
- Carr, R. S. & Smith, G. P. (2006). Linking of 2D and pipe hydraulic models at fine spatial scales. *7th International Conference on Urban Drainage Modelling and 4th International Conference on Water Sensitive Urban Design*, 2-7 April 2006, Melbourne, Australia, Vol. 2, pp. 361-368.
- Chang, T.J., Wang, C.H., Chen, A.S. (2015). A novel approach to model dynamic flow interactions between storm sewer system and overland surface for different land covers in urban areas. *Journal of Hydrology*.
- Chow, V. T. (1959). *Open – Channel Hydraulics*.
- Deltares (2018). *SOBEK. Hydrodynamics, Rainfall Runoff and Real Time Control. User Manual*. Deltares.
- Deltares (2019a). *D-Flow Flexible Mesh. User Manual*. Deltares.
- Deltares (2019b). *D-Flow Flexible Mesh. Technical Reference Manual*. Deltares.
- East China Normal University (2019). Data Digital Surface Model (5 meters).
- United States Environmental Protection Agency (U.S. EPA) (2003). Protecting Water Quality from Urban Runoff. https://www3.epa.gov/npdes/pubs/nps_urban-facts_final.pdf
- Fan, Y., Ao, T., Yu, H., Huang, G., & Li, X (2017). A Coupled 1D-2D Hydrodynamic Model for Urban Flood Inundation. *Advances in Meteorology*.
- GISGeography. DEM, DSM & DTM Differences – A Look at Elevation Models in GIS. <https://gisgeography.com/dem-dsm-dtm-differences/>
- Google Maps. <https://maps.google.com>
- Henonin, J., Russo, B., Mark, O., & Gourbesville, P. (2013). Real-time urban flood forecasting and modelling – a state of the art. *Journal of Hydroinformatics*, 717-736.
- Information Office of Shanghai Municipality. Mengqing Theme Park on Environmental Protection of Suzhou Creek. History of Environmental Protection for Suzhou Creek. <http://touch.shio.gov.cn/en/proposed-interviews/detailindex.aspx?id=8>

- INTERMAP. The Risks of Hazard. Three Common Types of Flood Explained. <https://www.intermap.com/risks-of-hazard-blog/three-common-types-of-flood-explained>
- IPA (Institute of Public Art). <https://www.instituteforpublicart.org/case-studies/jingan-sculpture-park/>
- Jiang, Y., Zevenbergen, C., & Ma, Y. (2018). Urban pluvial flooding and stormwater management: A contemporary review of China's challenges and "sponge cities" strategy. *Environmental Science and Policy*, 80, 132-143.
- Lashford, C., Rubinato, M., Cai, Y., Hou, J., Abolfathi, S., Coupe, S., Charlesworth, S., & Tait, S. (2019). SuDS & Sponge Cities: A Comparative Analysis of the Implementation of Pluvial Flood Management in the UK and China. *Sustainability*, 11, 213.
- Ke, Q. (2014). Flood risk analysis for metropolitan areas – a case study for Shanghai. *Delft Academic Press*.
- Ke, Q., Jonkman, S. N., van Gelder, P., & Bricker, J. (2018). Frequency Analysis of Storm-Surge-Induced Flooding for the Huangpu River in Shanghai, China. *Journal of Marine Science and Engineering*. 6(2), [70].
- Mapcarta. <https://mapcarta.com>
- Mark, O. & Drordjević, S. (2006). While waiting for the next flood in your city. *7th International Conference of Hydroinformatics*, 4-8 September 2006, Nice, France.
- Mark, O., Apirumanekul, C., Kamal, M., & Praydal, P. (2001). Modelling of Urban Flooding in Dhaka City. *UDM'01*, Orlando, Florida, USA.
- Mark, O., Weesakul, S., Apirumanekul, C., Aroonnet, S. B., & Drordjević, S. (2004). Potential and limitations of 1D modelling of urban flooding. *Journal of Hydrology* 299, 284-299.
- Meng, X., Zhang, M., Wen, J., Du, S., Xu, H., Wang, L., & Yang, Y. (2019). A Simple GIS-Based Model for Urban Rainstorm Inundation Simulation. *Sustainability*, 11, 2830.
- PagerPower, Urban & Renewables. Digital Elevation Models (DEM): Terrain (DTM) or Surface (DSM) Data? <https://www.pagerpower.com/news/differences-digital-elevation-model-dtm-dsm/>
- Poleto, C., & Tassi, R. (2012). Sustainable Urban Drainage Systems, Drainage Systems, Prof. Muhammad Salik Javaid (Ed.), ISBN: 978-953-51-0243-4.
- QGIS. <https://qgis.org/en/site/about/index.html>
- Schmitt, T. G., Thomas, M., & Ettrich, N. (2004). Analysis and modeling of flooding in urban drainage systems. *Journal of Hydrology* 299, 300-311.
- Shanghai Climate Center (2019). Data rainfall events (August 1997, September 2013, August 2005).
- Shanghai Daily. Shanghai merges downtown Jing'an with Zhabei District (2015). <https://archive.shine.cn/metro/public-services/Shanghai-merges-downtown-Jingan-with-Zhabei-District/shdaily.shtml>
- Shanghai Municipal People's Government. *Basic Facts*. Geographic Location. www.shanghai.gov.cn/shanghai/node23919/node24059/node24061/userobject22ai36489.html
- Shanghai Water Authority (2019). Data sewer system (Jingan District).
- Sutter, V. (2019). 2D urban flood modelling using a numerical model of Delft3D flexible mesh: A case study in downtown of Shanghai city, China. Delft University of Technology.

- Tomičić, B., Mark, O., & Kronborg, P. (1999). Urban Flooding Modelling Study at Playa de Gandia. *Third DHI User Conference*, Hørsholm, Denmark.
- Van de Ven, F. H. M. (2016). Water Management in Urban Areas. *Lecture notes CIE5510*. Faculty of Civil Engineering and Geosciences, Water Management, Section of Water Resources, Delft University of Technology.
- Wang, A., Qu, N., Chen, Y., Li, Q., & Gu, S. (2018). A 60-Minute Design Rainstorm for the Urban Area of Yangpu District, Shanghai, China. *Water*, 10, 312.
- World Meteorological Organization (WMO) and Global Water Partnership (GWP) (2008). Urban Flood Risk Management - A Tool for Integrated Flood Management, APFM Technical Document No. 11, *Associated Programme on Flood Management (APFM)*.
- Xie, J., Wu, C., Li, H., & Chen, G. (2017). Study on Storm-Water Management of Grassed Swales and Permeable Pavement Based on SWMM. *Water*, 9,840.
- Yuan, Y., Xu, Y., & Arulrajah, A. (2017). Sustainable Measures for Mitigation of Flooding Hazards: A Case Study in Shanghai, China. *Water*, 9, 310.

APPENDIX A: RAINFALL EVENTS

A.1 Rainfall events from Chicago design storm

The rainfall distribution over time for the rainfall events that were generated from the Chicago hydrograph is presented in Table 12.

Table 12: Rainfall distribution over time

Time Step (min)	Rainfall intensity (mm/min)				
	1yr	3yr	5yr	10yr	50yr
5	0.585	0.821	0.931	1.080	1.426
10	0.616	0.865	0.980	1.137	1.501
15	0.651	0.914	1.036	1.202	1.587
20	0.692	0.972	1.101	1.278	1.687
25	0.740	1.039	1.178	1.366	1.804
30	0.797	1.119	1.269	1.472	1.943
35	0.867	1.216	1.379	1.600	2.112
40	0.953	1.338	1.517	1.760	2.324
45	1.065	1.495	1.695	1.966	2.596
50	1.215	1.706	1.934	2.244	2.962
55	1.431	2.008	2.277	2.641	3.487
60	1.768	2.482	2.814	3.264	4.310
65	2.386	3.349	3.797	4.405	5.816
70	3.934	5.522	6.260	7.262	9.588
75	9.178	12.882	14.605	16.942	22.369
80	5.587	7.842	8.890	10.313	13.617
85	3.353	4.706	5.335	6.189	8.172
90	2.453	3.443	3.903	4.528	5.979
95	1.964	2.757	3.126	3.626	4.787
100	1.655	2.324	2.634	3.056	4.035
105	1.441	2.023	2.294	2.661	3.513
110	1.284	1.802	2.043	2.370	3.129
115	1.162	1.631	1.849	2.145	2.832
120	1.065	1.495	1.695	1.966	2.596
125	0.986	1.384	1.569	1.820	2.403
130	0.920	1.291	1.464	1.698	2.242
135	0.864	1.212	1.374	1.594	2.105
140	0.815	1.144	1.297	1.505	1.987
145	0.773	1.085	1.230	1.427	1.884
150	0.736	1.033	1.171	1.359	1.794
155	0.703	0.987	1.119	1.298	1.713
160	0.673	0.945	1.072	1.243	1.641
165	0.647	0.908	1.029	1.194	1.576
170	0.623	0.874	0.991	1.149	1.518
175	0.601	0.843	0.956	1.109	1.464
180	0.580	0.815	0.924	1.071	1.415

A.2 Historical rainfall events

The hydrographs for the historical rainfall events of August 1997 and September 2013 for the data from Pudong and Longhua stations are presented in Figure 48-Figure 51.

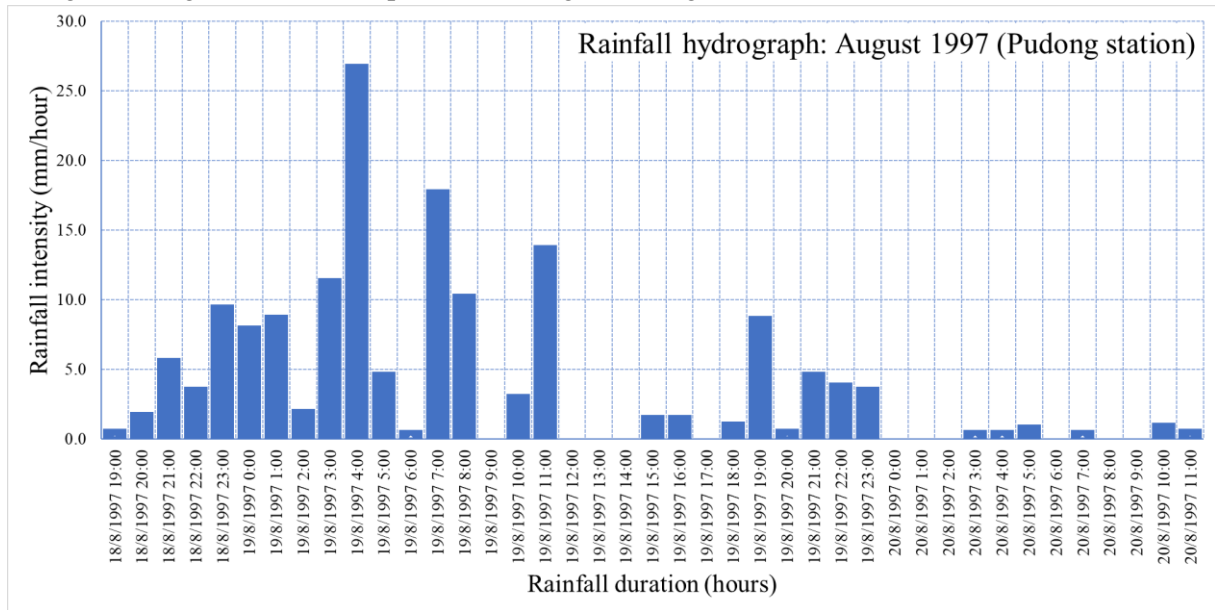


Figure 48: Rainfall hydrograph for August 1997 at Pudong station

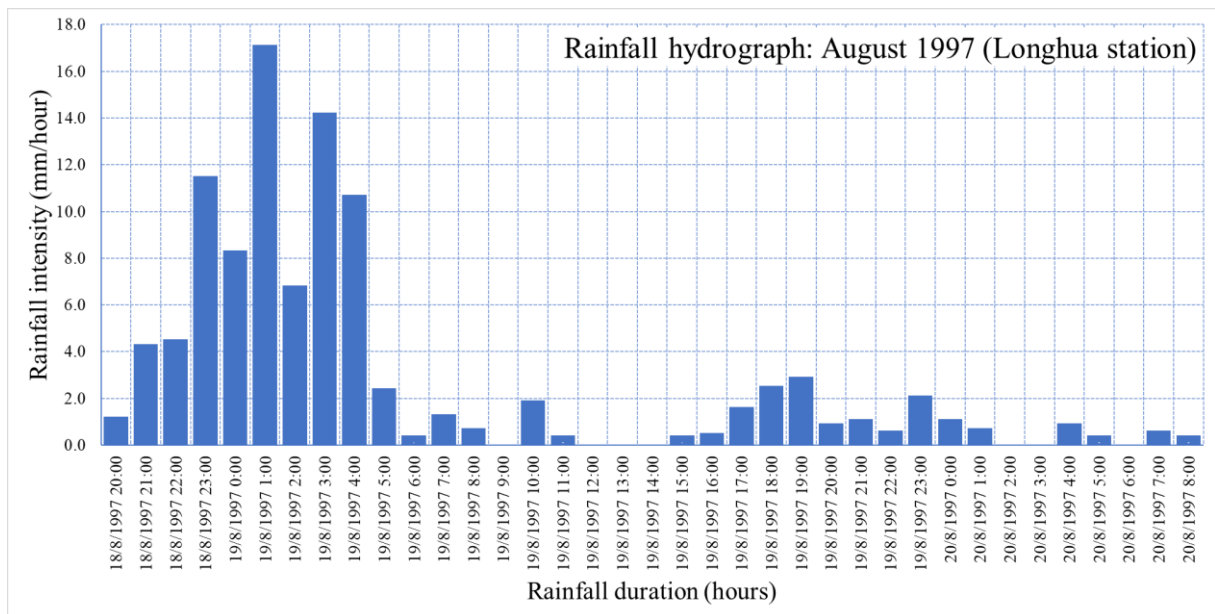


Figure 49: Rainfall hydrograph for August 1997 at Longhua station

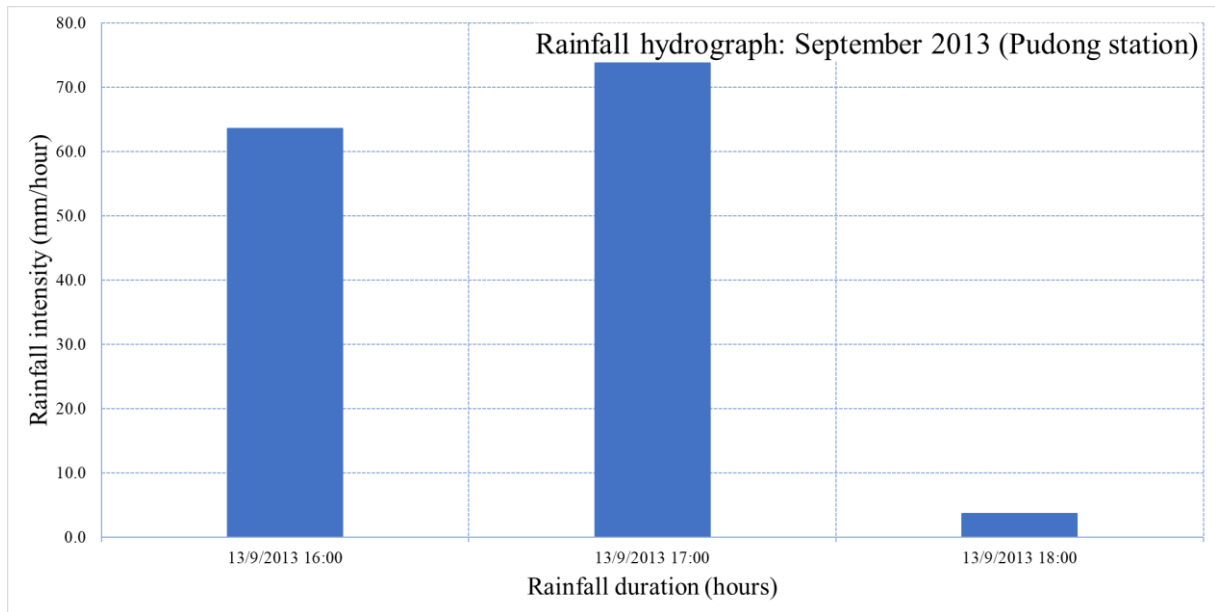


Figure 50: Rainfall hydrograph for September 2013 at Pudong station

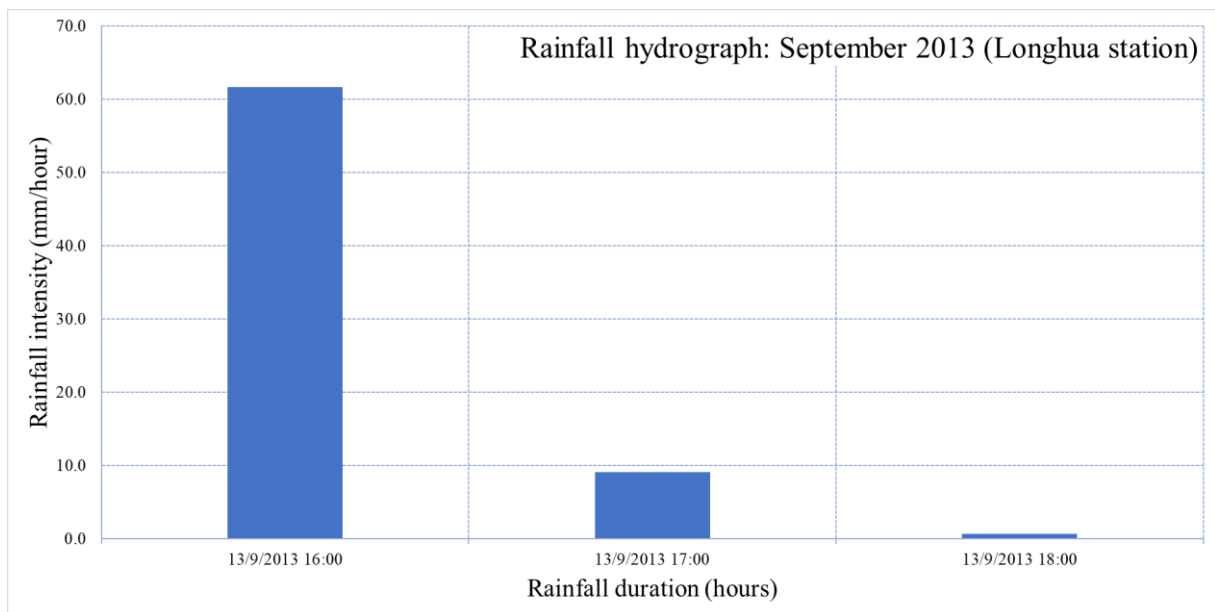


Figure 51: Rainfall hydrograph for September 2013 at Longhua station

The series of the rainfall intensity for the rainfall events of August 1997 and September 2013 at Pudong and Longhua stations are shown in Table 13 and Table 14, respectively. Also, the total storm volume is included in these tables.

Table 13: Time series of rainfall event of August 1997 for Pudong and Longhua station

Rainfall event of August 1997			
Pudong station		Longhua station	
Time	Rainfall Intensity (mm/hour)	Time	Rainfall Intensity (mm/hour)
18/8/1997 19:00	0.2	-	-
18/8/1997 20:00	1.4	18/8/1997 20:00	0.9
18/8/1997 21:00	5.3	18/8/1997 21:00	4.0
18/8/1997 22:00	3.2	18/8/1997 22:00	4.2
18/8/1997 23:00	9.1	18/8/1997 23:00	11.2
19/8/1997 0:00	7.6	19/8/1997 0:00	8.0
19/8/1997 1:00	8.4	19/8/1997 1:00	16.8
19/8/1997 2:00	1.6	19/8/1997 2:00	6.5
19/8/1997 3:00	11.0	19/8/1997 3:00	13.9
19/8/1997 4:00	26.4	19/8/1997 4:00	10.4
19/8/1997 5:00	4.3	19/8/1997 5:00	2.1
19/8/1997 6:00	0.1	19/8/1997 6:00	0.1
19/8/1997 7:00	17.4	19/8/1997 7:00	1.0
19/8/1997 8:00	9.9	19/8/1997 8:00	0.4
19/8/1997 9:00	0.0	19/8/1997 9:00	0.0
19/8/1997 10:00	2.7	19/8/1997 10:00	1.6
19/8/1997 11:00	13.4	19/8/1997 11:00	0.1
19/8/1997 12:00	0.0	19/8/1997 12:00	0.0
19/8/1997 13:00	0.0	19/8/1997 13:00	0.0
19/8/1997 14:00	0.0	19/8/1997 14:00	0.0
19/8/1997 15:00	1.2	19/8/1997 15:00	0.1
19/8/1997 16:00	1.2	19/8/1997 16:00	0.2
19/8/1997 17:00	0.0	19/8/1997 17:00	1.3
19/8/1997 18:00	0.7	19/8/1997 18:00	2.2
19/8/1997 19:00	8.3	19/8/1997 19:00	2.6
19/8/1997 20:00	0.2	19/8/1997 20:00	0.6
19/8/1997 21:00	4.3	19/8/1997 21:00	0.8
19/8/1997 22:00	3.5	19/8/1997 22:00	0.3
19/8/1997 23:00	3.2	19/8/1997 23:00	1.8
20/8/1997 0:00	0.0	20/8/1997 0:00	0.8
20/8/1997 1:00	0.0	20/8/1997 1:00	0.4
20/8/1997 2:00	0.0	20/8/1997 2:00	0.0
20/8/1997 3:00	0.1	20/8/1997 3:00	0.0
20/8/1997 4:00	0.1	20/8/1997 4:00	0.6
20/8/1997 5:00	0.5	20/8/1997 5:00	0.1
20/8/1997 6:00	0.0	20/8/1997 6:00	0.0
20/8/1997 7:00	0.1	20/8/1997 7:00	0.3
20/8/1997 8:00	0.0	20/8/1997 8:00	0.1
20/8/1997 9:00	0.0	-	-
20/8/1997 10:00	0.6	-	-
20/8/1997 11:00	0.2	-	-

Total storm volume (mm)	146.2	94.3
------------------------------------	-------	------

Table 14: Time series of rainfall event of September 2013 for Pudong and Longhua station

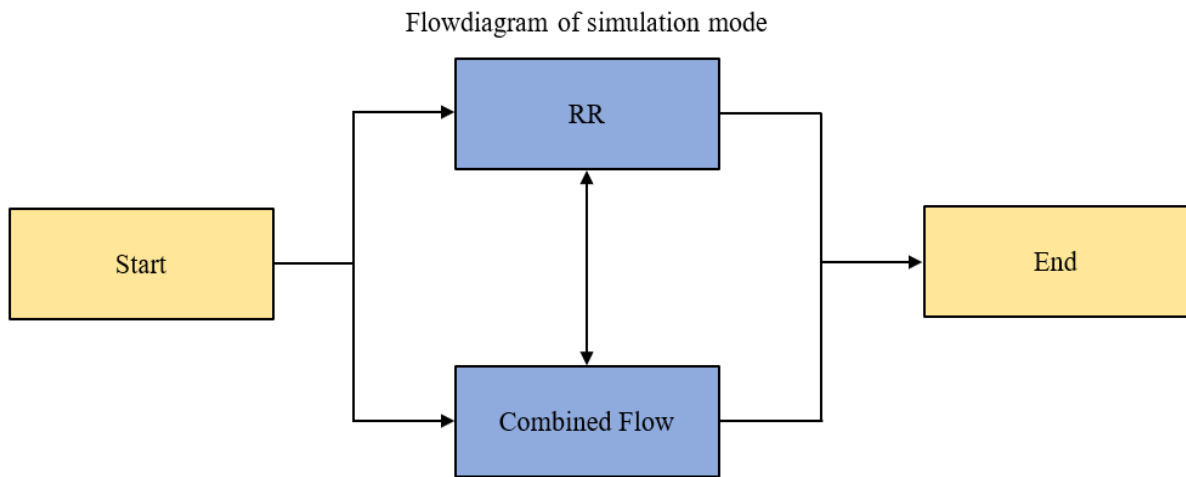
Rainfall event of September 2013			
Pudong station		Longhua station	
Time	Rainfall Intensity (mm/hour)	Time	Rainfall Intensity (mm/hour)
13/9/2013 16:00	63.6	13/9/2013 16:00	61.6
13/9/2013 17:00	73.8	13/9/2013 17:00	9.1
13/9/2013 18:00	3.6	13/9/2013 18:00	0.7
Total storm volume (mm)	141.0		71.4

APPENDIX B: SEWER SYSTEM IN SOBEK

The sewer system of Jingan district was integrated in the flood hazard model. The simulation of the flow in the sewer system was performed by using SOBEK. Due to the lack of preprocessing of the model and of the data, the following changes were made in the set-up of the model.

B.1 Settings

The selected SOBEK modules that were used in this project were 1DFLOW (Rural), 1DFLOW (Urban) and RR (Rainfall-Runoff). The simulation mode that was chosen is the RR (Rainfall-Runoff), 1DFLOW (Rural) and 1DFLOW (Urban) module simultaneously. This means that the rainfall event and the flow in the pipeline network were performed at the same time. The flow diagram of the simulation mode is shown in Figure 52.



RR (Rainfall - Runoff), 1DFlow (Rural) and 1DFlow module simultaneously

Figure 52: Selected simulation mode

Also, some computational parameters were set in this task block. The following assumptions were made:

- Simulation timestep: the time step in computation was set 5 minutes for the rainfall events with different return periods and 60 minutes for the historical rainfall events
- Simulation period: the simulation period was derived from the meteorological data (next section)
- Initial values: the initial flow was set 0 m³/sec and the initial depth in the channels was set 0.01 m.
- Timestep output: the output timestep was set 5 minutes for the rainfall events with different return periods and 60 minutes for the historical rainfall events

B.2 Meteorological data

The selected precipitation data (rainfall events) for this project were generated by the Chicago rainfall hydrograph with return periods of 1, 3, 5, 10 and 50 years (chapter 4.4). The duration of these rainfall events was 3 hours with a timestep of 5 minutes. The hydrographs of these rainfall events are presented in Figure 21. Also, three historical rainfall events were simulated in SOBEK for August 2005, August 1997 and

September 2013. The duration of these events was 59, 41 and 3 hours, respectively, with a timestep of 1 hour. The corresponding hydrographs are shown in Figure 22, Figure 23 and Figure 24, respectively.

B.3 Schematization

The schematization (model) and the data for the sewer system were provided (Shanghai Water Authority 2019). The schematization is presented in Figure 53. The number of the nodes was 2785 and the number of the pipes was 2872. No boundary conditions or outflow points to the adjacent river were provided.



Figure 53: Initial plan of pipeline network – manholes do not allow runoff

However, pre-processing of the data for the manholes and the pipelines of the sewer system should be done.

➤ Network nodes

- Flow - Manholes with Runoff

The type of the network nodes was initially provided to be Flow–Manhole. However, this type of node did not allow the precipitated water to enter the pipelines. This means that the manholes were closed on top. So, the type of Flow–Manholes with Runoff was selected which allowed runoff of the water. Also, the invert and the street level for each manhole were set from data that were provided. Finally, the surface area of each manhole was calculated based on the diameters that were given.

- Flow - External Weir

Since there were no data related to the specific location and the type of the outlets of the pipeline network, some assumptions were made. Firstly, a reasonable assumption for the location of the outlet points was based on the fact that these points should be located near the river that crosses the area next to the northeast side of the pipeline network (top right corner in Figure 54). Another assumption was based on the direction of the flow and the slope of the pipelines. This means that the lower points where the water is accumulated should be set as outlets to let the water escape from the pipeline network. Also, the property of an outlet was assigned for the nodes (gullies) that were dead-end for the flow of water in the northeast side of the pipeline network, the line across the river. Finally, considering the large area that was covered by the

system, additional outlets were assigned. In this way the distance between the abovementioned outlets reduced. In total 15 outlets were defined, as shown in Figure 54.

- Network Branches
 - Flow – Pipe

For the pipelines the type of Flow–Pipe was selected. The pipelines were round with diameters that were provided. For the friction coefficient of the pipes the Manning coefficient was used based on a concrete material with smooth surface. Chow (1959) suggests that for sewer with manholes, inlet etc., straight pipes, the normal value for the Manning coefficient should be 0.015 with minimum and maximum values of 0.013 and 0.017, respectively. In this case the normal value was selected, so 0.015. Finally, the upstream and downstream levels for each pipe were set by data that were provided.

The final plan of the pipeline network is shown in Figure 54.

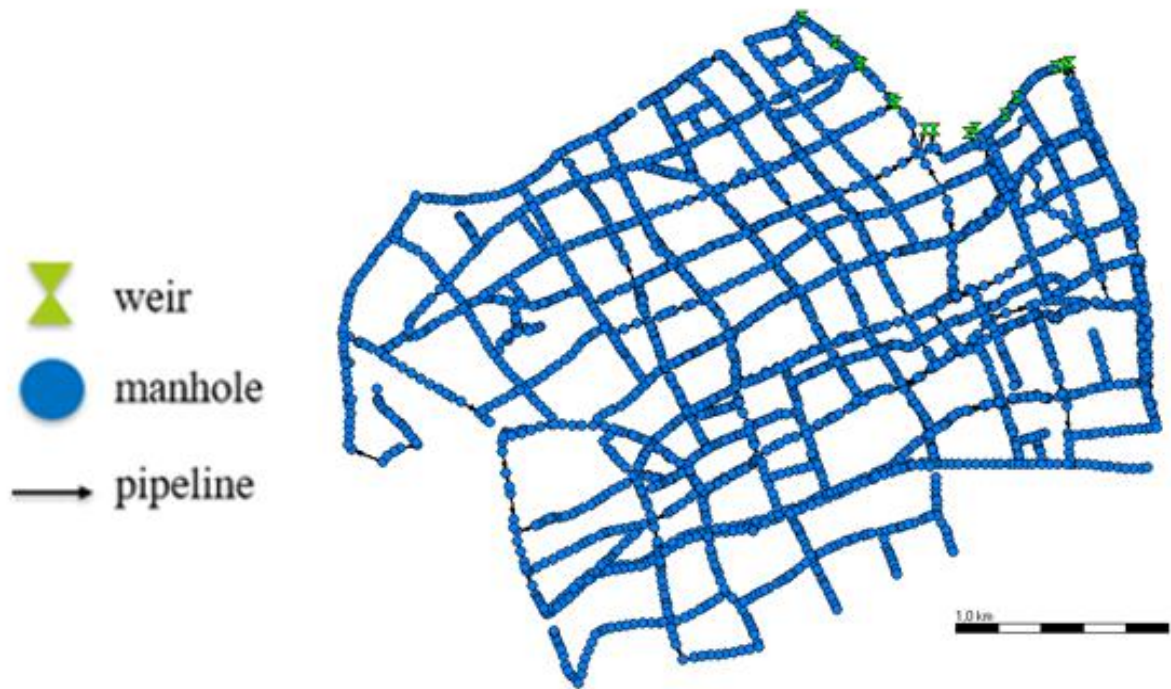


Figure 54: Final plan of pipeline network – manholes allow runoff

B.4 Integration of rainfall in SOBEK

B.4.1 Assumptions

As it is mentioned in the previous chapter, for the integration of the rainfall in the simulation of the flow in the sewer system, the type of the nodes in SOBEK should be changed from Flow-Manholes to Flow-Manholes with Runoff. However, for this type of node the infiltration capacity and the slope of the surface largely influence the rainfall-runoff process. The model distinguishes different types of surfaces, depending on the infiltration (closed paved, open paved, roof, unpaved) and the slope (area with a slope, flat, stretched flat) of the surface. In the case of the area of interest, the following assumptions were made:

- Infiltration: Closed paved areas
 - This refers to areas full of streets, roofs and parking lots which corresponds to the real situation of the surface area of Jingan District.
- Slope: Runoff type → flat
 - In SOBEK, an area with slope more than 4% is considered an area with slope. Since the surface elevation in Shanghai ranges between 2 meters and 4 meters, then the area was considered flat.

- Equal distribution of surface area to the manholes

Since the manholes have not equal distances from each other, a large amount of work was needed to calculate the actual surface runoff area that corresponds to them. For this reason, the simplification of an equally distributed surface runoff area was made.

B.4.2 Calculation of runoff area

Firstly, the surface area of each block was calculated in QGIS as illustrated in Figure 55.

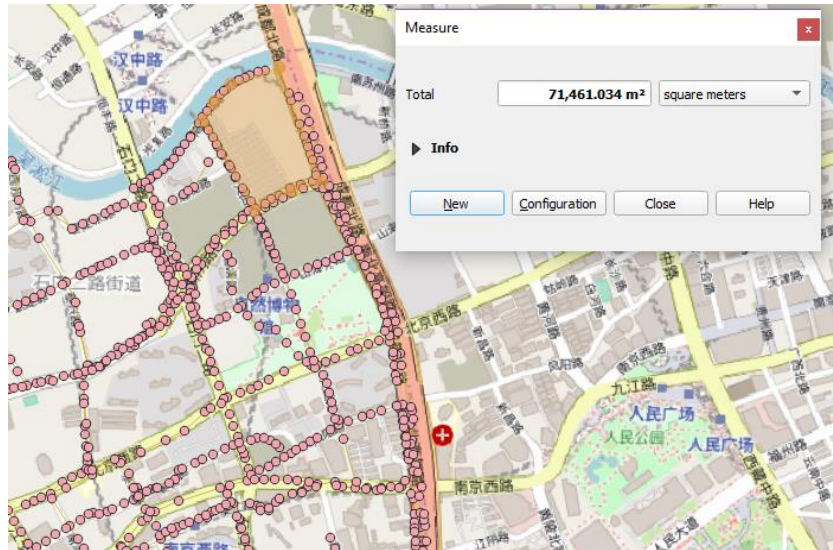


Figure 55: Calculation of the block surface area using QGIS

Then, this area was distributed to all the manholes that form each block by dividing the surface area with the number of the nodes of the block. This was the total runoff area for each node for the specific block. However, for the simulation the 70% of the total area was used as mentioned in chapter 4.3.

The calculation of the total runoff area for all the nodes after considering all the blocks was based on the following two formulas:

Edge manholes: manholes that are part of only one block area

$$S_i = A_j/n_j$$

Intermediate manholes: manholes that are part of more than one block area

$$S_i = \sum_{j=1}^m A_j/n_j$$

where:

S_i : surface area that corresponds to manhole i

A_j : surface area of block j

n_j : number of manholes in block j

m : total number of blocks that the manhole i is part

A schematic representation of the division of the pipeline network into blocks is shown in Figure 56.

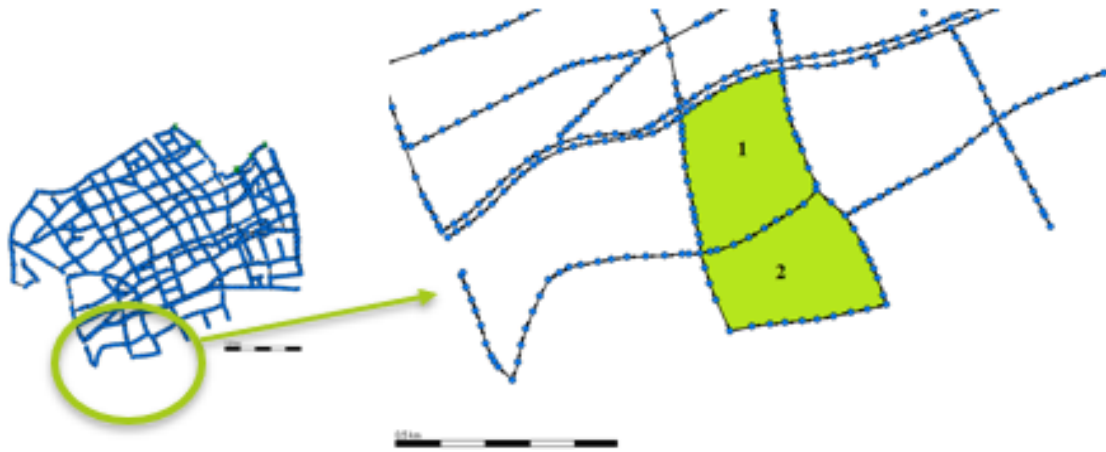


Figure 56: Schematic representation of blocks in the pipeline network

B.5 Output of SOBEK and connection with 2D model

One of the outputs of the simulation of the 1D flow in SOBEK was the runoff discharges of each node of the sewer system. These discharges referred to the water discharge that comes from the rainfall event and corresponds to each inlet of the pipeline network. In the 2D model these discharges represent the sink facilities as were described in chapter 4.3.

To include sinks in the 2D model, two types of files should be created: the first is related to the location (coordinates) of the sink facility (.pli file) and the second to the time series that describe the runoff discharges (.tim file). Based on this, the number of the .pli and .tim files is equal to the number of the inlets to the pipeline network, 2785.

However, these results should be processed before they can be used as inputs in DFM for the simulation of the overland 2D flow. For the preprocessing of these data a code was created in MATLAB that generates the .pli and .tim files. This code is included in Appendix D.

APPENDIX C: RESULTS (EFFECTIVENESS OF THE DRAINAGE SYSTEM)

C.1 Model 4: Rainfall event with 1-year return period

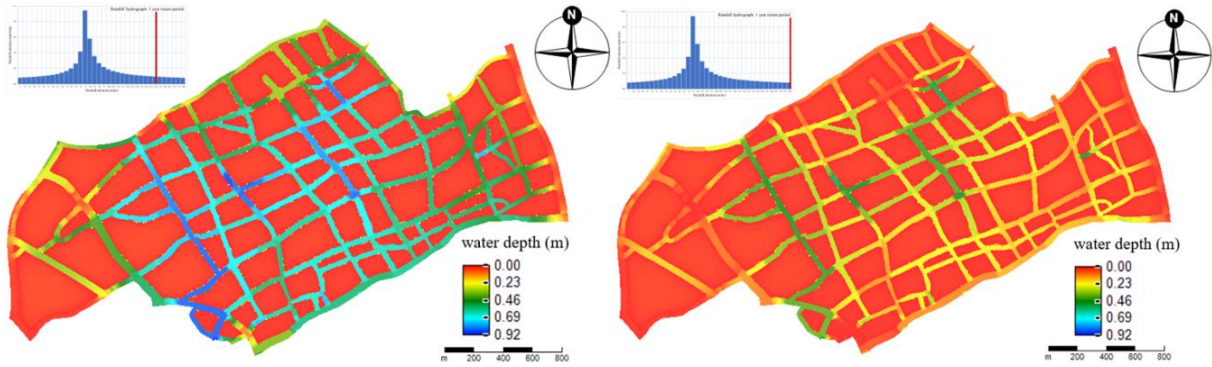


Figure 57: Maximum inundation depths for the rainfall event of 1-year return period, not including the drainage system (left panel), including the drainage system (right panel)

C.2 Model 5: Rainfall event with 3-years return period

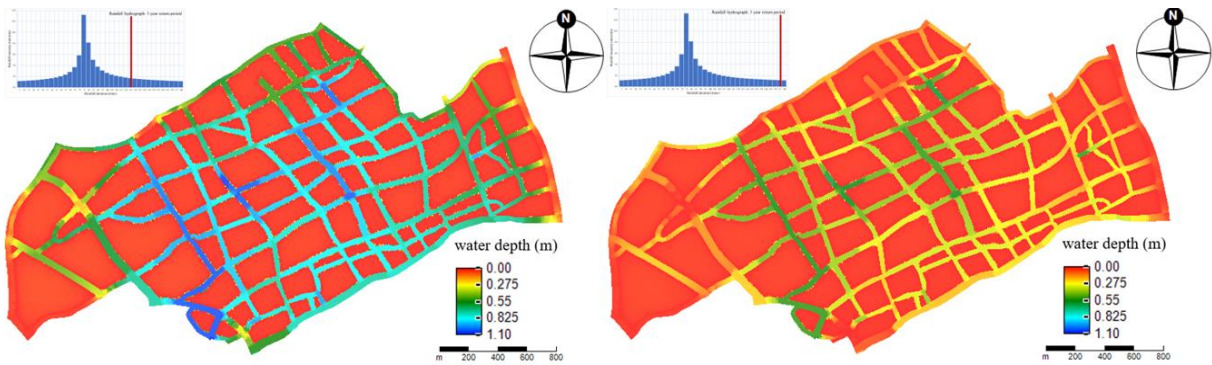


Figure 58: Maximum inundation depths for the rainfall event of 3-years return period, not including the drainage system (left panel), including the drainage system (right panel)

C.3 Model 6: Rainfall event with 5-years return period

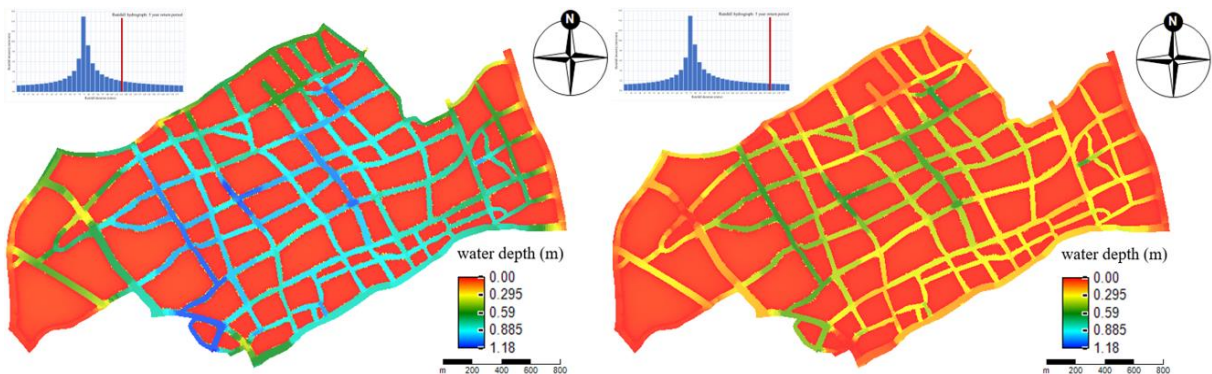


Figure 59: Maximum inundation depths for the rainfall event of 5-years return period, not including the drainage system (left panel), including the drainage system (right panel)

C.4 Model 7: Rainfall event with 10-years return period

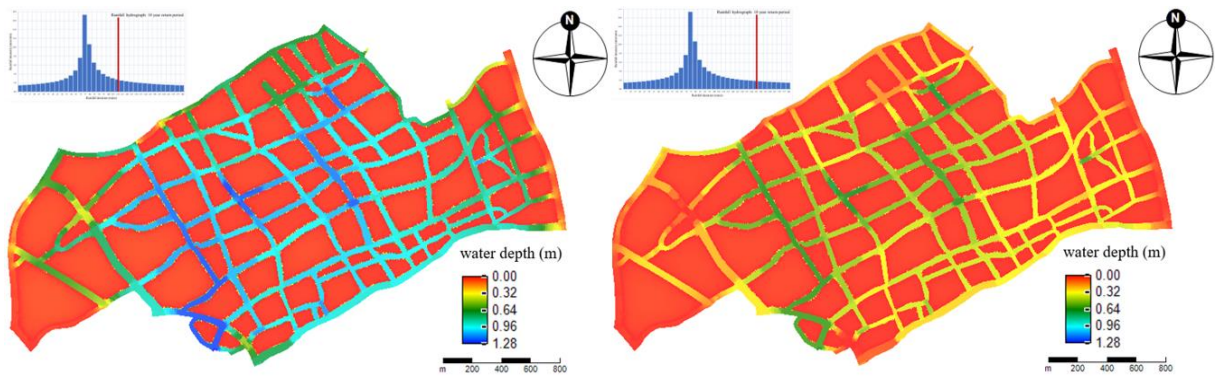


Figure 60: Maximum inundation depths for the rainfall event of 10-years return period, not including the drainage system (left panel), including the drainage system (right panel)

C.5 Model 8: Rainfall event with 50-years return period

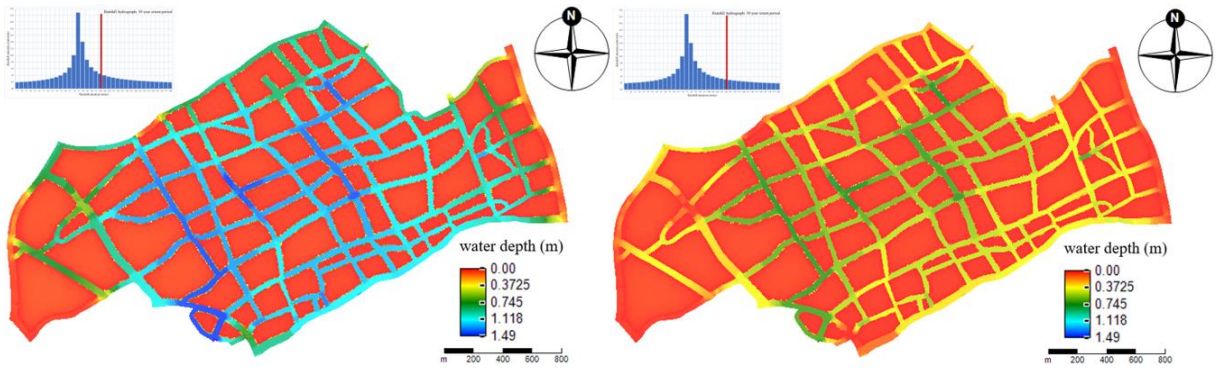


Figure 61: Maximum inundation depths for the rainfall event of 50-years return period, not including the drainage system (left panel), including the drainage system (right panel)

Table 15: Surface area of water storage areas as estimated in DFM

ID of water storage area	Surface area (m²)	ID of water storage area	Surface area (m²)
1	8742	15	3246
2	5928	16	483
3	5621	17	640
4	2083	18	2025
5	14400	19	3306
6	2550	20	1680
7	12243	21	5180

APPENDIX C: RESULTS (EFFECTIVENESS OF THE DRAINAGE SYSTEM)

8	2496	22	3960
9	1892	23	1849
10	3162	24	3906
11	3240	25	2940
12	6862	26	2700
13	3596	27	2736
14	4675		

APPENDIX D: MATLAB CODES

D.1 Preprocessing of surface elevation map

Elimination of nodata values from the original map

```

%%
clc
clear all;

filename1 = '___xyz'; % TYPE NAME OF DSM (XYZ FILE) WITH NODATA VALUES
delimiterIn = ' ';
DSM_with_nodata_values = importdata(filename1, delimiterIn);
N = length(DSM_with_nodata_values);

%%
j = 0;
for i = 1:N
    if (ne(DSM_with_nodata_values(i,3), ___)) % TYPE NO DATA VALUE (FROM DSM)
        j = j+1;
    end
end

DSM_without_nodata_values = zeros(j,3);

filename2 = '___xyz'; % TYPE PREFERRED NAME OF OUTPUT DSM (XYZ FILE) WITHOUT
NODATA VALUES
fileID = fopen(filename2, 'w');
w = 0;
for i = 1:N
    if (ne(DSM_with_nodata_values(i,3), ___)) % TYPE NO DATA VALUE (FROM DSM)
        w = w+1;
        DSM_without_nodata_values(w,1) = DSM_with_nodata_values(i,1);
        DSM_without_nodata_values(w,2) = DSM_with_nodata_values(i,2);
        DSM_without_nodata_values(w,3) = DSM_with_nodata_values(i,3);
        fprintf(fileID, '%.12f %.11f %.20f\n', DSM_without_nodata_values(w,1),
        DSM_without_nodata_values(w,2), DSM_without_nodata_values(w,3));
    end
end

fclose(fileID);

```

Change of elevation values lower than 2 meters

```

%%
clc
clear all;

filename1 = '___xyz'; % TYPE NAME OF DSM (XYZ FILE) THAT CONTAINS ELEVATION
VALUES LOWER THAN 2 METERS
delimiterIn = ' ';
DSM_initial = importdata(filename1, delimiterIn);
N = length(DSM_initial);
%%
DSM_processed = zeros(N,3);

```

```

filename2='___xyz'; % TYPE PREFERRED NAME OF OUTPUT DSM (XYZ FILE)
fileID=fopen(filename2, 'w');

for i=1:N
    if (lt(DSM_initial(i,3),2))
        DSM_processed(i,1) = DSM_initial(i,1);
        DSM_processed(i,2) = DSM_initial(i,2);
        DSM_processed(i,3) = 10;
    else
        DSM_processed(i,1) = DSM_initial(i,1);
        DSM_processed(i,2) = DSM_initial(i,2);
        DSM_processed(i,3) = DSM_initial(i,3);
    end
    fprintf(fileID, '%.12f %.11f %.20f\n', DSM_processed(i,1), DSM_processed(i,2),
DSM_processed(i,3));
end
fclose(fileID);

```

Set of maximum elevation

```

%%
clc
clear all;

filename1 = '___xyz'; % TYPE NAME OF ORIGINAL DSM (XYZ FILE)
delimiterIn = ' ';
DSM = importdata(filename1, delimiterIn);
N = length(DSM);

%%
filename2 = '___xyz'; % TYPE PREFERRED NAME OF OUTPUT DSM (XYZ FILE)
fileID = fopen(filename2, 'w');

for i = 1:N
    if
        (ne(DSM(i,3),2))&&(ne(DSM(i,3),2.05))&&(ne(DSM(i,3),2.1))&&(ne(DSM(i,3),2.15))&&(ne(DSM(i,3),2.2))&&(ne(DSM(i,3),2.25))&&(ne(DSM(i,3),2.3))&&(ne(DSM(i,3),2.35))&&(ne(DSM(i,3),2.4))&&(
        ne(DSM(i,3),2.45))&&(ne(DSM(i,3),2.5))&&(ne(DSM(i,3),2.55))&&(ne(DSM(i,3),2.6))&&(ne(DSM(i,3),2.65))&&(ne(DSM(i,3),2.7))&&(ne(DSM(i,3),2.75))&&(ne(DSM(i,3),2.8))&&(ne(DSM(i,3),2.85))&&(
        &(ne(DSM(i,3),2.9))&&(ne(DSM(i,3),2.95))&&(ne(DSM(i,3),3.0))&&(ne(DSM(i,3),3.05))&&(ne(DSM(i,3),3.1))&&(ne(DSM(i,3),3.15))&&(ne(DSM(i,3),3.2))&&(ne(DSM(i,3),3.25))
        DSM(i,3) = 5;
    end
    fprintf(fileID, '%.12f %.11f %.20f\n', DSM(i,1), DSM(i,2), DSM(i,3));
end

fclose(fileID);

```

D.2 Generation of PLI and TIM files

Generation of .pli, .tim files

```

%%
clc
clear all;

% import coordinates of nodes
filename1 = '____.txt'; % TYPE NAME OF FILE WITH THE COORDINATES OF THE NODES
delimiterIn = ',';
Coordinates_Nodes = importdata(filename1, delimiterIn);
N_Coor_Nod = numel(Coordinates_Nodes)/3;

% import ID of deleted nodes
filename2 = '____.txt'; % TYPE NAME OF FILE WITH THE ID OF THE DELETED NODES
ID_Deleted_Nodes = importdata(filename2);
N_ID_Del_Nod = numel(ID_Deleted_Nodes);

%%
% generate matrix containing the ID and coordinates of the used nodes
N_ID_New_Nod = N_Coor_Nod - N_ID_Del_Nod;
New_Nod = zeros(N_ID_New_Nod, 3);
j = 1;
for i = 1:N_Coor_Nod
    li = ismember(i, ID_Deleted_Nodes(:));
    if eq(li, 0)
        New_Nod(j, 1) = Coordinates_Nodes(i, 1);
        New_Nod(j, 2) = Coordinates_Nodes(i, 2);
        New_Nod(j, 3) = Coordinates_Nodes(i, 3);
        j = j + 1;
    end
end

%%
% generate pli files
C = zeros(1, 2);
for i = 1:N_ID_New_Nod
    ID = New_Nod(i, 1);
    filename3 = ['IDnode' sprintf('%d', ID) '.pli'];
    IDnode = ['IDnode' sprintf('%d', ID)];
    Rows_Columns = [1, 2];
    for j = 1:2
        C(1, j) = New_Nod(i, j + 1);
    end
    fileID = fopen(filename3, 'w');
    fprintf(fileID, '%s\r\n %d %d\r\n%15.8f %15.8f', IDnode, Rows_Columns, C);
    fclose(fileID);
end

%%
% import time series
filename4 = '____.txt'; % TYPE NAME OF FILE WITH TIME SERIES
Time = importdata(filename4);

```

```
N_Time = length(Time);

% import runoff discharges
filename5 = '____.txt'; % TYPE NAME OF FILE WITH TIME SERIES OF THE DISCHARGE
Run_Dis = importdata(filename5);

% generate tim files
Runoff = zeros(2,N_Time);
for i = 1:N_ID_New_Nod
    for w = 1:N_Coor_Nod
        if eq(New_Nod(i,1),Run_Dis(w,1))
            ID = New_Nod(i,1);
            file_name = ['IDnode' sprintf('%d',ID) '.tim'];
            fileID = fopen(file_name, 'w');
            for j = 1:N_Time
                Runoff(1,j) = Time(j,1);
                Runoff(2,j) = -Run_Dis(w,j+1);
            end
            fprintf(fileID, '%8.6f %8.6f\n', Runoff);
            fclose(fileID);
        end
    end
end
end
```

APPENDIX E: FIELDWORK IN SHANGHAI

E.1 Correction of surface elevation map

E.1.1 Introduction – Definition of problems

During extreme rainfall events, inundation may occur in many locations in Jingan District due to the insufficient drainage system of the urban area. This results in the development of a 2D (two-dimensional) overland flow of the rainwater which, especially at the beginning, takes place mainly on the areas with the lowest elevation, to wit the street system.

For Jingan District, the simulation of the overland 2D flow is performed by using the DFM (Delft3D Flexible Mesh). However, during the set-up of the model an important input parameter that has to be taken into account is the DEM (Digital Elevation Model). This is a map that illustrates the elevation of the surface of the earth including buildings, streets, parks, etc. and indicates the path that the water will follow during the inundation event.

However, by using the DEM several problems may arise by inaccuracies in the elevation of the street system. This may lead to unreliable results, to wit inundation maps based on unrealistic surface elevation and thus water flow path conditions. The origins of these inaccuracies may be attributed to several factors. However, in this chapter focus is given in the resolution of the DEM and the existence of elevated streets that block the measurement of the areas below them.

Influence of buildings on road elevation

The DEM that would be used initially in DFM for the simulation of the overland 2D flow in Jingan District had a resolution of 20 meters. This means that the information in the DEM is provided in pixels of 20×20 meters area.

However, Jingan District is a residential area where the maximum width of most of the streets is around 10-12 meters. This is calculated in QGIS by using the command Measure Line in combination with the OpenStreetMap provided by the software (Figure 62). The accuracy of this measurement may not be good, but it is a first estimation and assessment of the real situation.

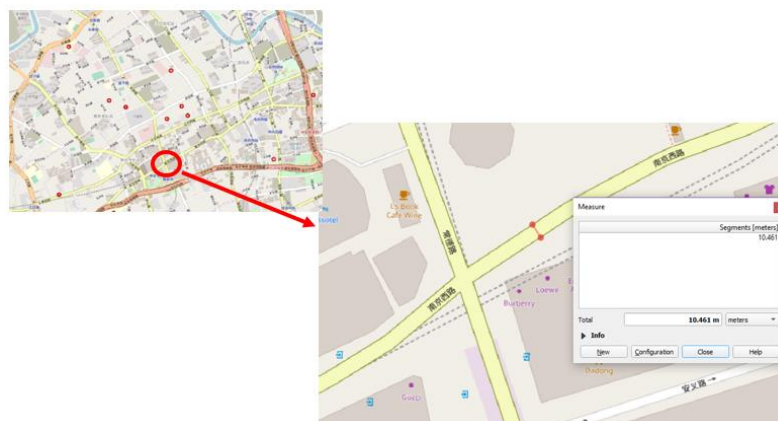


Figure 62: Estimation of the width of the road in Jingan District using QGIS

The same conclusion was made after visual observation and estimation of the width of the street during the fieldwork investigation in Jingan District. An example of such a street is illustrated in Figure 63.

covered by roads which have the same elevation with the perpendicular to them roads. This is illustrated in Figure 65.

In Figure 65, four pictures are depicted regarding some of the locations of the elevated roads that were visited. The combination of the following list and the spots in Figure 66 provide information about the actual location.

- Top left panel: Huashan Rd – Yan’an Middle Rd (spot 1 in Figure 66)
- Top right panel: Weihai Rd – Yan’an Middle Rd (spot 2 in Figure 66)
- Bottom left panel: Maoming N Rd – Yan’an Middle Rd (spot 3 in Figure 66)
- Bottom right panel: Chengdu N Rd – Nanjing W Rd (spot 5 in Figure 66)

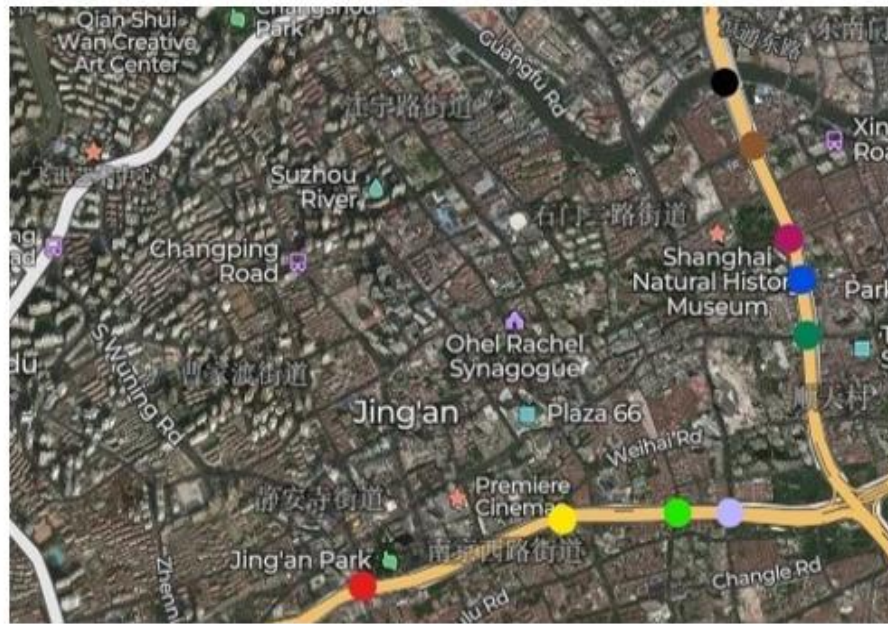


Figure 65: Elevated roads in Jingan District, Huashan Rd – Yan’an Middle Rd (top left panel), Weihai Rd – Yan’an Middle Rd (top right panel), Maoming N Rd – Yan’an Middle Rd (bottom left panel), Chengdu N Rd – Nanjing W Rd (bottom right panel)

E.1.2 Measurements – Correction of unrealistic values in DEM

To solve the problem of the influence of the buildings in the elevation of the road system, the elevation of each road in Jingan District was checked in QGIS and changes were made where it was necessary. The new assigned values for the elevation were based on the elevation of other parts of the road near the area of interest.

For the problem that was triggered by the presence of the elevated roads a different approach was chosen. During the fieldwork in Jingan District, measurements were performed, and estimations were made regarding the elevation of the elevated roads and the elevation of the areas below them. The measurements took place in 9 different locations across the elevated roads, 4 across the Yan’an Elevated Road and 5 across the North-South Elevated Road that leads to the river in the northern part of Jingan District. The exact locations of the measurements are illustrated in Figure 66.



- | Yan'an Elevated Road | North-South Elevated Road |
|--|---|
| ● Location 1: Huashan Rd – Yan'an Middle Rd | ● Location 5: Chengdu N Rd – Nanjing W Rd |
| ● Location 2: Weihai Rd – Yan'an Middle Rd | ● Location 6: Chengdu N Rd – Fengyang Rd |
| ● Location 3: Maoming N Rd – Yan'an Middle Rd | ● Location 7: Chengdu N Rd – Beijing W Rd |
| ● Location 4: Shimen 1 st Rd – Yan'an Middle Rd | ● Location 8: Chengdu N Rd – Xinzha Rd |
| | ● Location 9: Chengdu N Rd – S Suzhou Rd |

Figure 66: Locations of measurements across the elevated roads (Mapcarta)

The measurements were performed by using the Laser Rangefinder. The measured elevations for the selected locations, as well as the DEM values are summarized in Table 16. Also, in this table the corrected values for the elevation are presented based on the simple formula:

$$\text{Surface Elevation under elevated roads} = \text{DEM} - \text{Measured elevation}$$

$$(4) = (3) - (2)$$

Table 16: Measured elevation, DEM and estimated elevation under the elevated roads

Location (1)	Measured elevation of elevated roads (m) (2)	DEM (m) (3)	Elevation under elevated roads (m) (4)
1	11.0	13.825	2.825
2	10.1	12.960	2.800
3	11.4	14.686	3.286
4	10.0	12.614	2.614

5	9.4	2.790	2.790
6	8.8	2.793	2.793
7	10.4	2.142	2.142
8	9.2	2.142	2.142
9	7.4	3.636	3.636

From Table 16, it can be concluded that there were inaccuracies in the elevation of the areas only under the Yan'an Elevated Road. In the locations that the North-South Elevated Road crosses, the elevations are reasonable, and no changes were made in the DEM. Based on the last column of the above table, the DEM was modified by using the DFM.

E.2 Green areas in Jingan district

Another objective of the fieldwork investigation in Shanghai was to locate and list the already existing green infrastructure in the urban area of Jingan District. However, after investigation and discussion with local experts, it was concluded that Sponge City measures have not been implemented in Jingan District so far. The existing green areas in the urban area are mostly parks, gardens of residential blocks and green spaces between the buildings. It is emphasized that in contrast to the initial expectations, almost every block in Jingan District has at least a small part which is covered by green areas. However, it is not sure if the specific green spaces were constructed for water retaining purposes and thus their infiltration and retention capacity cannot be estimated.

During the fieldwork, it was planned to visit several green areas in Jingan District. However, due to the existence of closed residential areas and companies' restricted areas, the access to these places was not allowed. A list of the places that were visited is presented below and information about their location and covered area is given in Figure 67:

1. Environmental Theme Park of Suzhouhe Mengqing Garden
2. Jingan Park
3. Shanghai Rose Garden
4. Jingan Sculpture Park



Figure 67: Locations of visited green areas (Mapcarta)

From the abovementioned parks, only the Environmental Theme Park of Suzhouhe Mengqing Garden is relevant to water issues. In the following, a description is made of each location.

E.2.1 Environmental Theme Park of Suzhouhe Mengqing Garden

Mengqing Park is located in the Southern bank of Suzhou River (red spot in Figure 67). Its location is out of the limits of the investigated urban area of Jingan District, but its relevance with the water cycle makes it an important place to be visited. According to the Information Office of Shanghai Municipality, it is the first park in Shanghai with flowing water, which presents the rehabilitation of the creek and the technologies for the protection of the environment. At present, the creation of Mengqing Park, the changes in the Suzhou River and the other green areas and parks across the river, improve the conditions of the living environment for the citizens and make the Suzhou River an urban residential quarter with ecological characteristics. Some of the most important features of this park are presented below.

Rainwater Storage Tank

In the area of the park that is shown in Figure 68, according to the sign that is placed in this location, a storage tank of 25,000 cubic meters effective volume is six meters underground. This tank is used for the collection of the initial water that comes from the rain during a rainfall event. After the end of the rain, the tank through drain pipes pumps stormwater into the drainage network before the treatment of the rainwater in the treatment plants of the sewer system. The tank is linked to the ground with the more than 20 vent pipes, that are depicted in Figure 68, allowing the visitors to listen the natural sound coming from the underground water. According to the same sign a rainwater storage tank is a drainage system that is used in the developed nations in order to improve the quality of the water bodies in urban areas.



Figure 68: Location of underground rainwater storage tank

Also, in this location, a small-scale model of the sewer treatment plant and the rainwater storage tank is placed (Figure 69).



Figure 69: Model for sewer treatment plant and rainwater storage tank

Elevated water channel

According to the sign that is placed in the location that is depicted in Figure 70, the water of Suzhou River is treated by a biological purification system for the landscape water body of Mengqing Park. After this, the water is lifted by pumps and a cascade water channel is formed.

In Figure 70, the pool, a small part of the elevated water channel and the pumping system are illustrated. A closer look to the pumping system is given in the right panel of Figure 70.



Figure 70: Pool and elevated water channel (left panel) and pumping system (right panel)

After being pumped the water flows in the channel which has a length of 50 m (Figure 71) before it is collected in a reservoir (Figure 72).



Figure 71: Elevated water channel and flow direction



Figure 72: Reservoir that collects the water from the elevated channel

Moon-star Outfall

According to the sign in the location of Figure 73, the Moon-star Outfall is the outlet for the water that flows back to Suzhou River after the biological purification for the landscape water body of Mengqing Park.



Figure 73: Location of outfall to the Suzhou River for the water after purification

E.2.2 Jingan Park

Next to the entrance of Jingan Park, a sign with general information from Shanghai Jingan District Municipal, Greening Administration, September 1999, is placed. According to this sign, the park was founded in 1954 and is located in the area of Jingan Temple. This area has been one of the most famous cultural, tourist and business centers in Shanghai. The park has an important value with respect to ecology and is considered an oasis of this center of urban public activities. It was completely renovated in 1998 by the municipal government of Jingan District in order to be a human-oriented garden with historical and cultural characteristics and entertainment, fitness, leisure, tourism and sightseeing activities. The total area of the park is 33,600 square meters, with a coverage rate of green of 70%. Many green landscapes have been added in the park while the old and big trees were retained.

A sloped and a flat green area in the Jingan Park is shown in Figure 74 and Figure 75, respectively.



Figure 74: Sloped green area in Jingan Park

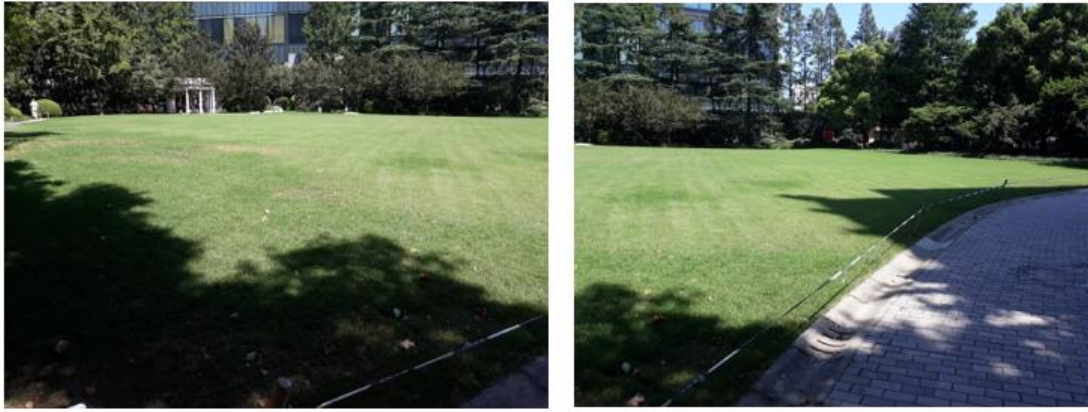


Figure 75: Flat green area in Jingan Park

E.2.3 Shanghai Rose Garden

Shanghai Rose Garden is a small green area which is located among buildings in the urban area of the Jingan District (Figure 76). Due to the small area that this garden covers, it could be considered a part of the final section of this chapter "Green areas across the road network".



Figure 76: Green space in Shanghai Rose Garden

E.2.4 Jingan Sculpture Park

According to IPA (Institute for Public Art), the Jingan Sculpture Park was founded in October 2007 and is located close to the center of Shanghai. The total coverage area of the park is 60,000 square meters. It is divided into six areas, among them four landscape areas. The combination of sculpture layout, landscape construction and terrace garden scenery create a clean and abundant park environment.

In Figure 77 and Figure 78, the roof and the side view of the main building in Jingan Sculpture Park are depicted, respectively. Since, the capacity of a green area to retain rainwater depends on many factors such

as the properties of the soil, the thickness of the soil layer etc. it is not known whether these green areas were developed to retain rainwater or for architectural purposes.



Figure 77: Roof garden on the main building in Jingan Sculpture Park



Figure 78: Side view of the main building in Jingan Sculpture Park

Examples of the landscape with the big green areas of the Jingan Sculpture Park are shown in Figure 79.



Figure 79: Green areas in Jingan Sculpture Park

E.2.5 Green areas across the road system

Apart from the parks and the gardens that were described above, green areas across the road system may play an important role in retaining rainwater during extreme pluvial events. Some pictures that were taken in the Jingan District are presented in Figure 80 - Figure 82. Also, the locations where the pictures were taken are indicated in these figures.



Figure 80: Green areas across the Nanjing W Road



Figure 81: Green area in Qinghai Road

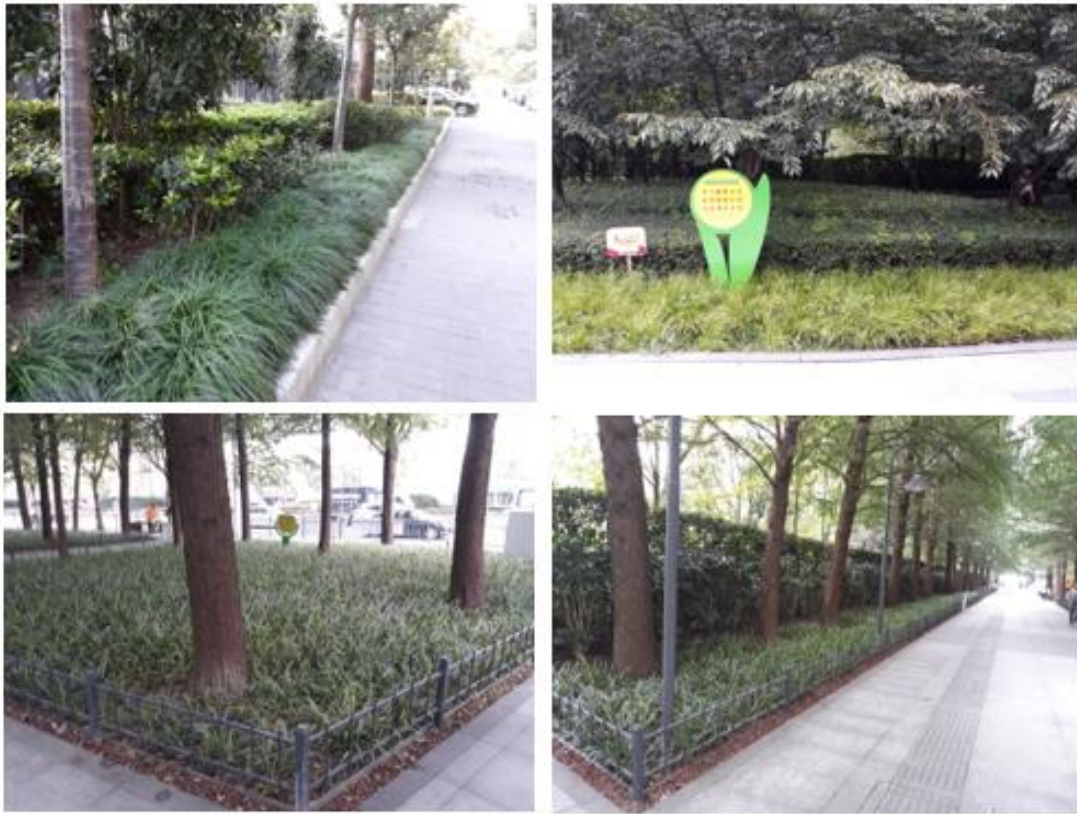


Figure 82: Green areas across the Chengdu N Road

E.3 New buildings vs Old buildings

The combination of extreme weather conditions, that trigger severe rainfall events in Shanghai, and the inadequate capacity of the underground pipeline network in Jingan District to collect and transfer the rainwater, usually leads to pluvial flooding events, causing severe damage to people's properties like houses and stores. This damage is highly related to the inundation depth.

For this reason, a video recording of all the buildings in Jingan District was initially planned. This would lead to useful remarks regarding the protection of these buildings against flooding events and would help in the production of damage maps. However, due to the large area that Jingan District covers, this plan was abandoned and instead of that photos were taken for some specific buildings.

The investigation was mainly focused on the differences between new and old buildings. It was observed that in Jingan District the new buildings are elevated from the road a considerable number of meters by means of stairs. This can be seen in Figure 83 (upper panels). However, this comes in contrast with the view of the old buildings. The entrance to the old buildings is usually located in the same level as the pavement in front of them as shown Figure 83 (lower panels), making them more vulnerable to flooding compared to the new buildings.

It is not clear yet if a structural code has been established for newly designed buildings in order to avoid the contact with water in case of extreme flood events in the area, however, it is a fact that there are obvious differences.



Figure 83: Elevated entrances in new buildings (upper panels) vs street level entrances in the old buildings (lower panels)

E.4 Flood event / Bad maintenance / Possible outlet locations

E.4.1 Flood event (6th September 2019)

During the second day (6th September 2019) of the investigation fieldwork in Shanghai, a pluvial flood event took place in the campus area of Shanghai Normal University. The torrential rainfall event was originated by Typhoon Lingling that crossed the coastal area of Shanghai these days and lasted for almost 12 hours, causing inundation conditions in some locations. This is illustrated in Figure 84.



Figure 84: Inundation in the campus of Shanghai Normal University

Also, it was observed that although the entrance of the water flow to the underground pipeline network was not hampered by any kind of trash, leaves from the trees or sediment, the water remained stagnant for over 5 hours. This situation is presented in Figure 85.



Figure 85: Stagnant water on top of inlets (Shanghai Normal University campus)

After discussion with local people, four possible explanations were given related to this issue:

- The intensity of the rainfall event was so high that the underground pipeline network was filled with water for some hours reducing its drainage capacity
- The pipeline system is constituted by pipes of small diameter which sometimes may be filled with sediment or trash
- The gates of the pipeline system outlets in the river were closed (maybe due to high water level in the river)
- The capacity of the pumping stations in Shanghai is not adequate

E.4.2 Bad maintenance

In Jingan District, the underground pipeline network that collects and transfers the rainwater is a quite complex system. It consists of a considerable number of inlets on top of the road system and pipelines that allow the water to flow under the surface of the urban area. However, the inundation situations that are usually observed in Jingan District due to extreme rainfall events, are aggravated as a result of bad maintenance of the underground network.

For this reason, an inspection of the inlet systems and the pipes was initially planned to be performed. However, the access to the pipeline network is not allowed. Thus, only the inspection of the condition of the inlet system was done. Two examples that illustrate the current condition of the inlets are presented in Figure 86.



Figure 86: Examples of inlets for the rainwater in Jingan District

In this figure, it is shown that the inlets are clear from trash and sediment. However, a closer look to the inside will prove that the maintenance in the underground pipeline network is bad and may only be performed in the hot spots of the system, to wit the points where regular hampering of the flow and thus surface inundation occurs.

E.4.3 Possible outlet locations

The northern part of Jingan District borders the Suzhou River. Consequently, it is reasonable to assume that the outlets of the drainage system may be located across this river. During the fieldwork investigation in Jingan District, the areas next to the river were visited. Examples of the inlets of the drainage system are presented in Figure 87.



Figure 87: Inlets and manholes across the river

In this figure, it can be observed that a manhole is always presented in the middle of the road which may be used in situations that inspection and maintenance actions take place. In the edges of the road (connection with the pavements) two inlets are placed to allow the water to flow in the underground pipeline network. During the fieldwork in Jingan District, it was also observed that the same pattern of manholes and inlets was presented approximately every 40 meters across the Suzhou River.

E.5 Expert Judgement

During the fieldwork investigation, several discussions took place with local experts regarding the problem of urban pluvial flooding in the downtown area of Shanghai. In order to draw useful deductions, a questionnaire was developed with specific questions oriented to the problems that arose during the 1D modelling and the proposal of the measures to deal with the flood hazard problem. The questionnaire is presented in chapter E6 of Appendix E. In the following, a summary is presented of the conversations that took place and the respective conclusions.

Pluvial flooding events in the urban area of Shanghai take place quite often, two to three times per year, with some of them to cause serious damages. The last pluvial flooding event in the urban area of Shanghai was caused by Lichma typhoon on August 2019. The inundation depth was up to 20 to 30 cm, while the strong winds caused many trees to fall. The result of that event was that 200,000 people evacuated their houses. The drainage system has been designed to withstand rainfall events with 3 years return period; however, the capacity of the system may be reduced due to the bad maintenance. This causes the system to be able to deal with rainfall events of 1-year return period. However, there are plans for the system to be upgraded and withstand rainfall events with 3 to 5 years return period in general and 10 years return period in the most important places. In particular, for Jingan District that is located in the downtown of Shanghai

and is the area of interest of this part of the fieldwork, the drainage system has been designed with 1-year return period.

In general Shanghai had a combined drainage system, so the rainwater and the sewer were collected in one underground pipeline network. However, during the last two to three decades, actions have been taken to separate the drainage system. Today most of the system is considered separated, with the sewer system to end up in the sea and the rainwater system to the river. Due to the location of Jingan District, separation of the system is not an easy task since the required construction works affect the daily activities of people in the downtown area of Shanghai. For this reason, in Jingan District the system is considered combined.

In the last years, some pluvial flood reduction measures have been implemented in the urban area of Shanghai. Firstly, the small in diameter pipes of the pipeline network have been replaced by larger ones and the pumping stations have been upgraded increasing their capacities to discharge water out of the urban area. Also, the construction of underground tunnels has taken place to retain and reuse water, e.g. the underground tunnel 60 meters below the Suzhou creek. Furthermore, another action that has been taken is the implementation of the Sponge City Project which includes hard and soft measures and green infrastructure. In the framework of this project, about 30 cities were selected, among them Shanghai, as pilot cities to assess the effectiveness of the Sponge City measures. Finally, additional indirect measures have been considered such as the development of a warning system in case of upcoming extreme rainfall events, the education of people related to flood problems, the development of emergency plans and the gathering of stockpile (preparation of material, equipment and goods before flood events). However, especially for Jingan District, there is not information whether flood reduction measures have taken place or not since it is an area in the downtown of Shanghai and intervention is a difficult and expensive task.

The main water control structures in Shanghai are the pumping station. In Jingan District there is only one pumping station. Apart from the pumping stations, other water control structures are the floodwalls in the connection with the Suzhou river and the floodgates in the outlets in case the water level in the river exceeds the level of the outlet. Regarding the outlets of the pipeline network there is no information neither for the number of them nor for the actual location. This makes the simulation of the water flow in the pipeline network harder since in place of the actual situation some reasonable assumptions will need to be made.

Moreover, the materials that the pipes of the pipeline network are made of concrete and steel, but there are no data regarding the actual location of these pipes. For the concrete pipes the condition may not be good since on one hand the maintenance takes place only in the hot spots, to wit the locations with the maximum recorded inundation depths and on the other hand the sewer water causes damage to the material.

Summarizing, the recommended measures for pluvial flood reduction in the downtown of Shanghai are the Sponge City measures, the construction of deep underground tunnels and the upgrade of the old pumping stations. These measures would improve the capacity of the drainage system and would help in reducing the frequency of the flood events. Finally, it is quite important for a risk assessment to be done.

E.6 Questionnaire

1. How often is pluvial flooding in the urban area of Shanghai and especially in Jingan District?
2. What was the last pluvial flooding in the urban area of Shanghai and what were the damages?
3. Does Jingan District have a combined or a separate sewer system?
4. What pluvial flood reduction measures have been implemented in Jingan District in the last years?
5. What are the measures that deserve priority in the urban area of Shanghai and in Jingan District?
 - Green roofs/rooftop gardens
 - Permeable pavement
 - Half open pavement with grass
 - Sidewalks
 - Rain gardens
 - Bioswale

- Separation of rainwater from the sewer system
 - Regular cleaning of sewer system from waste, debris, sediment, tree roots
 - Upgrading/enlarging the capacity of drainage system
 - Construction of more outflow points in the sewer system
 - Installation of water infiltration and attenuation systems
 - Infiltration basins
 - Floodplains restoration
6. What are the locations (hot spots) in Jingan District with the biggest inundation problems due to rainfall events?
 7. What is the condition of the material (concrete, steel) that the pipelines of the rainwater collecting system are made of in Jingan District? (Roughness)
 8. How often is maintenance done in the pipeline network of Jingan District?
 9. Are there any rainwater control structures inside Jingan District?
 10. What is the number and the location of the outlets of the rainwater collecting system to the river?
 11. What is the position of the outlets with respect to the water surface on the river? Above or below the water surface? What mechanism is used (pumping system)?
 12. Is the rainwater of the adjacent districts transferred in the pipeline system of Jingan District before it ends up in the river?
 13. What kind of measures do you recommend for pluvial flood reduction in Shanghai and in Jingan District in particular?